

**Design and Analysis of Diesel Exhaust After-Treatment for Heavy-Duty
Vehicle Emission Control System In Workshop**



Obse Regasa Dechasa

A Thesis submitted to the Department of Mechanical Engineering
School of Mechanical, Chemical and Materials Engineering

Presented in Partial Fulfillment of the Requirement for Master of Science in
Automotive Engineering

Office of Graduate Studies

Adama Science and Technology University

June, 2024

Adama, Ethiopia

**Design and Analysis of Diesel Exhaust After-Treatment for Heavy-Duty
Vehicle Emission Control System In Workshop**

Obse Regasa Dechasa

Advisor: Alemayehu Wakjira (Phd)

A Thesis Submitted to the Department of Mechanical Engineering

School of Mechanical, Chemical and Material Engineering

Presented in Partial Fulfillment of the Requirement for Master of Science in
Automotive Engineering

Office of graduate studies

Adama Science and Technology University

June, 2024
Adama, Ethiopia

DECLARATION

I hereby declare that this thesis entitled “**Design and analysis of diesel exhaust after-treatment for heavy-duty vehicle emission control system in workshop**” is my own work and has not been submitted for the award of any academic degree, diploma or certificate in any other university. All sources of materials that are used for this thesis have been duly acknowledged through citation.

Obse Regasa Dechasa

Name of the student

Signature

Date

RECOMMENDATION

I, the advisor of this thesis, hereby certify that I have read the revised version of the thesis entitled “**Design and analysis of diesel exhaust after-treatment for heavy-duty vehicle emission control system in workshop**” prepared under my guidance by Obse Regasa Therefore, submitted in partial fulfillment of the requirements for Master of Science in Automotive Engineering. Therefore, we recommend the submission of the revised version of the thesis to the department following the applicable procedures.

Dr. Alemayehu Wakjira Huluka

Major Advisor

Signature

Date

ACKNOWLEDGMENT

I want to thank God first and foremost for his generosity, for the wisdom and bravery he gave me, for the blessings and protection I experienced while working on my thesis, and I also want to thank His mother. I would like to express my gratitude to Dr. Alemayehu Wakjira, my advisor, for his excellent effort in setting the foundation for my thesis. I now know how to carry out research and present the findings in an easily comprehensible manner thanks to him. It was truly an honor and a delight to work for him. Furthermore, I express my gratitude to Mr. Garibe Chukulu, a PhD candidate student, for his academic expertise, advice, during my master's program and thesis work. This job could not have been finished without your assistance. Lastly, I want to express my gratitude to my families and friends for their important support, guidance, and assistance.

TABLE OF CONTENTS

DECLARATION	i
RECOMMENDATION	ii
APPROVAL	iii
ACKNOWLEDGMENT	iv
LIST OF FIGURES	ix
LIST OF TABLES.....	xi
ACRONYMS.....	xii
ABSTRACT	xiii
CHAPTER ONE.....	2
1. INTRODUCTION.....	2
1.1. Background of study.....	2
1.2. Statement of problem	4
1.3. Objectives	4
1.3.1. General Objective	4
1.3.2. Specific Objectives	4
1.4. Significance of study	5
1.5. Scope of the study	5
1.6. Research Outline.....	6
CHAPTER TWO.....	7
2. LITERATURE REVIEW	7
2.1. Introduction	7
VOCs Treatment Techniques	7
2.7.1. Technology of Catalytic combustion treatment.....	7
2.8. Wet scrubber for stationary	8
2.9. Local exhaust ventilation as a control mechanism.....	8
2.10. Refining and treating industrial waste gas.....	9
2.10.1. Composition of pollutant in flue gas	9
2.11. NOx purification technology for power plant and automotive industrial process	9
2.12. Health and Pollution Risks at Vehicle Repair Workshops.....	11
2.13. Respiratory health and Occupational exposure in small scale enterprise.....	11
2.14. Protecting garage workers	12
2.15. Construction and supervision of vehicle maintenance workshop	12

2.16.	Diagnose Faults through Exhaust Gas Color.....	12
2.17.	Simple approach for evaluating exposure	13
2.18.	Catalytic convertor diesel engine emission control methods	13
2.18.1.	Two-way.....	14
2.18.2.	Three-way.....	14
2.18.3.	Four-way	14
2.19.	Muffler and SRC for heavy duty truck.....	15
2.20.	Emission from heavy-duty vehicles	16
2.22.	Summary from Literature Survey.....	17
2.22.1.	Research Gap.....	18
CHAPTER THREE		19
3.	MATERIALS AND METHODS	19
3.1.	Introduction	19
3.2.	Materials	19
3.2.1.	ANSYS FLUENT Simulations:	19
3.2.2.	CHEMKIN Simulations	19
3.2.2.1.	Analysis and plot on CHEMKIN	20
3.3.	MATLAB/Simulink:	20
3.4.	Methods and methodology	21
3.5.	Data collection methods	22
3.5.1.	Original primary data	22
3.5.2.	Secondary data	22
3.7.	Catalytic convertor design calculation	23
3.7.1.	Shape of emission reduction device.....	23
3.7.2.	Space velocity	24
3.8.	Hose Selection	29
3.8.1.	Exhaust Pipe Size Estimate.....	30
3.9.	Design of gas inlet compartment tank	31
3.10.	Design of the multiple cylindrical pipe	32
3.10.1.	Material selection	33
3.10.2.	Circumferential.....	33
3.10.3.	Longitudinal Stress.....	34
3.10.4.	Steady Heat Conduction for circular pipe	35

3.10.5. Temperature Drop inside the tank.....	36
3.11. MATHLAB/Simulink to keep constant tank temperature.....	36
3.11.1. Heat gain formula.....	37
3.11.2. Heat Loss formula.....	38
3.11.3. Heater.....	39
3.11.4. Thermostat.....	39
3.11.5. Model of Tank.....	40
3.11.6. Integrate Tank, thermostat and heater.....	41
3.12. Single pipe with divergent cover.....	41
3.12.1. Water pump selection.....	42
3.13. Electrical fan selection.....	43
3.15. Mesh independence test.....	46
3.15.1. 2D model for combustion chamber simulation analysis.....	49
3.15.2. Boundary condition and possible assumption.....	50
3.15.3. ANSYS fluent meshing watertight (polyhedral mesh).....	51
3.16. Engine exhaust-after-treatment with a transient inlet flow.....	54
3.16.1. Project setup.....	54
3.16.2. Configuration of reactor.....	56
3.16.3. Engine-out.....	58
3.16.4. Solver panel.....	59
3.17. Catalyst selection.....	59
3.17.1. Catalyst.....	59
3.17.2. Substrate.....	59
3.17.3. Catalytic coating material (washcoat).....	60
3.18. Temperature range of catalytic convertor.....	61
3.19. Water cooling through single pipe.....	62
3.19.1. Newton cooling law.....	63
CHAPTER FOUR.....	65
4. RESULTS AND DISCUSSIONS.....	65
4.1. . Results from ANSYS 2023 R1 fluent reaction.....	65
4.2. Cylindrical multiple pipe.....	69
4.3. Catalytic convertor.....	75
4.4. The temperature versus time variation:.....	76

4.5.	Oxygen concentration (in mass-fraction)	77
4.6.	Nitrogen concentration (in mass fraction)	79
4.7.	CO ₂ concentration (mass fraction)	79
4.8.	CO concentration (mass fraction).....	80
4.9.	NO _x concentration (in mass-flow)	81
4.10.	Concentration of HC (mass fraction).....	82
4.11.	Inlet flow rate of engine out	85
4.12.	Verification.....	87
CHAPTER FIVE		89
5.	CONCLUSION AND RECOMMENDATION	89
5.1.	Conclusion.....	89
5.2.	Recommendation	90
5.3.	Future work	90
REFERENCES		91
APPENDIX I: Engine-out data for Chemkin		xv
APPENDIX II: Result value from design calculation		xvi
APPENDIX III: Full assembly design.....		xvii
APPENDIX IV: Data from Chemkin inlet engine out and after treatment at transient ...		xvii

LIST OF FIGURES

Figure 2-1: Classification of VOCs end processing technologies	7
Figure 2-2: Wet scrubbing diagram.....	8
Figure 2-3: Basic local exhaust ventilation system	9
Figure 2-4: Post and pre combustion NO _x removal technologies.....	10
Figure 2-5: Schematic of the SNCR process	11
Figure 2-6: Basic catalytic convertor	13
Figure 2-7: Three-way catalytic convertor	14
Figure 2-8: Diesel engine emission control technology	15
Figure 2-9: SCR system.....	16
Figure 3-1: methodology	21
Figure 3-2: Sinotruk HOWO WD615, 69,336HP	22
Figure 3-3: Heat conduction through a plane wall	35
Figure 3-4: 3D of cooling pipe where water circulate through	36
Figure 3-5: Heater modeling and response time.....	39
Figure 3-6: Thermostat model	40
Figure 3-7: Total heat gain and heat lose for tank temperature.....	41
Figure 3-8: Integrate Tank, Heater and Thermostat	41
Figure 3-9: Pipe with divergent cover	42
Figure 3-10: Water pump	43
Figure 3-11: (a) Fan assembled before refrigerant box, (b) fan assembled after refrigerant box	45
Figure 3-12: Single refrigerant liquid pack	45
Figure 3-13: 2D model of combustion mesh	47
Figure 3-14: Velocity verses number of element	48
Figure 3-15: 2D model of combustion chamber.....	49
Figure 3-16: Polyhedral mash multiple cylindrical pipe	53
Figure 3-17: Surface reaction on 3-way catalyst	54
Figure 3-18: Perfectly-stirred reactor model (PSR).	57
Figure 3-19: C1_PSR (psr_after_treatment) (C1)	58
Figure 3-20: Conversion efficiency for CO and HC as a function of temperature	62
Figure 3-21: Temperature verses time.....	64
Figure 4-1: Contour static temperature.....	65

Figure 4-2: Contour Pollutant NO (thermal or prompt)	66
Figure 4-3: Contour Mass fraction of C ₁₀ H ₂₂	66
Figure 4-4: Rate of soot	67
Figure 4-5: Contour mass fraction of O ₂ , N ₂ , and CO ₂	68
Figure 4-6: Mass fraction of C ₁₀ H ₂₂ , and soot	69
Figure 4-7: temperature drop due to cold circulating water	72
Figure 4-8: Pressure, temperature, turbulence kinetic energy and velocity distribution inside the multiple circular pipe	73
Figure 4-9: Temperature variation.....	75
Figure 4-10: Catalytic wall, boundary condition, pressure contour, velocity streamline....	76
Figure 4-11: Temperature versus time	77
Figure 4-12: Oxygen concentration (mass fraction).....	78
Figure 4-13: Concentration of nitrogen (mass fraction).....	79
Figure 4-14: CO ₂ concentration (mass fraction)	80
Figure 4-15: CO concentration (mass fraction).....	81
Figure 4-16: NO _x concentration (mass fraction).....	82
Figure 4-17: HC concentration (mass fraction).....	83
Figure 4-18: inlet flow rate of engine-out	85
Figure 4-19: engine-out, CO, NO, and HC	86

LIST OF TABLES

Table 3-1: Specification of WD615.69, 336hp.....	23
Table 3-2: Firing Order of 6- Cylinder Engine(James, 2018).....	26
Table 3-3: Recommended capacities.....	30
Table 3-4: Exhaust pipe size estimation.....	30
Table 3-5: Standard dimensions.....	32
Table 3-6: Aluminum property (Liu, 2020).....	33
Table 3-7. Standard table for water pump selection.....	43
Table 3-8: number of element versus velocity.....	48
Table 3-9: Refinement ratio.....	48
Table 3-10: Grid independence index value.....	49
Table 3-11: Boundary Conditions and related input values.....	51
Table 3-12: Boundary condition.....	53
Table 3-13: P _{sr} -after-treatment input parameter.....	56
Table 3-14: Temperature range for specific condition in a catalytic convertor adapted.....	62
Table 3-15: Time based temperature variation.....	64
Table 4-1: Average mass fraction at combustion chamber outlet.....	68
Table 4-2: Temperature inlet and outlet gas domain.....	70
Table 4-3: Percentage Conversion of CO.....	83
Table 4-4: Percentage Conversion of NO.....	84
Table 4-5: Percentage Conversion of UHC.....	84
Table 4-6: Overall Average mass-fraction.....	87

ACRONYMS

IARC	International agency for research
Psr	perfectly-stirred reactor
AHP	Air Horsepower
FPM	Feet Per Minute,
CFM	Cubic feet meter
UHC	Unburned hydro carbon
MVRW	Motor vehicle repair workshop
GVWRs	gross vehicle weight ratings
WHO	World health organization
3D	Three dimensional (x,y,z)
DPF	Diesel particulate filter
EGR	Exhaust gas recirculation
VOCs	Volatile organic compounds
CAD	Computer aided design
MTTR	Mean time to repair
FWC	Four-way catalytic convertor
RH	Relative humidity
SCR	Selective catalytic reduction
DOC	Diesel oxidation catalyst

ABSTRACT

The growing number of vehicles on the road has led to a parallel expansion of auto repair workshops. However, the environmental impact of emissions from vehicle exhaust systems during maintenance procedures has often been overlooked. According to the World Health Organization, diesel engine is major contributor of six primary air pollutants comprise particle pollution, ground-level ozone, carbon monoxide, sulfur oxides, nitrogen oxides, and lead. Both prolonged and brief exposure to airborne toxicants yield varying toxicological consequences for humans, encompassing respiratory and cardiovascular ailments, neuropsychiatric complications, eye irritation, skin disorders, and enduring chronic illnesses like cancer. The study is a second-generation pollution reduction system used for workshop of heavy-duty vehicles. The primary objective is to mitigate air pollution by stabilizing the temperature of the catalytic converter. A finite element model was employed to evaluate the system's performance. Given the high temperatures generated by heavy-duty engines, multiple cooling pipes was designed to reduce the initial exhaust temperature of 1235K (962°C) to 919K (646°C) at an ambient water temperature of 292K. To maintain the optimal operating temperature range of 550-650°C for the catalytic converter, a mathematical model was developed using MATLAB/Simulink, incorporating a thermostat and heater as temperature controllers. Additionally, a 2D model of the HOWO Sino-truck WD615.69, 336HP combustion chamber was designed to obtain real engine-out data on ANSYS. The emission reduction reactions was studied using the "psr_after treatment.ckprj" project file from the CHEMKIN sample library, with a focus on the surface reaction mechanism for catalytic conversions of NO_x, CO, and unburnt hydrocarbons (UHCs) using a Platinum (Pt) three-way catalyst. The model demonstrated significant reductions in emissions, with CO decreased by 83.3%, NO_x by 51%, and UHCs by 60.08%, while also contributing 67.6% of CO₂ and 30.7% of O₂ to the surrounding workshop environment. This research provides a comprehensive solution to address the environmental concerns associated with vehicle maintenance in auto repair workshops, contributing to improved air quality and reduced health risks for workers and local communities.

Keywords: vehicle emission, after-treatment, heater, diesel exhaust, catalytic convertor.

CHAPTER ONE

1. INTRODUCTION

1.1. Background of study

Diesel-powered heavy-duty vehicles are widely used in various industries, including transportation, construction, and mining. While these vehicles provide reliable performance and efficiency, their exhaust emissions can have significant environmental and health impacts, particularly in enclosed workshop environments where maintenance and repair activities take place.

The primary pollutants of concern from diesel exhaust classified into two groups, invisible emissions and visible emissions. Like, nitrogen oxides (NO_x), carbon monoxide (CO), hydrocarbons (HC), and various other harmful compounds are invisible and Visible emissions consist of soot, smoke (carbon particles), and particulates. The accumulation of these emissions in the confined workshop spaces can expose workers to elevated levels of air pollution, leading to respiratory issues, cardiovascular problems, and other health concerns.

To address this challenge, effective exhaust after-treatment systems have become increasingly important for heavy-duty vehicle maintenance workshops. These systems aim to reduce the emission of pollutants before they are released into the workshop environment, thereby improving air quality and ensuring a safer and more comfortable working condition for the technicians and staff.

Existing after-treatment technologies, such as diesel oxidation catalysts (DOCs), selective catalytic reduction (SCR) systems, and diesel particulate filters (DPFs), have demonstrated their effectiveness in reducing emissions from heavy-duty vehicles. However, the integration and optimization of these technologies within the specific context of workshop environments, considering factors like space constraints, noise levels, and maintenance requirements, warrant further investigation.

Additionally, the emergence of alternative fuels and lean-burn combustion technologies for heavy-duty engines presents new opportunities to explore their impact on exhaust emissions and the subsequent design of after-treatment systems. Understanding the emission characteristics of these advanced combustion strategies and alternative fuels can lead to the development of more comprehensive and tailored solutions for workshop environments.

(Guo & Wang, 2018).

Automotive repair businesses provide a range of tasks associated with the upkeep and repair of automobiles, those activity produce waste material poses health risks and can harm the environment if not managed appropriately. Such businesses are subject to conventional norms for the control and prevention of potential environmental impacts in addition to government licensing requirements. But a lot of business owners are unaware of their responsibilities regarding environmental laws and permits (Dutra & Victório, 2020). A particular category of automotive repair service encompasses engine repair, bodywork correction, maintenance of oil supply systems, electrical system upkeep, tire balancing and repair, four-wheel alignment testing and adjustment, air conditioning servicing, sheet metal work, and touch-up painting. This range of services can produce various pollutants, including oil, wastewater, hazardous waste, exhaust emissions, and other byproducts. (Guo & Wang, 2018). Therefore the absence of regulation, supervision, and implementation of standards by relevant authorities makes occupational risk assessment in small-scale sectors high. The majority of workers in low-income nations lack formal education and take risks, leading to a significant increase in unlicensed and temporary garages. The majority work in jobs where they are constantly exposed putting their health at risk without their knowledge (Ataro et al., 2018). Maximum exposure those frequently found in vehicle repair workshops, traffic-heavy areas, and roadside locations such as petrol stations, bus stops, and pedestrians navigating roadsides. (Ahmad et al., 2016).

Over the past few decades, increasingly stricter pollution restrictions have applied to HDVs and HD engines. As a result, emissions from more recent diesel engines have decreased significantly over time. This includes selective catalytic reduction for reducing NO_x and diesel particle filters for reducing PM. Heavy motors are expected account for 10% PM also 24% NO_x, despite these notable reductions. Given that trucks only account for 8% of all motor vehicle greenhouse gas emissions (Tan et al., 2019).

This research aims to design and analyze a diesel exhaust after-treatment system that can effectively control emissions from heavy-duty vehicles during maintenance activities in workshop settings. By integrating advanced technologies and considering the unique operational and environmental factors of workshops, the system seeks to enhance air quality, worker safety, and environmental sustainability in these critical industrial facilities .According to polish law, the car store ran the risk of being negligent and of not following healthy advice. Therefore the installation of an exhaust extraction system is regarded as a

basic necessity in order to enhance working conditions and protect employees from dangerous exposure.

1.2. Statement of problem

Heavy-duty motors generate a blend of harmful gases and particles throughout the combustion procedure. Exposure to these toxic substances can lead to various respiratory issues, cardiovascular problems, and other health complications for the workshop staff. Moreover these discharges present a serious environmental problem and accumulation of these emissions in the work area can diminish the overall efficiency and productivity of the workers, as they may experience discomfort, fatigue, and reduced concentration due to the polluted atmosphere. The negative impact on worker health and well-being ultimately affects the quality and timeliness of the vehicle repair and maintenance services provided by these workshops.(Weitekamp et al., 2020).

Undeveloped country, Upkeep and repair tasks conducted by automotive mechanic operators and technicians fail to adhere to any of the regulations established by international organizations or the standards set by the Federal Ministry of Environment (Abutu Francis, 2018). Many local garages lack proper exhaust gas removal systems, exposing staff to harmful pollutants and compromising their health. Traditional methods like basic filtration and long, flexible hoses are often ineffective. These hoses can trap pollutants and create backpressure on the engine over time due to carbon buildup, further hindering performance and potentially causing damage on engine. Demanding environmental regulations for emission reduction are becoming increasingly common. To create a healthier and safer work environment for all, garages need to adopt more advanced exhaust gas removal solutions.

1.3. Objectives

1.3.1. General Objective

The general objective of this thesis is to design and analyze diesel exhaust after-treatment for heavy-duty vehicle emission control system for workshop.

1.3.2. Specific Objectives

The specific objectives are as follows:

- ✓ To design exhaust emissions treatment system for heavy-duty repair workshop.
- ✓ To model, three-way catalytic convertor, multiple cylindrical pipe and combustion chamber of WD615, 336hp, via the ANSYS for engine-out data
- ✓ To Model and simulate temperature variation control system on matlab/Simulink

- ✓ To Investigate and characterize exhaust gas flow on CHEMKIN, and reactions occurring within the after-treatment devices
- ✓ To compare performance of after-treatment device with the conventional how much exhaust gas converted

1.4. Significance of study

The significance of this thesis

- ✓ Environmental impact mitigation involves reducing harmful pollutants
- ✓ Improving the pollution phenomenon in heavy-duty vehicle repair workshops by reducing emissions
- ✓ Ensure a safer and healthier working environment for mechanics and maintenance staff.

1.5. Scope of the study

The extent of this investigation is centered on exhaust gas flow characteristics and reduction reactions under various engine maintenance circumstance and fault correction. Through the Chemkin-Pro software, mathematical modeling for temperature variation through the system on matlab/Simulink to understand and the temperature control within optimal requirement for system. The design and development of an effective catalytic converter system is a critical component of the study, with the aim of significantly reducing HC, CO, NO_x of engine exhaust. This aspect of the research was involve investigation into the catalytic surface reaction kinetics ,exploring the complex interplay between the catalyst formulations, influence of various condition, of exhaust gas and space velocity, on the overall efficiency and performance of the catalytic converter system.

As well as developing a diesel engine exhaust emission treatment system for heavy-duty vehicles in workshops capable of servicing three vehicles simultaneously. The system is workshop-specific and not intended for anchoring vehicles exceeding three at a time.

For understanding of the system's performance, each component, Modeled utilizing the ANSYS Fluent computational fluid dynamics (CFD) solver. Provide valuable insights into the complex fluid dynamics, heat transfer, and chemical reactions within the exhaust after-treatment system, by analyzing this data, can improve the design of the entire system for better performance.

Finally, a thorough analysis and presentation of the findings in a variety of formats, including tables, and graphs, was conclude off the research. This make it easier to understand system's

capabilities, the effectiveness of the emission control techniques, and the possibility of future improvements and practical application in heavy-duty vehicle applications.

1.6. Research Outline

Chapter 1: Introduction, Problem Statement where Outline the issue of harmful emissions and pollution from heavy-duty vehicle exhaust in auto repair workshops, Objectives of the Study Develop an effective exhaust gas management system to mitigate emissions in vehicle repair workshops Improve the working environment and safeguard the well-being of workshop personnel and Significance of the Study

Chapter 2: Literature Review, Review of existing literature on heavy-duty vehicle emissions and their impact Evaluation of previous studies and solutions related to exhaust gas reduction systems for workshops Identify gaps and limitations in current approaches

Chapter 3: Methodology, Description of the materials and methods used in the study detailed explanation of the design, development, and Design Calculations and Considerations, Detailed design calculations for the key components of the exhaust gas management system Thermal analysis, fluid dynamics, and emission reduction performance calculations Incorporation of safety, efficiency, and regulatory compliance considerations

Chapter 4: Results and discussion, Present the results of the system's performance evaluation Analyze the effectiveness of the proposed solution in reducing emissions and improving the working environment

Chapter 5: Conclusion and Recommendations, Summarize the key findings and achievements of the study discuss the limitations and potential areas for further research Provide recommendations for the implementation and adoption of the proposed exhaust gas management system in auto repair workshops. Finally References and Appendices, List of all the references cited in the thesis Inclusion of relevant supplementary information, such as data, drawings, or additional analyses, in the appendices

CHAPTER TWO

2. LITERATURE REVIEW

2.1. Introduction

The section, different related research works that have been done on similar problems have been gathered and reviewed to show the available knowledge and literature gaps. The scientific knowledge level that has been reached and the conclusions made by different scholars have been reviewed.

VOCs Treatment Techniques

There are two categories of industrial VOC tail-end treatment methods available today: destruction technology and recycling technology. Membrane separation, adsorption, adsorption, and condensation processes are examples of recycling technologies. Technologies for destruction include low-temperature plasma, combustion, photo-catalysis, and biodegradation. The gas atmosphere and other surroundings are more complicated during emission mechanism of industrial volatile organic compounds VOCs, poor treatment technology selection will lead to re-pollution and additional environmental harm (Tannous, 2024)

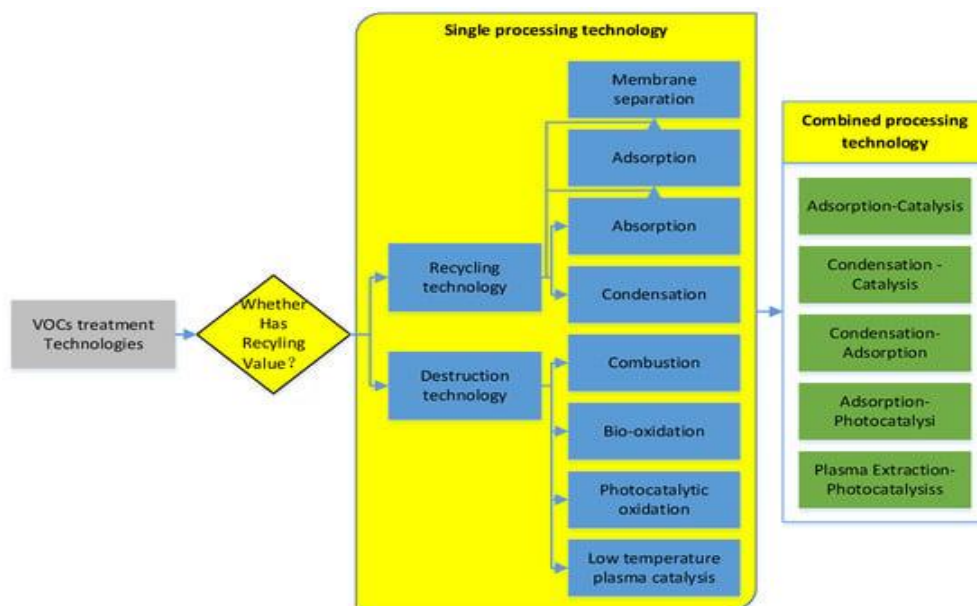


Figure 2-1: Classification of VOCs end processing technologies

2.7.1. Technology of Catalytic combustion treatment

The majority of the precious metals in the current catalysts are still Nano-scale, and their loading amounts range from 0.5 to 10%. As a result, certain catalysts are quite expensive and operate weakly catalytically. As a result, one of the challenges in environmental catalysis is the creation of low-loaded noble metal particle-supported catalysts for the effective

catalytic combustion of volatile organic compounds. Though the synergistic mechanism between the components is unknown, the catalytic performance of two-component or even multi-component active materials has improved significantly in numerous aspects when compared to single-component active materials. Under the assumption of the most efficient catalyst products can be synthesized by examining their mutual effects on particle size and dispersion degree of each other (K. Li & Luo, 2023).

2.8. Wet scrubber for stationary

Particles eliminated by a wet scrubber both acid gasses and PM. The diesel engine of an underground vehicle is linked to this scrubber in the exhaust gas stream within the dry particle filter and the combustion process. When exhaust gas enters the scrubber beneath the surface of the scrubbing liquid, the concentrations of some soluble particles and the temperature of the gas both drop. This process results in an increase in the relative humidity (RH) of the gas at the scrubber discharge. This high relative humidity restricts the downstream dry particle filter. Within the tests include those transient heat loss estimation, flow visualization, and heating. The transient heat loss estimation tests are used to evaluate the scrubber's steady-state heat loss. Conduction, convection, and radiation are some of the heat-loss tests that are compared and examined. The scrubber's heat loss is then calculated using the most accurate one (Abdulwahid, 2020).

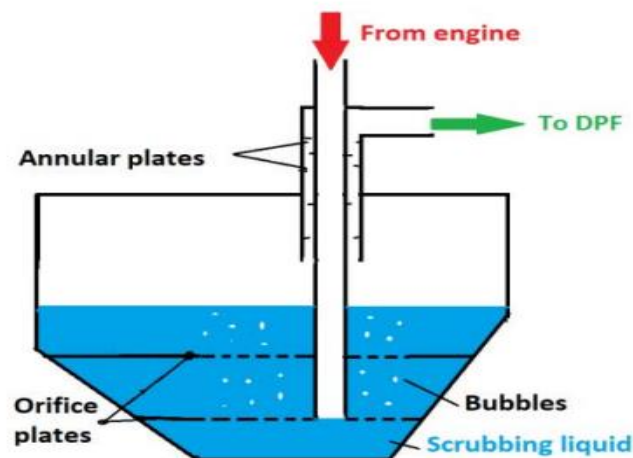


Figure 2-2: Wet scrubbing diagram

2.9. Local exhaust ventilation as a control mechanism

A number of potentially dangerous airborne pollutants, types of gases can be produced by welding and other heated processes like thermal cutting. Gases include metal vapors with manganese and hexavalent chromium, ozone, oxides of nitrogen, and carbon monoxide.

Welding comes in a lot of forms and is a widely used process in many different sectors. Inhaling welding fumes can result in chest tightness, coughing, and a dry, tickly throat. Blood and fluid can accumulate in the lungs as a result of Plasma-arc, metal inert gas (MIG), and tungsten inert gas (TIG) processes produce ozone gas. There is a common correlation between emissions from stainless steel and occupational asthma. Asthma is brought on by the chromium and nickel oxides found in stainless steel fume. Breathlessness, wheezing, and pressure in the chest are among the symptoms (Flynn & Susi, 2012).

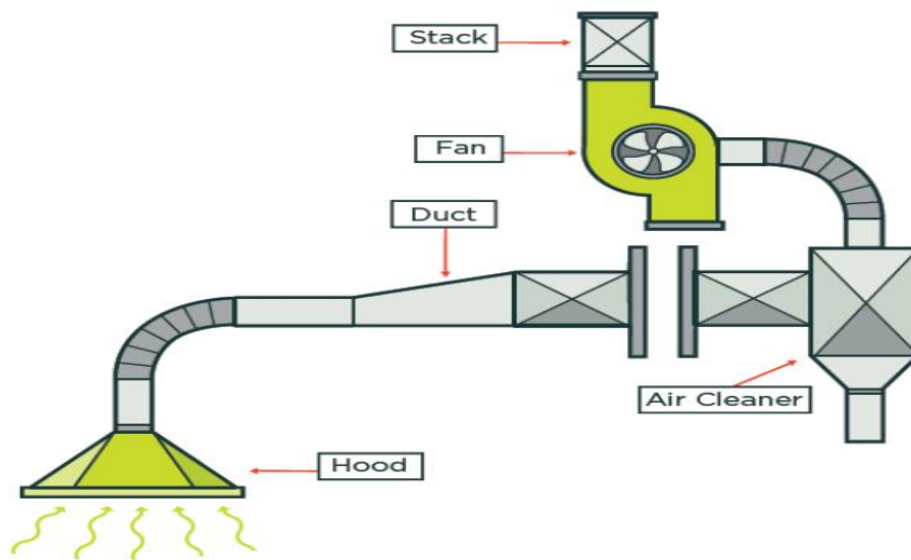


Figure 2-3: Basic local exhaust ventilation system

2.10. Refining and treating industrial waste gas

2.10.1. Composition of pollutant in flue gas

Four harmless elements, namely N_2 , O_2 , CO_2 , and H_2O , make up the majority of the volume of flue gas produced by waste incineration and so constitute its principal constituents. Dioxins and other left over organic compounds are mostly found in the flue gas, but there are also trace amounts of heavy metals like mercury and cadmium, as well as particles (PM_{2.5} and PM₁₀), strong adsorption acid gases (SO_2 , NO_2 , HCl , and HF), and other air pollutants due to the unpredictability of the waste type and combustion process.

(H. M. Li et al., 2020)

2.11. NO_x purification technology for power plant and automotive industrial process

The main pollutants generated by manufacturing facilities, power plants, and the burning of urban solid waste are particulate matter, nitrogen oxides, and sulfur oxides. (H. M. Li et al., 2020). The two primary forms of NO_x in flue gas are NO (90–95%) and NO_2 (5–10%). In addition to causing acid rain, fog, photochemical smog, depletion of ozone, and greenhouse

gas emissions, also lead to a number of environmental issues, including headaches, nausea, and irritation of the throat and eyes (Shan et al., 2021). The various Selective non-catalytic reduction, wet scrubbing, adsorption, electron beam, non-thermal plasma, and electrochemical reduction of NO_x are a few of the post-combustion techniques for removing NO_x. Selective catalytic reduction involves using a variety of reducing reagents, such as ammonia, hydrogen, hydrocarbons, and carbon monoxide. Based on the different stages of combustion, NO_x control techniques can be grouped into three groups: pre-combustion, in-combustion, and post-combustion. (Gholami et al., 2020).

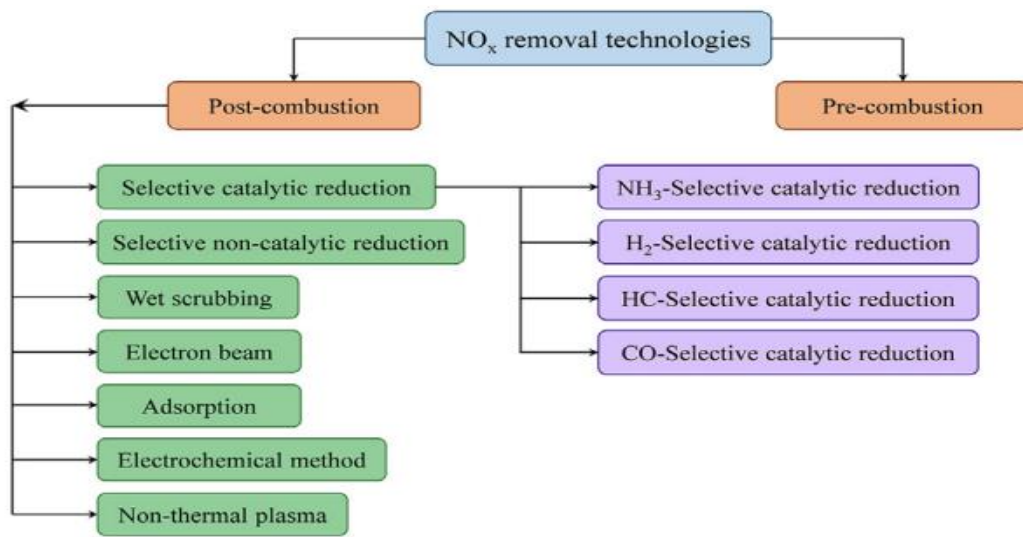


Figure 2-4: Post and pre combustion NO_x removal technologies

One method of post-NO_x reduction is selective non-catalytic reduction (SNCR), which uses high temperatures to drive the process rather than a catalyst. NO_x is chemically reduced to provide the basis for SNCR. By injecting a reduction reagent into hot flue gas, it reacts with the gas and produces H₂O and N₂ vapor. In terms of chamber design, fuel type, and atomizer geometry and performance, there are differences in the NO_x reduction performance and temperature window. The 850 °C to 1100 °C temperature range is where SNCR functions effectively (Pronobis et al., 2017). Reducing agent chemicals have a significant influence on the chemical pathways for NO_x reduction via SNCR. The common SNCR reagents include cyanuric acid, urea, and ammonia. NH₂ radicals are created when ammonia undergoes NH₃ decomposition. Two products of the reaction between NO and NH₂ are N₂ and H₂O. First, (CHNO)₃ must break down to isocyanic (HNCO) acid in order to produce cyanuric acid. NH₂ and NCO are produced when HNCO reacts with H and OH radicals. N₂O and CO are produced when NO interacts with NCO, a significant intermediate. Depending on the temperature, N₂O can either break down into N₂ or be eliminated as a byproduct. The

removal of NO_x is determined by several variables, including the type of reagents utilized, the amount and composition of chemicals and additions (such as hydrogen and hydrogen peroxide), temperature, length of stay, molar ratio of NH_3/NO , and flue gas O_2 concentration. Reduced nitrogen oxide levels are significantly impacted by the way NH_3 and flue gas are mixed. Since NH_3 is present in large quantities and the reaction rate is sluggish, NH_2 radicals do not react with NO_x at lower temperatures. NH_3 slip increases as a result of a decrease in NO_x reduction at higher temperatures, nitrogen dioxide radicals and O_2 react, creating NO_x rather than removing it. (Blejchař et al., 2018).

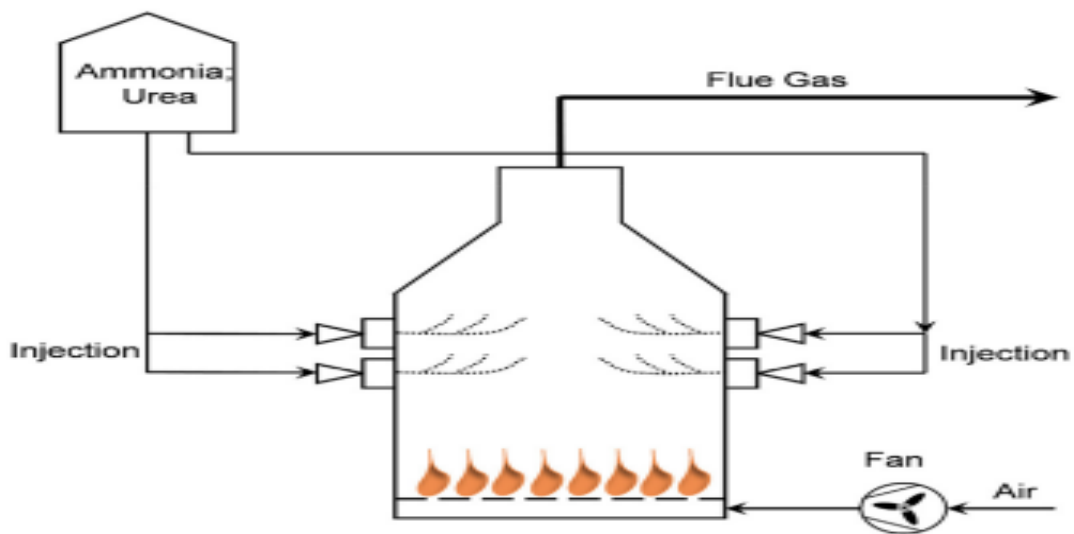


Figure 2-5: Schematic of the SNCR process

2.12. Health and Pollution Risks at Vehicle Repair Workshops

Health Risks and Pollution in Auto Repair Shops Recently, cars have become an essential part of modern life; the MVRW sector, which includes small and medium-sized businesses, is categorized as an unorganized sector. MVRW workers are subject to a variety of dangers, including those related to their physical health, accidents, chemicals, biology, and ergonomics, as well as exposure to dangerous pollutants like benzene, PAHs, VOCs, heavy metals, PM, NO_x , and SO_x . Every year, more than 270 million incidents and 2 million injuries are reported worldwide. Moreover, some severe collisions leave victims disabled; they may also lose bodily parts or experience problems with their musculoskeletal system, reproductive system, skin, or nervous system (Parrish & Stockwell, 2015).

2.13. Respiratory health and Occupational exposure in small scale enterprise

Urban air pollution primarily caused due to NO_x , SO_x , VOC_s , all over worldwide due to rapid urbanization, automobiles, and industrial activity.(Chawla & Lavania, 2008). Some task such as, such as welding, painting, car maintenance, and repair, include working with

fumes, vapors, gasses, exhausts, and dust. possessing several related to small-scale enterprises whose employees are frequently exposed to such work-related exposures (Ahmad & Balkhyour, 2020).

Urban air pollution affects general public's health, also workers, particularly employed in roadside small-scale industries and environments with heavy traffic. Because it is released at a height that is close to breathing and exposes people to the greatest amount of pollution, vehicle exhaust is the worst kind of exhaust (Ahmad & Balkhyour, 2020).

2.14. Protecting garage workers

According to investigator Gary Warner, the manager at Auto Extract Systems, located in Leigh, Greater Manchester, smaller garages typically choose exhaust extraction reels that are fixed to the wall or ceiling. In order to capture at-source pollutants and prevent them from dispersing into the atmosphere, he investigate that ideally each bay would have a car exhaust extraction system with a fan. Small or backstreet garages frequently don't want to invest in solutions and will just open the doors, but a manufacturer's dealership will install the necessary equipment. It is acceptable during the summer, but in the winter, a reputable employer would use an exhaust extraction system, turn on (Swallow, 2023).

2.15. Construction and supervision of vehicle maintenance workshop

The significance of workshop management, vehicle maintenance, and workshop layout in lowering emission levels and enhancing automotive maintenance operations. Depending on Mean Time TO Repair (MTTR), Possibilities for different workshop layouts are evaluated. Enhancing the structure of maintenance workshops and management techniques, enhance the quality of maintenance operations, and shorten the mean time between failures. When the layout is well-designed and adaptable, the system improves and the mean time between failures (MTTR) drops. Costs and maintenance quality are also significant considerations (Almomani & Almutairi, 2020).

2.16. Diagnose Faults through Exhaust Gas Color

The engine exhaust pipe makes abnormal noises and releases black smoke when the truck is operating. Due to The mixture's excessive richness and incomplete combustion are the primary causes of black smoke. The car engine can be overloaded, the cylinder pressure might be low, the engine temperature might be too low, the air filter element might be clogged, some cylinders might not be operating, or the ignition might be turned on too late. The main reason that exhaust pipe emits blue smoke or gray smoke, is because of oil enters to the cylinder combustion chamber to participate in combustion. When the oil enters the

cylinder and evaporates into blue after heating, the oil and gas are discharged out of the cylinder together with the exhaust gas, and the blue flue gas will be seen at the exhaust pipe. White smoke is discharged from the exhaust pipe. The cause is a large amount of white smoke is discharged from the air pipe. Large amount of water vapor and white smoke are discharged from the exhaust pipe, and there are water droplets at the outlet of the exhaust pipe. Due to the coolant jumps into the cylinder or the water vapor formed by water in gasoline (Denton, 2020).

2.17. Simple approach for evaluating exposure

Personal portable monitor, very sensitive instrument designed to identify small amounts of pollution. By choosing a small sample size, personal monitoring techniques are utilized to quantify exposures across huge populations. Various studies indicate that this method is a simple way to measure SO₂, CO, NO_x, formaldehyde, organic vapors, and respirable particles (Ahmad et al., 2016a).

2.18. Catalytic convertor diesel engine emission control methods

Most present cars use an internal combustion engine, which can emit less pollution when operated through a catalytic converter. To transform toxic byproducts such as nitrogen oxides, carbon monoxide, and gasoline hydrocarbons into less dangerous materials like Carbon dioxide, water vapor, and nitrogen gas, exhaust systems employ catalytic converters as a site for oxidation and reduction (Guoquan et al., 2021).

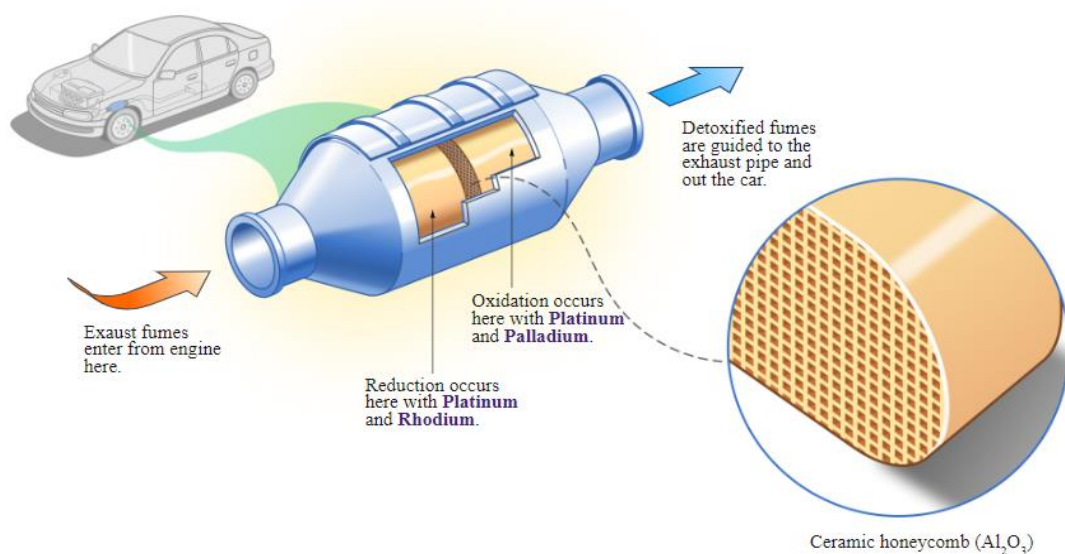


Figure 2-6: Basic catalytic convertor

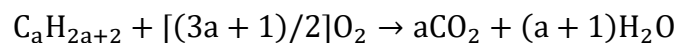
2.18.1. Two-way

Used on diesel engines to decrease HC and CO emissions is produced when fuel is partially consumed about. In two-way catalytic converter typically, two tasks are carried out at once. The first is the conversion of carbon dioxide from carbon monoxide. Oxidation is an additional one. unburned hydrocarbon to carbon dioxide and water (Gupta et al., 2017).

CO Oxidation of two CO₂



HC Oxidation to CO₂ and H₂O



2.18.2. Three-way

Addition to oxidation a reduction catalyst to regulate using a catalytic converter NO_x can be employed. The oxidation system's outflow is where the reduction catalyst has been fixed. Catalytic reduction is the initial step in the process. Nitrogen oxide emissions are decreased with the usage of rhodium and platinum. The catalyst releases O_2 . When it comes into contact with these molecules, separating and holding onto the nitrogen atom in the process. In the catalyst, the nitrogen atoms form connections with additional nitrogen atoms that are trapped, generating (Gupta et al., 2017).

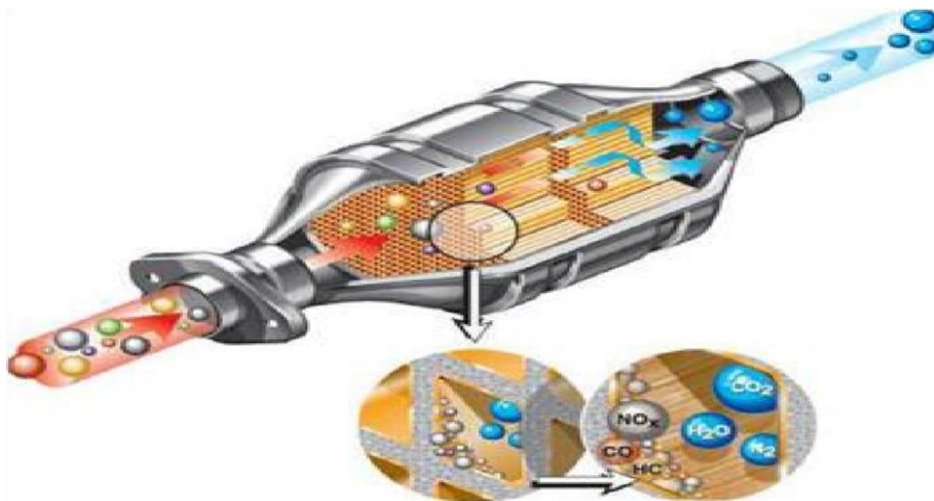


Figure 2-7: Three-way catalytic convertor

2.18.3. Four-way

A recent study to regulate emissions from diesel engines used a four-way catalytic system. It combines several different pollution control techniques into one small device. Nitrogen oxides, particulate matter, hydrocarbons, and carbon monoxide released by diesel engines are all simultaneously removed by the FWC system through the employment of a

combination of oxidation and reduction catalysts. The CO and HC are oxidized to H_2O and CO_2 by the DOC, which is composed of Pt and Al_2O_3 on a monolith. The DPF collects and holds soot particles with a 99% effectiveness rate in trapping. The SCR process uses the urea solution as a reducing agent to change NO_x into N_2 and H_2O (Trivedi & Prasad, 2018).

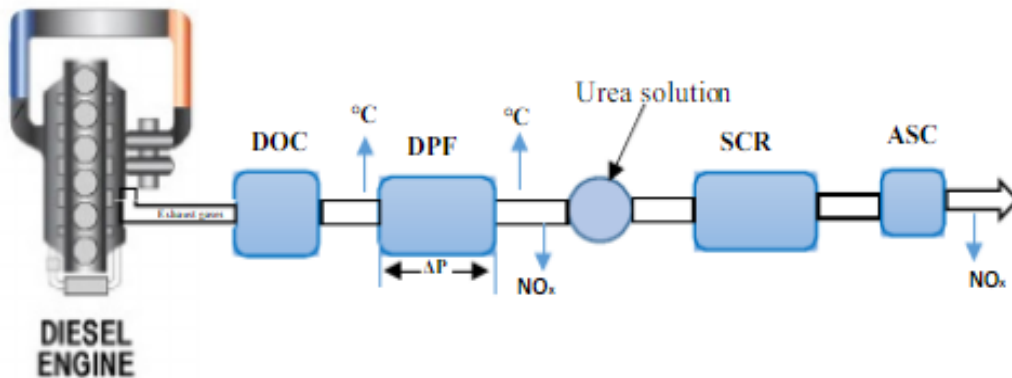


Figure 2-8: Diesel engine emission control technology

2.19. Muffler and SRC for heavy duty truck

In addition to lowering NO_x , the combined SCR catalytic and muffler systems also lower the noise of truck. This is small in size, has a compact structure, and is simple to install. Thus, it's been applied broadly. However, there hasn't been much through research done on the integrated systems' acoustic performance, pressure loss, or NO_x conversion efficiency.

As illustrated in Figure 2.10, the SCR system is comprised of the non-heated urea pipe, the control sensor, the wiring, the urea box, the muffler with a catalytic converter, and the urea supply measurement and control system, investigator used a perforated tube, and the cavity of the muffler was to be modeled using the equivalent acoustic impedance technique. One way to limit the low-frequency energy sound is to change the level suddenly. The medium-high frequency sound energy can be eliminated by using perforated pipes of various sizes. (Chen & Zhang, 2013).

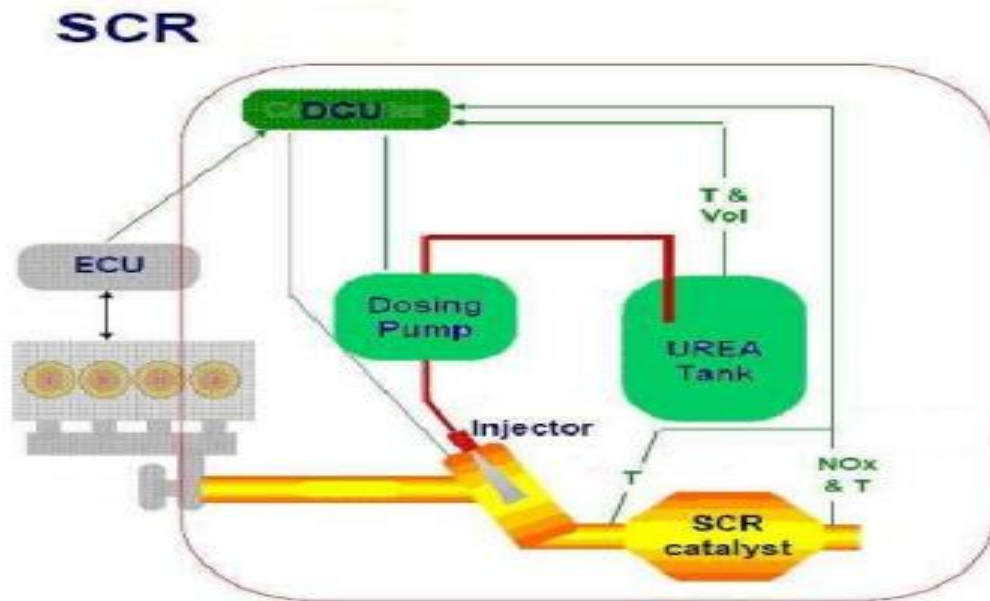


Figure 2-9: SCR system

2.20. Emission from heavy-duty vehicles

As to the EPA assessment, heavy-duty truck pollution is a major cause of poor air quality and health nationwide, particularly in underprivileged and stressed neighborhoods. These cars are the main source of mobile source emissions of particulate matter, carbon monoxide, and air toxics, as well as NO_x (which reacting in the atmosphere, generate smog, or ground-level ozone) (about 32% of 2017, the most current inventory available). Furthermore, 456.6 million metric CO_2 tons were released by medium and heavy-duty vehicles in 2019, accounting for approximately 25% of the transportation sector's total CO_2 the EPA's Inventory of U.S. Greenhouse Gas Emissions, which tracks emissions in the country (Gas & Standards, 2023).

2.21. ANSYS Software governing equation

The governing equation, used for this paper on ANSYS fluent in order to achieve the required result. Governing equations solved by the software for this study is (Vaghela et al., 2024).

$$continuity = \rho \left(\frac{\partial U_j}{\partial X_j} \right) = 0 \quad (2.1)$$

$$momentum = \rho \frac{\partial}{\partial x_j} (U_j U_i) = - \frac{\partial P + \partial \tau_{ij}}{\partial x_i} + S_{cor} + S_{cf g} \quad (2.2)$$

$$energy = \frac{\partial(\rho E)}{\partial t} + \nabla(\rho u E) = \nabla(k \nabla T) + \Sigma(h_{i_{mi}}) + Q \quad (2.3)$$

2.22. Summary from Literature Survey

In emission control, the overall capacity of the device is determined by cleaning capacity of pollutant from engine-out to the environment. Where this cleaning capacity depends on different factors, many researchers try to improve those factors and achieve the required reduction. At present there are different pollution control ways: VOCs Treatment Techniques, wet scrubber, selective catalytic converter.

- ✓ The SCR method's high efficiency, low operating costs, and relatively easy installation make it the perfect solution for removing NO_x from flue gas. However, there are still certain drawbacks to this approach, including expensive limited catalytic life, high operating temperature, here high temperature demand Low efficiency, the requirement for downstream cleaning equipment, and other disadvantages of SNCR and restricted application for feeds with low NO_x concentrations (Gholami et al., 2020)
- ✓ A wet scrubber: A wet scrubber is designed to eliminate (PM) and acid gases from exhaust gases. In this system, the exhaust gas is introduced into the scrubber below the liquid surface, leading to a decrease in gas temperature and the concentration of soluble particles. Wet scrubbers are widely utilized in research studies as they offer a straightforward and comprehensible method for evaluating gas cleaning efficiency of workshop. However Wet scrubbers can have a high-pressure drop, which requires more energy-intensive fans and blowers, also generate wastewater that requires proper handling and disposal, which can be an additional operational challenge, Even if no chemicals are used, the dissolved gases in the scrubber liquid can make the effluent unsuitable for direct discharge to public waters. and become clogged with accumulated particulate matter, especially if the inlet gas has high particulate concentrations (Abdulwahid, 2020).
- ✓ VOCs Treatment Techniques: is the basis for pollution control technique, which used improved capacity by using destruction technology and recycling technology as the research objective. Membrane separation, absorption, adsorption, and condensation processes are examples of recycling technologies. Technologies for destruction include low-temperature plasma, combustion, photo-catalysis, and biodegradation. However, harm Re-pollution Risk, Improper technology selection can lead to incomplete VOC removal or even the creation of secondary pollutants during the

treatment process. This can result in re-pollution and negate the purpose of the treatment system (Kamp et al., 2017)

2.22.1. Research Gap

Where Numerous research studies worldwide have analyzed the issue of exhaust emissions from heavy-duty vehicles and the effectiveness of various control systems for huge repair workshop, while these studies have provided valuable insights, but the necessary level of emission reduction is still an open question as long as poor treatment technology lead to re-pollution with lack of sufficient temperature and additional environmental harm due to waste byproduct where requires further methods.

Extensive research has been conducted on various emission control devices and their mechanisms for transforming pollutants. These mechanisms typically involve oxidation and reduction reactions within the catalyst, while the importance of catalytic converter efficiency is well understood, existing research often overlooks the critical role of temperature control in maintaining optimal performance. Literature suggests a focus on the mechanisms within the converter itself, with less emphasis on maintaining a consistent operating temperature range. This research gap presents an opportunity to investigate the effectiveness of incorporating a temperature control system utilizing a thermostat and heater within the exhaust system. Improved Conversion Efficiency and Extended Converter Lifespan, as long as Temperature fluctuations can stress the catalyst, potentially leading to premature degradation.

CHAPTER THREE

3. MATERIALS AND METHODS

3.1. Introduction

Thorough out literature survey helped in the proper choice of working materials, research methodology, and simulation software. In this chapter sources and techniques employed in the model and analysis was be discussed below.

3.2. Materials

3.2.1. ANSYS FLUENT Simulations:

2D modeling of Combustion Chamber WD615.69, 336HP on (solid work) edit on ansys space claim. These models captured the geometry and characteristics of the chamber, allowing simulate real-world engine operation.

Engine-Out Data Generation, ANSYS FLUENT simulations provided critical engine-out data for subsequent analysis. This data encompassed crucial parameters within the combustion chamber, including: Temperature Contours, Detailed maps depicting the temperature distribution throughout the chamber. This information is vital for understanding heat transfer and high-Temperature Regions. Pressure Distributions, Variations in pressure across the chamber, which influence fluid flow and engine performance. Velocity Profiles, The speed and direction of the flowing gases within the chamber, essential for analyzing combustion efficiency and turbulence. Species Concentrations, In addition to the above, ANSYS FLUENT simulations provided data on the mass fractions or mole fractions of various chemical species present in the exhaust gases after combustion. This data is crucial for understanding the composition of the engine's exhaust and potential pollutant formation. Analyzing these species concentrations allows you to identify the presence and concentration of pollutants like, CO, NO_x, and HC in the exhaust. Evaluate efficiency of the combustion process and identify for improvement. Provide valuable input data for subsequent simulations using CHEMKIN-PRO.

3.2.2. CHEMKIN Simulations

After the critical engine-out data is exported from ANSYS FLUENT, CHEMKIN takes center stage. This powerful software, specializing in chemical kinetics, transforms the raw data into valuable insights about the chemical composition of the engine's exhaust.

The data from ANSYS FLUENT, likely including temperature, pressure, and species concentrations, serves as the foundation for CHEMKIN's analysis. This data provides a

representation of the conditions within the combustion chamber after the engine has completed a combustion cycle.

Chemical Equilibrium Calculations: CHEMKIN's core functionality lies in its ability to perform chemical equilibrium calculations. Based on the engine-out data and the known chemical properties of the fuel and air entering the engine, CHEMKIN predicts the most likely stable combination of chemical species (molecules) present in the exhaust gases.

3.2.2.1. Analysis and plot on CHEMKIN

Mass Fraction Analysis: Once CHEMKIN determines the most likely stable species, it calculates the mass percentage of every species in the mixture of exhaust gases. The fraction of mass is the mass of a specific species divided by the mixture's total mass. By analyzing these mass fractions, Quantify the amount of pollutants like NO_x, CO and HC after-treatment.

3.3. MATLAB/Simulink:

Model, the thermostat and heater together form a control system designed to maintain a constant temperature within a tank.

- ✓ **Thermostat:** This acts as a sensor and a switch. It continuously monitors the heat of gas in the tank. When it decrease below a predefined set-point (desired temperature), the thermostat activates the heater. Conversely, and as it increase above the set-point, the thermostat deactivates the heater.
- ✓ **Heater:** This component adds heat to the liquid in the tank. When activated by the thermostat, the heater increases the temperature of the liquid until it reaches the desired amount. Once the point is reached, the heater is turned off by the thermostat.

By working together, the thermostat and heater create open-loop control system. The thermostat provides feedback on the current temperature, and the heater adjusts the heat input based on this feedback. This feedback loop ensures the temperature stays within a desired range, preventing the liquid from becoming too hot or too cold. Therefore Simulink allows to model and simulate the behavior of the thermostat and heater system before implementing it in a real setup. This helps to, Verify that the control system functions as expected. Fine-tune the set-point and control parameters (e.g., how much the heater increases the temperature) for optimal performance. Simulink can generate plots that show how the temperature in the tank changes over time and how the thermostat and heater interact to maintain the desired temperature.

3.4. Methods and methodology

Several procedures or methods was been used in order to accomplish the general and focused goals. Figure below provides a summary and list of all the process steps, it shows the procedures followed to complete the research.

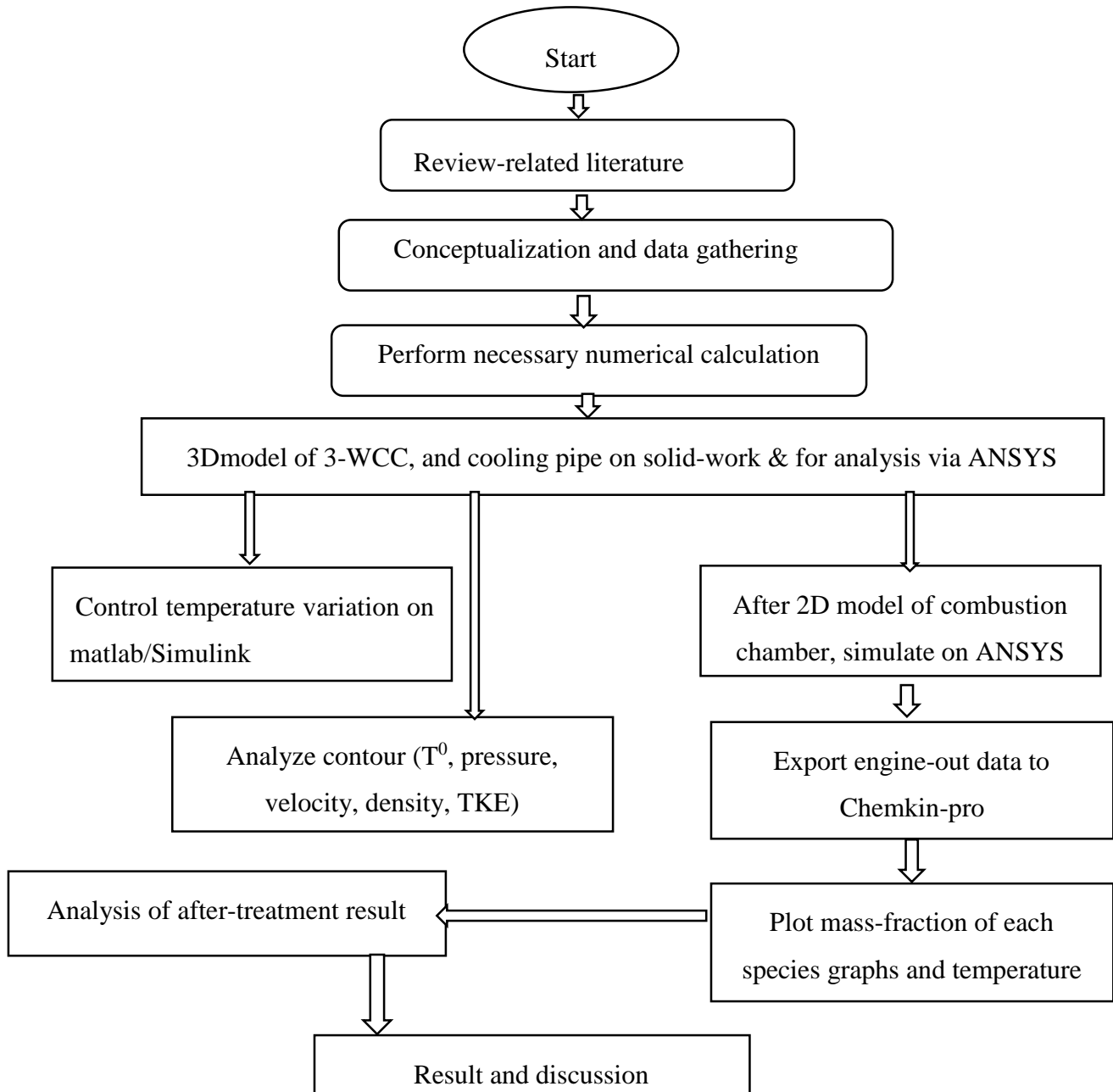


Figure 3-1: methodology

3.5. Data collection methods

Primary and secondary data collection are the two categories of data collection techniques used in this study. Primary and secondary data were gathered from the sources that were accessible and arranged appropriately.

3.5.1. Original primary data

Primary data were the original data collected by observation at different garages, took different measurements, interview with lab workers (mechanics) and workshop /Garage/ stake holders at their work place, visiting various governmental heavy vehicle workshops in Adama, (Bekelcha and, trans)

3.5.2. Secondary data

The data were available in the as books, published /unpublished papers, internets (Wikipedia, etc.) and websites. Searching for different related literatures about the drawbacks effects of diesel engine exhaust emission of heavy duty vehicles in workshop and how to solve such kinds of problem in the workshop. Also find the right and appropriate methods and methodology that should be used to minimize the effect of diesel engine exhaust emissions of heavy duty vehicle in workshops. This work helps to identify the effect of diesel engine exhaust emissions from heavy duty vehicle in workshops on human and environmental health, in Ethiopia.

3.6. Heavy duty vehicle specification

Vehicle Type: Sinotruk Howo Wd615.69, 336 / 371 / 420Hp Euro-II

Ease of Selection: the selected track was highly operated in the area of study in larger quantity and frequently brought to the garage for easy to complex maintenance and overhaul.



Figure 3-2: Sinotruk HOWO WD615, 69,336HP

Table 3-1: Specification of WD615.69, 336hp

Serial	HOWO, Sino-truck WD615.69 EURO-II
Inlet-air type	Intercooling, Turbo-charging
Exhaust	9.726L
Rotating speed at rated, Max output	2200rpm, 247kw
Torque and HP	1350N/m, 336hp,
Rotating torque speed	1100 to 1600rpm
Consumption	≤191g/kwh
Type	4 _stroke, direct injection, cooler water,
Noise	≤98Db
Compressional	17:01
Bore and stroke	126 x 130mm
Oil capacity	23 liters
Oil pressure	420-550 (rate) / 120-250 (idle point)

3.7. Catalytic convertor design calculation

3.7.1. Shape of emission reduction device

The cylinder shape consideration is required when selection the shape of emission reduction device to ensure that it meets specific requirements and objectives. The cylinder shape chosen after careful consideration of various factors;

- ✓ Ease of fabrication: the cylinder shape is relatively easy to manufacture compared to more complex shape. It may involve simpler production techniques and require fewer manufacturing steps, resulting in cost and time saving.
- ✓ Minimum assembly time: the cylindrical shape might allow for efficient assembly processes, reducing the time required for putting the device together. This can contribute to improved productivity and faster production cycles.

- ✓ Rigidity: the cylinder shape often provides inherent structural rigidity, which can be beneficial for emission reduction device. Rigidity helps maintain the shape integrity, withstand operational stresses, and enhance overall durability.
- ✓ Easier maintenance: the cylindrical shape might facilitate easier maintenance procedures. It can potentially offer better accessibility to internal components, simplifying inspection, cleaning, and potential repairs. This can contribute to improved operational efficiency and reduced downtime.

By considering these factors and selecting the cylindrical shape, the aim is to optimize the fabrication process, assembly time, structural integrity, and maintenance aspects of emission reduction device.

3.7.2. Space velocity

Space velocity, also known as the flow rate of volume, is a quantify of how quickly the gas passes over chemical reactor relative to the reactor volume. It represent the percentage of the fluid's volume flow rate to the reactor's size. The space velocity is often expressed in units of inverse time, such as reciprocal hours or reciprocal seconds, indicating the number of reactor volumes of the fluid processed per unit time, it is also referred to a holding time or residence time, as it represents The duration needed for one reactor volume of fluid to be processed.

The volume of catalysts within the reactor plays a crucial role. The space velocity helps determine the efficiency of the catalysts by indicating the rate of gas is passing on the catalyst surface. An increased speed in space means that the gas is passing over the catalyst more quickly, allowing for faster reaction rates but potentially reducing the duration of the gas-catalyst interaction conversely, a lower space velocity provides a longer contact time between the fluid and catalyst, allowing for more through reaction processes but possibly reducing the overall reaction rate (Couper et al., 2012).

Assuming for single cylinder engine space velocity = 30,000 hr⁻¹

$$Sv = \frac{V_f}{C_v} \quad (4.1)$$

Where:

- ✓ Sv_ space velocity
- ✓ Vf_ volume flow rate
- ✓ Cv_ catalyst volume
- ✓ Swv_ swept volume

- ✓ Is_ Intake stroke per hour
- ✓ Fi_ firing interval
- ✓ Nc_ number of cylinder
- ✓ Ed_ engine displacement

$$S_v = S_{wv} * I_s \quad (4.2)$$

From equation (2) we have:

$$C_v = \frac{V_f}{S_v} \quad (4.3)$$

3.7.3. Shell _value

The cylindrical portion in the middle between the inlet and outflow cones is called the shell. There are circular disks in this part. These discs are likely positioned perpendicular to the length of the shell, forming horizontal layers or section within the structure.

Circular discs within the shell of a structure can serve several common purposes, including:

1. Structural support: the disc can provide structural reinforcement and stability to the shell, helping to maintain its shape and integrity.
2. Compartmentalization: the discs can divide the internal space of the shell into separate compartments or sections. This division can be useful for organizing different processes or material within the structure.
3. Flow distribution: the disc can be designed to control and distribute the flow of gases within the shell. They can help ensure even distribution and promote efficient movement through the structure.
4. Mixing and agitation: the disc can be used to promote mixing and agitation of gases within the shell. They may have specific designs or features that enhance fluid movement and improve the efficiency of chemical reaction or other processes taking place within the structure
5. Heat transfer enhancement: the circular disc can be utilized as heat transfer surface, either for heating or cooling purposes. They can increase the surface area available for heat exchange, enhancing the efficiency of heat transfer processes within the shell.
6. Separation or filtration: in certain application, the discs may act as separation or filtration of elements. They can help remove impurities or different components from gas stream as it flow through the shell (Fornalczyk et al., 2016).

$$C_v = \frac{\pi}{4} * D^2 * L \quad (4.4)$$

Where: D- catalyst-diam

L- catalyst-length (Assume l= 3D)

$$C_v = \frac{\pi}{4} * (D^2) * (3D) \quad (4.5)$$

As it is evidence from the firing order of six cylinder engine, mostly exhaust gases are released twice per recur. If the sizing of the emission treating system also need to be doubled as follows

$$DF = 2D$$

$$LF = 2L$$

3.7.4. Firing

Both primary and secondary balance is achieved by using the firing directive of 1-5-3-6-2-4 in straight inline-six engines. 1-4-2-6-3-5 firing sequence is also the most frequently utilized firing order. In a four-stroke cycle, two of the engine's cylinders are idle while the other four complete one of the cycle's power-producing strokes (James, 2018)

$$f_i = \frac{720^0}{N_c} \quad (4.6)$$

Table 3-2: Firing Order of 6- Cylinder Engine

Firing order	Strokes					
1	Pow	Exh	In	Com	Pow	Exh
5	Com	Pow	Exh	In	Com	Pow
3	In	Com	Pow	Exh	In	Com
6	Exh	In	Com	Pow	Exh	In
2	Pow	Exh	In	Com	Pow	Exh
4	Com	Pow	Ex	In	Com	Pow

0 120⁰ 240⁰ 360⁰ 480⁰ 600⁰ 720⁰

Where: P- Power stroke

E- exhaust stroke

C- Compression stroke

I- intake stroke

3.7.5. Exhaust

To produce place of mixture following duration, high-pressure gases left over after combustion is finished and provide toward the cylinder in order to work on the driveshaft

along the expansion stroke. There are two stages to this: the exhaust cycle and blow-down. At the TDC of the power strokes, when the valve for the exhaust starts to open, at approximately 600 _400 BDC, blow down happens. The temperature in the cylinder has reached above 1000 K, however the pressure is still only at 4-5 pa. The pressure differential happens once the valve is opened the exhaust system approximately one atmosphere of pressure enables exhaust gases to flow out of the system immediately (Jason et al., 2024)

$$\left[\frac{P1}{P2}\right] = \left[\left(\frac{K + 1}{2}\right)\right]^K \quad (4.7)$$

The k value for air is, 1.35

Where:

- ✓ P₁- pressure of upward
- ✓ P₂- pressure of downward
- ✓ k - specific heats
- ✓ R - Gas Constant
- ✓ T - Temperature

The gas undergoes expansion cooling, which causes a pressure and temperature drop as it moves from the cylinder toward the exhaust system. The exhaust temperature is frequently determined.

$$T_{ex} = T_{EVO} \left[\frac{P_{ex}}{P_{EVO}}\right]^{\frac{(k-1)}{k}} \quad (4.8)$$

Where:

T_{ex}, P_{ex} = Temperature and pressure of the exhaust

In exhaust stroke, the engine's piston is moving past bottom dead and towards top dead during blow-down. Valve still open. The exhaust system's ambient pressure is somewhat higher than the inside cylinder that is in this motion, limiting the piston. The slight pressure Differential created by the valve's flow when the engine piston forces the pollutants emerging from the cylinder is what separate the pressure from cylinder pressure. The exhaust valve is where there is the minimal. Decrease pressure all over the exhaust cycle and exhaust maximum flow is constraint.

Based on the selected Vehicle Specification: The engine specifications for the WD615.69, 336hp engine can vary depending on the specific model and manufacturer. However, here are some general specifications that you might find helpful:

Engine Speed:

- ✓ **Rated speed:** Typically around 2200 RPM (rotations per minute). This is the speed at which the engine produces its maximum rated power output.
- ✓ **Maximum speed:** Usually around 2400-2500 RPM. This is the highest speed the engine can safely operate at for short periods.
- ✓ **Idle speed:** Around 600-800 RPM. When engine operating speed is not under load.

Temperature:

- ✓ **Coolant temperature:** Typically maintained between 80°C and 90°C. Exceeding this range can lead to overheating and engine damage.
- ✓ **Oil temperature:** Similar to coolant temperature, typically around 80°C to 90°C.

Pressure:

- ✓ **Oil pressure:** Varies depending on engine speed and load, but typically ranges from 3-5 bar at idle to 7-10 bar at rated speed. Low oil pressure can indicate insufficient lubrication and potential damage.
- ✓ **Boost pressure (turbocharged engines):** If the engine is turbocharged, the boost pressure typically falls between 1 and 2 bar. Higher boost pressure can increase power output but requires careful monitoring to avoid exceeding safe limits.

Motor valve opens at bottom dead (56°)

1. Explosion time is 56° bBDC and BDC.

$$T_b = \frac{\alpha}{360} * \frac{60}{RPM} \tag{4.9}$$

Where:

- ✓ T_b _ time of Blowdown
- ✓ α _angle of explosion

2. Gas exits during explosion

CV is the volume of the combustion area above the piston at top. The following formula can be used to get the clearance volume (Jason et al., 2024).

$$S_{wv} = \frac{E_d}{N_c} \tag{4.10}$$

$$rc * cv = S_{wv} + cv \tag{4.11}$$

To find volume when the exhaust valve opens:

$$\frac{V_{EVO}}{VC} = 1 + \frac{1}{2}(r_c - 1) \left[R + 1 - \cos\theta - \sqrt{R^2 - \sin^2\theta} \right] \quad (4.12)$$

As the valve opens

$$T_{EVO} = T_3 \left(\left(\frac{V_3}{V_{EVO}} \right)^{k-1} \right) \quad (4.13)$$

$$P_{EVO} = P_3 \left(\left(\frac{V_3}{V_{EVO}} \right)^k \right) \quad (4.14)$$

$$M_{EVO} = \frac{PV}{RT} \quad (4.15)$$

$V_4 = V_1$ $P_0 = 101\text{kpa}$ (atmospheric pressure)

$$T_4 = T_3 \left(\left(\frac{1}{rc} \right)^{k-1} \right) \quad (4.16)$$

$$P_4 = P_3 \left(\left(\frac{1}{rc} \right)^k \right) \quad (4.17)$$

$$V_{BDC} = V_4 = V_1 = (V_c + V_d) \quad (4.18)$$

$$V_{EVO} = \sqrt{KRT_{EVO}} \quad (4.19)$$

Inside the cylinder pressure increase leads the exhaust valve open, causing exhaust gas to exit the combustion chamber faster. The exhaust gas temperature could range from 700_1100 °C and higher. For this application, materials need to be highly durable and reliable at the lowest possible cost, able to withstand a variety of thermo-mechanical strains and stresses. Select the appropriate casting materials based on the engine type and exhaust gas temperature. Ferritic ductile cast irons are the less expensive option at lower temperatures, but as the temperature rises, more advanced materials are required. Ferritic ductile cast iron SiMo51 is a common material for exhaust systems, and it can withstand temperatures up to 750 degrees (Nunez, 2019).

3.8. Hose Selection

Select the proper hose for the right application is not an easy task. All exhaust hoses used are depend on the type systems and required there is Hoses are offered with several standard sizes, diameters, and temperature ranges available in market. They can be selected according to the required. A determination of hose type can be made after the designer established the real operating conditions, the way in which the cars are driven in the garage, and the length of the operation. Overall Recommendation Choose a hose with a plastic abrasion where

feasible, a galvanized steel externally helix, and special-coated high temperature fabric (Mizell et al., 2024)

Table 3-3: Recommended capacities

Vehicle	Temp (k)
Small vehicle	573 _ 623k
Truck	773_ 873k
Heavy off-road	1023_ 1473k
Dyno	843_2283k

Based on this criteria, the recommended hoses for diesel truck service is that of 500°C to 600 °C Continuous Operation

3.8.1. Exhaust Pipe Size Estimate

Table 3-4, provides the expected maximum horsepower for each common pipe size as well as the CFM that each pipe size will flow (Mizell et al., 2024).

Table 3-4: Exhaust pipe size estimation

Pipe diam(inch)	Area in ²	CFM	HP/ pipe	HP/dual hose
1	2.48	171	78	155
2	2.76	318	144	289
2 ¾	5.41	622	283	566
3	6.49	747	339	679
3 ¼	7.67	882	401	802
5	8.95	1029	420	935

Therefore the based on Turbo charger vg1560118229 wd615.69, 336HP and 410HP with a dual exhaust system only needs 5 inches is equivalent 127mm

1. Determine the airflow volume required for the specific vehicle type according to industry standards

- ✓ Automotive: 275-300 CFM through a 4-inch hose
- ✓ Pick-ups: Same as automotive
- ✓ Motorcycles: 600–650 CFM with a 6-inch pipes (two 5-inch legs can be separated for dual exhaust).
- ✓ Trucks: 500-550 CFM through a 5-inch hose

Find the cross-sectional area (A):

$$Q = A * V \quad (4.20)$$

Convert Q from m³/s to CFM to know the volumetric flow of air through the hose:

The volumetric flow is approaches to the standards of straight pipe suitable for capturing exhaust gases from various sources, 480CFM, so the hose is safe from back pressure.

$$\dot{m} = \rho Q \quad (4.21)$$

Where:

- ✓ \dot{m} _ Mass flow rate,
- ✓ ρ _ Density of air,
- ✓ Q _volumetric flow

The volumetric flow is approaches to the standards of straight pipe suitable for capturing exhaust gases from various sources, to calculating the volumetric flow rate of exhaust gas:

$$Q_v = \frac{Q_m}{M_w * P} \quad (4.22)$$

Where:

- ✓ Q_{vol} _ volumetric flow rate,
- ✓ Q_{m_mass} flow rate,
- ✓ M_w _ weight molecular weight and

P- Atmospheric pressure for simplicity, assume atmospheric pressure 101 kPa or 1 bar) and convert the mass flow rate to grams per second:

3.9. Design of gas inlet compartment tank

Formula for calculating the outlet temperature and inlet heat in an exhaust tank is challenging due to the various factors involved. However, here's a simplified approach using the **heat balance equation** under specific assumptions:

- ✓ **Steady-state operation:** The system maintains a constant temperature over time.
- ✓ **Uniform flow:** Exhaust gas flows through the tank at a constant rate and with a uniform temperature profile.

To find the rectangular prism volume, multiply all the dimensions of the tank (Jason et al., 2024).

$$V_{tank} = l * w * h \quad (4.23)$$

To calculate the pressure of the air inside a tank, we can use different methods, here are some common approaches (Jason et al., 2024).

Ideal Gas Law: for a gas in a tank, to determine the pressure:

$$PV = nRT \quad (4.24)$$

From equation (4.24) we can find pressure of tank and mas of air inside the tank

$$P_{tank} = \frac{nRT}{V}$$

$$M_{air} = \frac{PV}{RT}$$

To calculate the input heat required to raise the temperature of the air inside the rectangular tank,

$$Q = MCp\Delta T \quad (4.25)$$

From equation (25) re-arrange for temperature out and heat out from the tank

$$T_{out} = T_{air} - \frac{Q}{M * Cp}$$

$$Q_{out} = M * Cp(T_{in} - T_{out})$$

3.10. Design of the multiple cylindrical pipe

Most common wall thickness for heat pipe is 0.3mm. For heat pipe that require, the thickness is about 0.4 to 0.5mm. this helps to achieve better flatness and good Transfer of heat from the storage vessel to the wall (Truth et al., 2023).

Table 3-5: Standard dimensions

Diameter	4	5	6	8	10
Length	80-600mm	80-600mm	80-600mm	80-600mm	80-600mm

The thin cylindrical shell design process was followed in the creation of this component. Requirements for thin cylindrical the narrow cylinder's wall thickness cannot be more than one-twentieth the internal

$$\text{Diameter or Thickness} < \left[\left(\frac{1}{20} \right) * \text{internal diameter} \right]$$

$$t < \frac{d}{20} \text{ or } \frac{t}{d} < \frac{1}{20} \quad (4.26)$$

The requirement that needs to be met in order to classify a spherical or cylindrical shell as thin. The following assumption explain both developed stress on in a thinly cylindrical body and stress due to internal force:

- ✓ Cylinder wall's curvature is not taken into consideration.
- ✓ The section of the walls has a uniform distribution of tensile stresses.
- ✓ The effects of the pressure vessel's heads acting as a control is neglected.

A thin cylindrical shell tends to failure in one of two ways when it experiences internal pressure:

- ✓ It could fracture either horizontally or across the axial section, splitting the cylinder into two cylindrical shells.
- ✓ It could fracture either circularly or horizontally, collapsing the cylinder into two troughs.

Therefore, when an inner cylinder experiences pressure inside, its outer layer needs to be sufficiently rigid to withstand. Longitudinal stress as well as circumferential tension, also known as hoop stress.

3.10.1. Material selection

The selected material for the construction of the thin cylindrical shell is Aluminum and its mechanical properties are given below in the table (Liu, 2020).

Table 3-6: Aluminum property

Aluminum Property	Numerical value
Young's modulus	70 GPa
Yield Strength	7 – 11MPa
modulus of symmetric	27 GPa
Modulus of bulk	75 GPa
Hardiness of Poisson	0.34
hardness	161–349 M/Pa
Point of melting	933.32k
point of boiling	2737k
Density at room temperature	2.65 g/cm ³

The internal pressure of the pipe is calculated at maximum yield strength

$$p_{in} = \frac{2 \cdot s_t \cdot t}{d_{out}} \quad (4.27)$$

3.10.2. Circumferential

Circumferential tension, is a form of tensile stress that acts perpendicular to the circle. In differently, the tensile stress on a longitudinal section (or on the cylindrical barriers) corresponds to the total force acting on the region along the entire length X-X of the cylinder (Wuryanti & Fitriyani, 2019).

$$p * l * d \quad (4.28)$$

The entire force that is acting against the exterior surface of the cylinder

$$\delta_{t1} * 2t * L(\text{for two section})$$

$$\delta_{t1} = \frac{p*d}{2t} \text{ or } t = \frac{p*d}{2\delta_{t1}} \quad (4.29)$$

$$t < \frac{d}{20} = \frac{10\text{mm}}{20} = 0.2\text{mm take } 0.3\text{mm}$$

Where

- ✓ P_ pressure of inner
- ✓ d _diameter of inner
- ✓ l _Length
- ✓ t_ thickness
- ✓ σ_{t1} _ Circular stress
- ✓ Young's modulus
- ✓ μ _ hardness of Poisson's ratio

3.10.3. Longitudinal Stress

Assume an inner pressure-filled limited, closed cylindrical shell. Tensile tension that acts perpendicular to the axis is called longitudinal stress. the ends the transverse or circular section Y-Y is subject to tensile stress. The force operating along the Y-Y segment, or transverse section (Wuryanti & Fitriyani, 2019)

$$\delta_{t2} * \pi * dt \quad (4.30)$$

Where:

δ_{t2} = Longitudinal Stress and total resisting force from equation above

$$\delta_{t2} * \pi * d * t = p * \frac{\pi}{4} (d^2) \quad (4.31)$$

$$\delta_{t2} = \frac{p * d}{4t} \text{ or } t = \frac{p * d}{4\delta_{t2}}$$

Variation of a thin cylindrical wall dimensions as a result of internal pressure an internal pressure applied to a thin cylindrical shell will cause both the shell's diameter and length to expand. The shell's increased diameter (δd) as a result of internal pressure can be measured by

$$\delta d = \frac{p * d^2}{2t * E} \left(1 - \frac{\mu}{2}\right) \quad (4.32)$$

Inner pressure increase (δl)

$$\delta l = \frac{pdl}{2t * E} \left(\frac{1}{2} - \mu \right) \quad (4.33)$$

The cylinder's load increase with diameter and length. The shell's increased volume as a result of internal pressure is calculated using

$$\begin{aligned} \delta v &= \text{final volume} - \text{original volume} \\ &= \frac{\pi}{4} (d + \delta d)^2 (l + \delta l) - \frac{\pi}{4} * d^2 * l \end{aligned} \quad (4.34)$$

3.10.4. Steady Heat Conduction for circular pipe

The existence of a temperature differential is necessary for heat transmission. Heat transfer is caused by temperature differentials. Conduction is the process via which energy is transferred by interactions between the most charged particles of the substance and its less active, adjacent ones. Regarding to continuous conduction over big flat sidewall with width $\Delta x = L$ and area of surfaces A . A temperature differential of $\Delta T = T_2 - T_1$ exists across the wall. Keep in mind that heat transport is the only energy interaction; the wall's energy balance can be stated as (Braga da Costa Campos, 2020).

$$Q_{in} - Q_{out} = \frac{dE_{wall}}{dt} \quad (4.35)$$

For steady-state operation,

$$Q'_{in} = Q'_{out} = \text{constant}$$

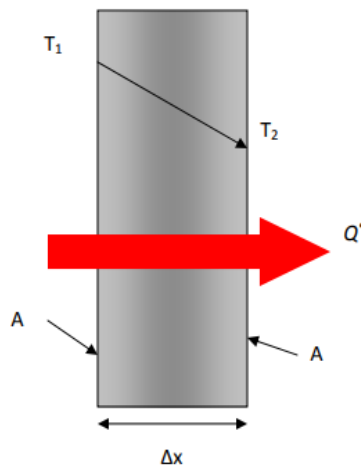


Figure 3-3: Heat conduction through a plane wall

$$Q_{rate} \propto \frac{A * \Delta T}{t} \quad (4.36)$$

$$Q_{conv} = hA(T_{\infty 1} - T_1) \quad (4.37)$$

$$Q_{cond} = kA(T_2 - T_1) \quad (4.38)$$

$$Q_{conv} = hA(T_{\infty 2} - T_2) \quad (4.39)$$

3.10.5. Temperature Drop inside the tank

The temperature of exhaust gases exiting an engine exhaust manifold reaches 1235k, depending on the engine's operating conditions. This high temperature poses a challenge for catalytic converters, as they are designed to operate within a specific temperature range for optimal performance and durability. This design allows for a more moderate temperature to be reached, ensuring the catalytic converter operates within its intended temperature range. To investigate the temperature drop in the exhaust pipe, a simulation approach can be employed. By changing the inlet water ambient temperature circulating through the pipe and analyzing the temperature profile along the pipe length, the effectiveness of the temperature drop can be assessed.

The simulation should consider factors such as:

1. Pipe geometry: Length, diameter, and material properties.
2. Exhaust gas properties: velocity magnitude and initial temperature.
3. Ambient conditions: Temperature and heat transfer coefficients.

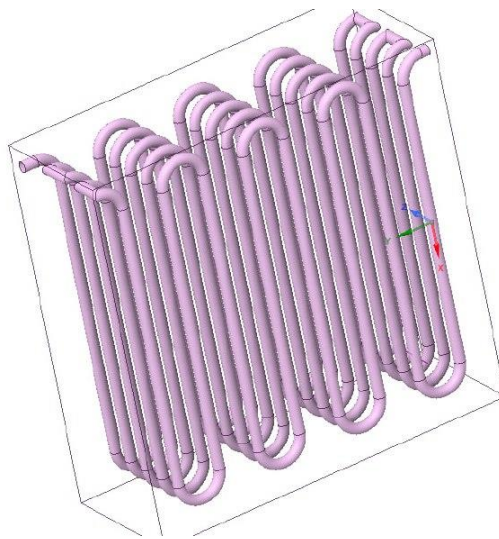


Figure 3-4: 3D of cooling pipe where water circulate through

3.11. MATHLAB/Simulink to keep constant tank temperature

This Simulink illustrates how to design and simulate a dynamic system using Simulink software. This instance is intended to be used a cooling uses thermostat (controller model) to regulate the temperature of a tank (environment model) using a cooling (plant model). The procedures for designing the algorithm and the model's structure are shown below. Tasks outside of the Simulink software environment completed before modeling can begin.

Define the parameters of the model and mathematical algorithms. Gather information for the model's parameters and measure the output signal to verify the outcomes of the simulation.

In-order to keep constant at moderate temperature of tank.

- ✓ Keep an eye on how the shifting temperature impacts on cooling system
- ✓ Keep constant temperature of tank in constant range.

Once understand modeling requirements. List the system elements. Tank cooling this model shows the link between a cooling system and a tank as system. It consists of,

- ✓ Tank temperature features,
- ✓ cooling tank temperature features,
- ✓ heater temperature features, and
- ✓ temperature control thermostat

The thermostat frequently detects the temperature in the tank and, based on the difference between the set temperature and the tank temperature, determines whether to turn on or off the heater. There are four parts to this system model: the tank, thermostat, heater, and cooling unit. The heat exchange in the tank is determined by three time-dependent variables.

- ✓ Tank temp (T-tank).
- ✓ Heat gain: the heat energy that is delivered to the tank from the exhaust gas (Q_{gain}).
- ✓ Heat loss: The cooling system receives thermal energy from the tank (Q_{loss}).

The link between these variables is defined by a differential equation; however, only tank temperature is a state variable because heat transfer is defined in terms of changing temperature.

3.11.1. Heat gain formula

Convection of hot air with a capacity of C_{air} from the heater provides thermal energy to the tank. The swing in temperature between the warm device and tank determines how much heat is gained by a mass of air in the heater,

$$Q_g = m_h T_h \quad (4.40)$$

The heater's rate of temperature gain is

$$\frac{dQ_g}{dt} = \frac{dm_h}{dt} c (T_h - T_r) \quad (4.40.1)$$

Where:

- ✓ $M_{h_}$ mass of heater air
- ✓ $T_{r_}$ room temperature
- ✓ $T_{O_}$ temperature of hot water out from the pipe
- ✓ $Q_{g_}$ heat gain

✓ Q_l heat loss

The heater produces a constant amount of air per unit time, mass of heater air; substituting that constant for dm heater air/ dt simplifies the calculation to

$$\frac{dQ_g}{dt} = m_h c(T_h - T_r) \quad (4.40.2)$$

3.11.2. Heat Loss formula

The storage vessel loses its heat through conduction along the hot gases and cold water via the cooling pipe, and this loss is proportionate to the temperature differential between the water outside and within the tank (Truth et al., 2023).

$$Q_l = kA \frac{(T_r - T_o)t}{D} \quad (4.41)$$

Replacing $\frac{kA}{D}$ with $\frac{1}{R}$, where R is the thermal resistance.

$$\frac{dQ_l}{dt} = \frac{(T_r - T_o)}{R} \quad (4.41.1)$$

Rearrange the above equation for changing tank temperature equation

$$\frac{dT_r}{dt} = \frac{1}{m_h} \left(\frac{dQ_g}{dt} - \frac{dQ_l}{dt} \right) \quad (4.41.2)$$

Standard property tables provide the majority values used for parameters required tank cooling. Specify every variable and coefficients in the equations, verify unit's dimensions agree with one another.

Where:

Description	Units
Area	m^2
Depth	M
Distributed heated energy_ Q	J
Temperature energy transfer rate $\frac{dQ}{dt}$	J/hr
Temperature conductivity _K	W/m.k
Resistance to heat _R	J/s.k
M_heater_air =3600	Kg/hr
Specific heat capacity, 1005.4	J/kg.k
Temperature of air in the tank T _{air} , 1235	K
Temperature of water cooling at exhaust pipe	K

3.11.3. Heater

- ✓ Use the thermostat's control signal and the tank's current temperature as inputs.
 - ✓ Finds out the heater's heat gain and outputs it when the control signal is activated.
- Represent the rate of heat gain equation using Simulink blocks from above equation in order to represent the heater subsystem.

$$\frac{dQ_g}{dt} = m_h c (T_h - T_r)$$

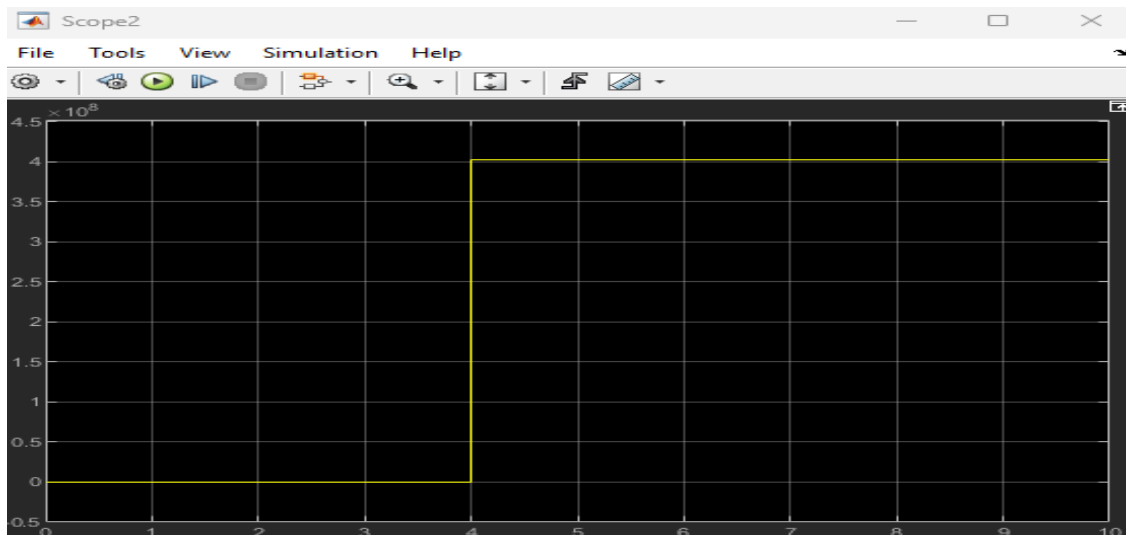
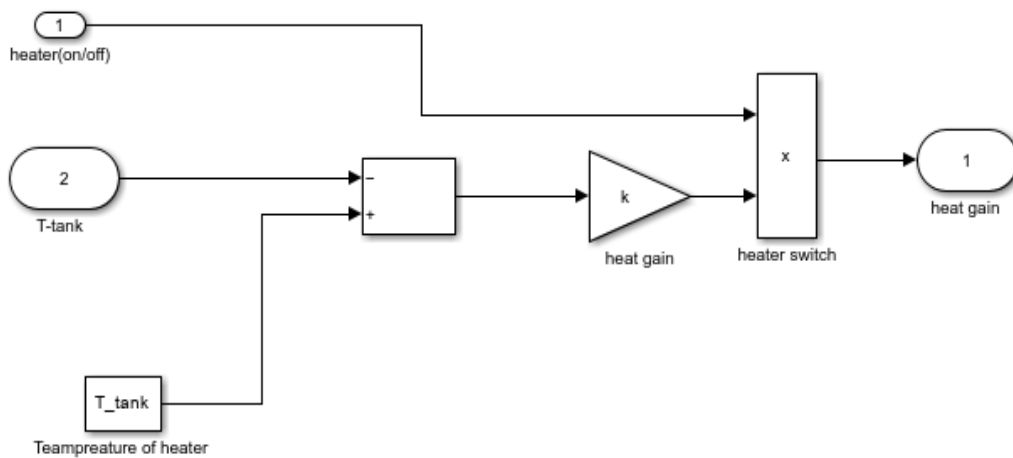


Figure 3-5: Heater modeling and response time

3.11.4. Thermostat

No need to use mathematical equations while modeling a thermostat. This component has the following requirements:

- ✓ The heater must be on and the control signal must equal 1 when the tank temperature drops below the predetermined level. The control signal equals 0 when the tank temperature is higher than the predetermined temperature
- ✓ The thermostat enables a 50 degree range around the temperature set point in order to prevent frequent switching.
- ✓ The tank temperature must rise by 50 degrees over specified temperature if thermostat is on before it turns off.
- ✓ The tank temperature must drop by 50 degrees below the desired temperature in order for the thermostat to turn on if it is off.

The one that determines whether the heating system is on or off by simulating how a thermostat works. Despite having one relay block, consider of it as the thermostat in the mode.

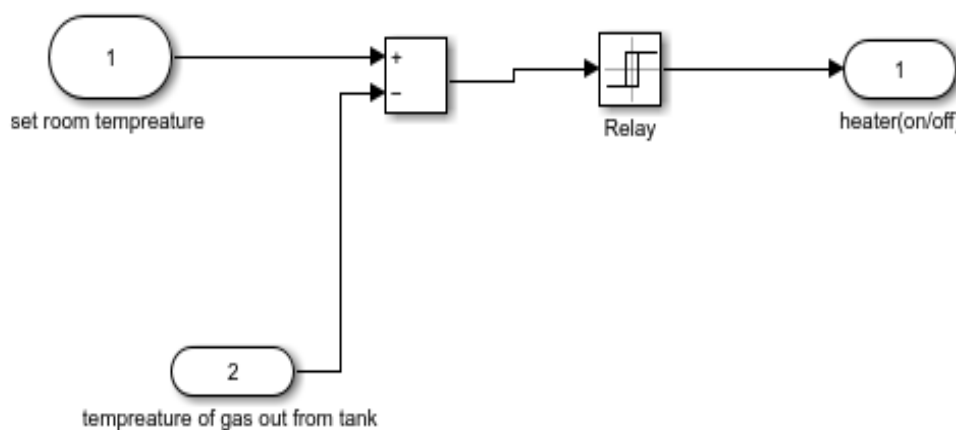


Figure 3-6: Thermostat model

3.11.5. Model of Tank

Inputs to the tank component are heat flow from the heater component and the external air temperature. The tank component uses these inputs to compute heat loss through the walls, heat loss through the cooling water, and the current tank temperature. To design the room subsystem, use the rate of heat loss equation and the changing tank temperature equation.

$$\frac{dT_r}{dt} = \frac{1}{m} \left(\frac{dQ_g}{dt} - \frac{dQ_l}{dt} \right)$$

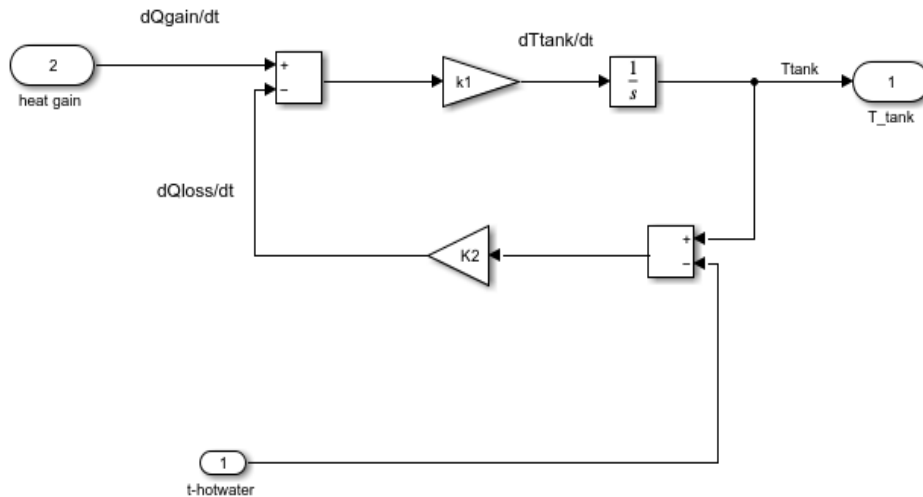


Figure 3-7: Total heat gain and heat lose for tank temperature

3.11.6. Integrate Tank, thermostat and heater

Essential to alter the outside temperature in order to simulate the thermostat and heater subsystems with the room system. How the cooling system and thermostat setting impact the outside temperature by simulating the model.

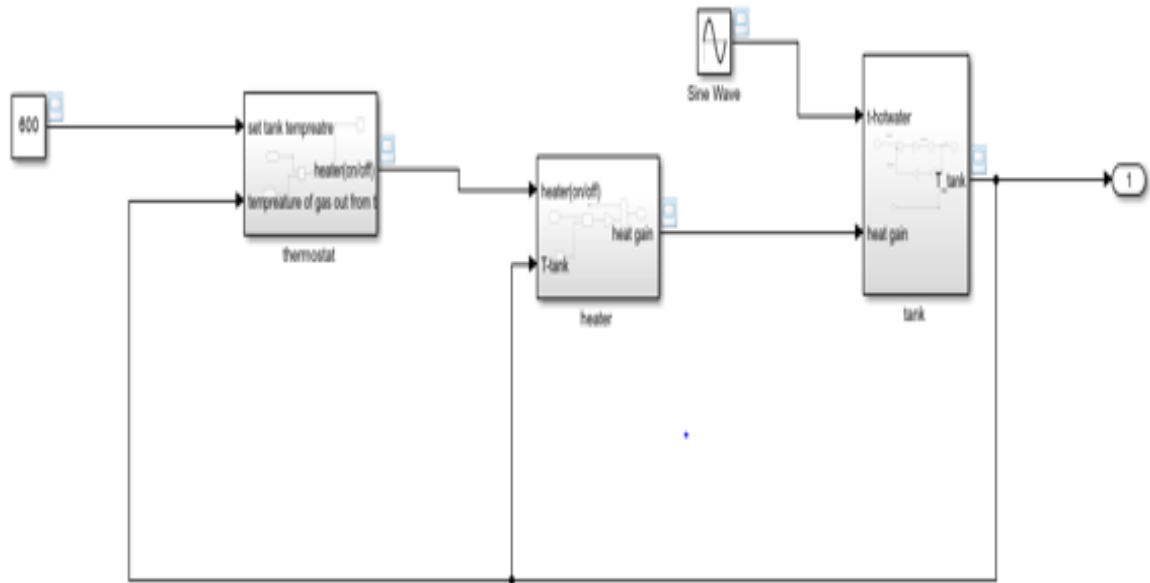


Figure 3-8: Integrate Tank, Heater and Thermostat

3.12. Single pipe with divergent cover

Follow similar calculation with multiple cylindrical pipe design calculation Conditions for thin cylindrical Wall thickness of thin cylinder must be less than one twentieth of the internal diameter or Thickness < $\left[\left(\frac{1}{20}\right) * internal\ diameter\right]$

$$t < \frac{d}{20} \text{ or } \frac{t}{d} < \frac{1}{20} \quad (4.42)$$

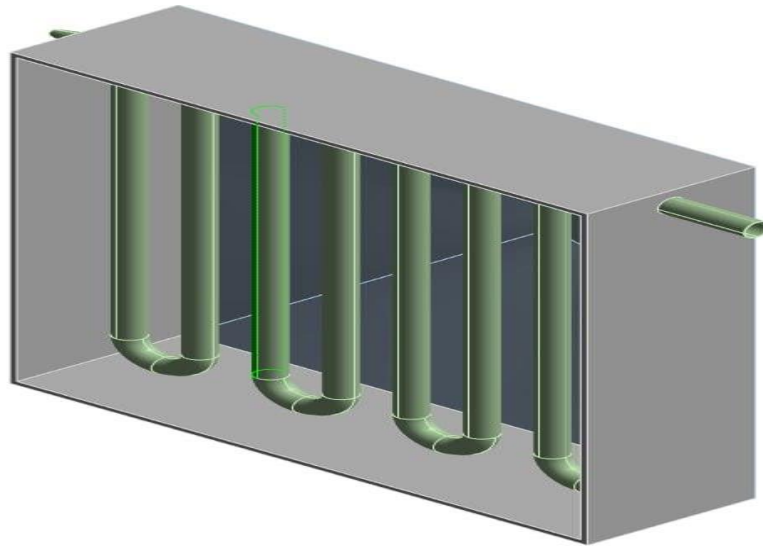


Figure 3-9: Pipe with divergent cover

3.12.1. Water pump selection

It is mechanical device designed to move water from one place to another. It operates by creating a flow of water through the use of centrifugal force or other mechanical means. Water pumps are commonly used in various applications such as pumping water from wells, Circulating water in heating and cooling systems. Flow Rate (GPM), this represents the volume of water the pump needs to deliver per unit time, usually expressed in Gallons per Minute (Roy et al., 2020). Pump horsepower is calculated:

$$PHP = \frac{TDH * Q * SG}{3960} \quad (4.42.1)$$

$$TDH = V_h + P_f \quad (4.42.2)$$

Where:

- ✓ TDH_ Total dynamic head (ft)
- ✓ Q_ Flow rate in (gallon per minute)
- ✓ SG _ specific gravity (1 for water)
- ✓ Vh_ vertical height (ft)
- ✓ Pf _ pipe friction loss (ft)

Table 3-7. Standard table for water pump selection

220v		Pipe size mm ²							
HP	KW	1.5	2.5	4	6	10	16	25	35
0.5	0.37	120	200	320	480	810	1260	1900	2560
0.75	0.55	80	130	220	320	550	850	1290	1760
1.0	0.75	60	100	170	250	430	670	1010	1380
1.5	1.1	40	70	120	180	300	470	710	980
2.0	1.5	30	60	90	130	230	550	760	1060

As far as the horse power of the pump is known it is easy to select the water pump

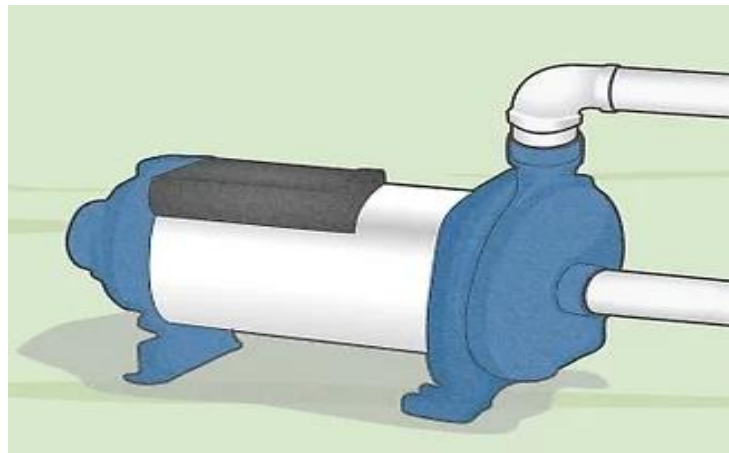


Figure 3-10: Water pump

3.13. Electrical fan selection

Based on the ANSYS result the temperature of a compartment drop at the temperature of 292k, therefore to get this ambient temperature external ventilating fan is required (AMCA, 2018)

$$Q = hA(T_{amb} - T_{cold}) \quad (4.43)$$

$$Q = C_p \dot{m}(T_{amb} - T_{cold}) \quad (4.44)$$

$$T_{cool} = \frac{Q}{C_p \dot{m}(T_{amb})} \quad (4.44.1)$$

$$V_m = \frac{\dot{m}}{\rho} \quad (4.45)$$

Where:

- ✓ \dot{m} mass flow rate
- ✓ V_m Velocity flow rate

- ✓ T_p Total air pressure
- ✓ S_p pressure at rest
- ✓ V_p pressure and velocity at every step of a ventilation
- ✓ CFM volume of air circulated in a minute
- ✓ FPM air stream velocity

A motor along to a centrally rotating hub drives the blades of an electric fan. Fans move air across a room to reduce heat, improve ventilation, and regulate humidity. The work done by the fan is on air is calculated as,

AHP– Air Horsepower is work done by the fan expressed as horsepower.

$$AHP = \frac{CFM * TP}{6356} \quad (4.46)$$

$$AHP = \frac{43.056CFM * 101pa}{6356} = 0.72 \text{ hp (537watt)} \quad (4.47)$$

$$TP = SP + VP \quad (4.48)$$

$$VP = \left(\frac{FPM}{4005}\right)^2 \quad (4.49)$$

$$AHP = \frac{CFM * \left(SP + \left(\frac{FPM}{4005}\right)^2\right)}{6356} \quad (4.50)$$

Therefore the appropriate horse power for the design is 0.72kw (537W), 220v of electric power consumption

3.14. Refrigerant box selection

Refrigerator is a device that transfers heat from indoor to outdoor spaces to create a cold temperature by lowering the interior space's temperature relative to the outside air. The idea of energy conservation states that heat is transferable rather than destroyed. A portable plastic bag filled liquid refrigerant is called a gel pack. Drop Before the temperature increases above, significant heat can be absorbed by refrigerant liquid (Redho et al., 2023)

In order to keep the required temperature phase change material should have to be used. This PCMs are effective alternative to store and release heat at specific range of temperature

For a refrigerant fluid in the 19°C to 20°C temperature range, possible to use a paraffin wax-based phase change material (PCM).

Some specific paraffin waxes that could work well for this application include:

- ✓ n-Eicosane ($C_{20}H_{42}$), the melting point is 36.4 degree, this provides phase change slightly above 19-20 degree target range

- ✓ n-Nonadecane ($C_{19}H_{40}$), the melting point is 31.1 degree, close to the desired temperature range
- ✓ therefore blends of two paraffin's n-Eicosane and n-Nonadecane, can fine tune melting point to be within the 19_ 20 °C

The advantage of using paraffin waxes is they are relatively inexpensive, non-toxic, and have predictable phase change characteristics. The melting/freezing points can also be adjusted by blending different paraffin compounds (Horton et al., 2024)

Therefore the main aim of selecting refrigerant fluid is, in-order to cool the water circulating through the single pipe, a number of small box type refrigerant (<200ml)is selected and where a multiple of small refrigerant box is placed inside a rectangular tank, where it is placed in front/ back of fan as the room/ambient temperature of pass through the surface of refrigerant it drop the desired temperature. This is because surface temperature and outer temperature of the fan without refrigerant it's not effective to reduce circulating water as much as required temperature. This is achieved by assembly the refrigerant rectangular tank with fan shown in the figure below.

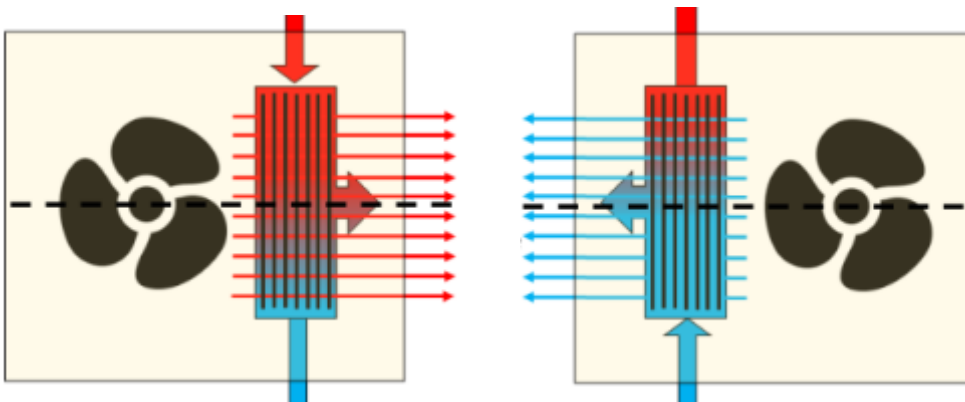


Figure 3-11: (a) Fan assembled before refrigerant box, (b) fan assembled after refrigerant box



Figure 3-12: Single refrigerant liquid pack

$$Q_{amb} = h_{amb}A(T_{\infty rom} - T_{sur}) \quad (4.51)$$

$$Q_{re} = h_{re}A(T_{\infty re} - T_{sur}) \quad (4.52)$$

By Heat flux

$$\frac{Q_{amb}}{A} = h(T_{\infty rom} - T_{sur}), \quad \frac{Q_{re}}{A} = h_{re}(T_{\infty re} - T_{sur}) \quad (4.53)$$

In order to get free-stream temperature of refrigerant re-arrange equ1 and 2

$$T_{\infty re} = \frac{h_{amb}}{h_{re}}(T_{\infty} + T_{sur}) \left(1 - \frac{h_{amb}}{h_{re}}\right) \quad (4.54)$$

Use ideal gas law

$$T_{\infty re} = \frac{pv}{nR_{re}} \quad (4.54.1)$$

Substitute this to equation to (4.54)

$$T_{sur} = \frac{\frac{pv}{nR_{re}} - \frac{h_{amb}}{h_{re}}T_{\infty}}{1 - \frac{h_{amb}}{h_{re}}} \quad (4.55)$$

Conductive heat transfer

$$Q = kA(T_s - T_o) \quad (4.56)$$

$$\frac{Q}{A} = h(T_{\infty amb} - T_s) = \frac{k(T_s - T_o)}{\Delta x} \quad (4.57)$$

$$T_o = T_s - \frac{h\Delta x(T_{\infty} - T_s)}{k} \quad (4.58)$$

3.15. Mesh independence test

Grid, interest is divided into small elements or cells, forming a grid. This grid is used to approximate the continuous governing equations of the physical phenomenon being studied into a system of algebraic equations that can be solved by a computer. Grid Refinement, Refining the grid refers to increasing number of cells in the grid, by making the cells smaller. Grid Coarsening, Coarsening the grid refers to decreasing the number of cells, typically by making the cells larger. This reduces the computational cost of the simulation but can also lead to a loss of accuracy. Grid Refinement Ratio, refining the grid, the grid refinement ratio determines how much smaller the cells become in each direction. A ratio of 2, for example, means that the cell size is halved in each direction (length, width, and height in 3D). Therefore the recommended to use a grid refinement ratio greater than 1.3 to effectively

isolate the discretization error from other error sources. the process might work (Knotek et al., 2021).

- ✓ **Grid Independence Test:** grid independence test to determine the optimal grid resolution for the simulation. This involves running the simulation with different grid resolutions and monitoring the results of interest
- ✓ **Medium Grid as Reference:** The grid resolution obtained from the grid independence test is designated as the medium grid. This serves as the baseline for comparison with coarser and finer grids.
- ✓ **Coarse and Fine Grids:** Based on the chosen grid refinement ratio (e.g., 1.4), a coarser grid and a finer grid are defined. The coarser grid will have larger cells than the medium grid (by a factor of the refinement ratio), and the finer grid will have smaller cells.
- ✓ **Richardson Extrapolation:** The Grid Convergence Index (GCI) is then calculated using Richardson extrapolation to estimate the discretization error based on the results obtained with the coarse, medium, and fine grids

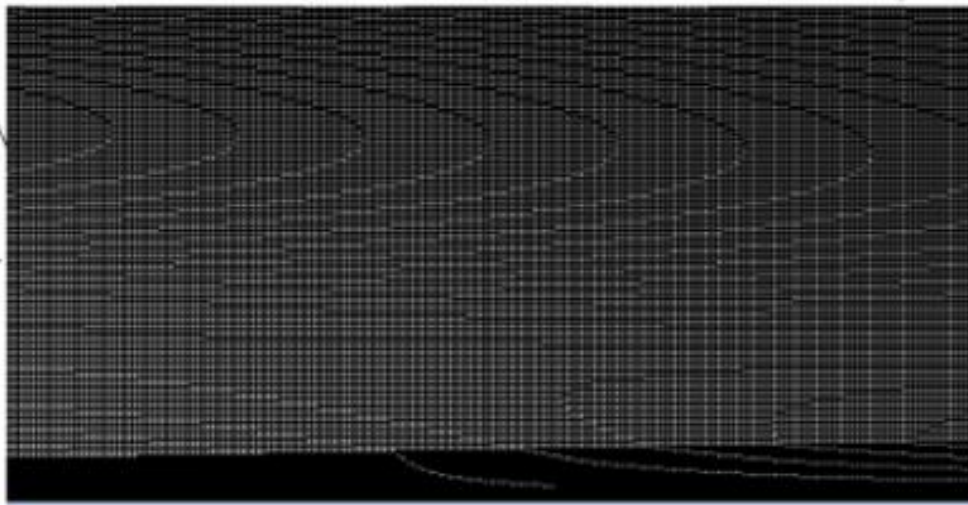


Figure 3-13: 2D model of combustion mesh

- ✓ The GCI is calculated according to the Richardson

$$GCI = f_s \frac{\epsilon}{r^p - 1} \quad (4.62)$$

- ✓ To calculate the GCI, the grid refinement ratio r .

$$r = \left(\frac{\Delta_{fine}}{\Delta_{coarse}} \right)^{1/3} \quad (4.63)$$

- ✓ The value of 1.25 to comparing three or more grids. is calculated

$$p = \frac{\ln \left| \frac{(F_{corse} - F_{medium})}{(F_{medium} - F_{fine})} \right|}{\ln r} \quad (4.64)$$

✓ for the error of the numerical solution for each grid condition is calculated

$$\varepsilon = \frac{f_{corse} - f_{fine}}{f_{fine}} \quad (4.65)$$

Table 3-8: number of element versus velocity

Parameters	Coarse mesh (1)	Medium mesh (2)	Fine mesh (3)
Element number	48568	53303	147426
Velocity (m/s)	261.63849	306.93849	297.67929

The graph below clearly shows that the red color indicates the region where the 53,303 medium mesh size is associated with good convergence, as evidenced by the graph. Where the velocity is 306.93m/s

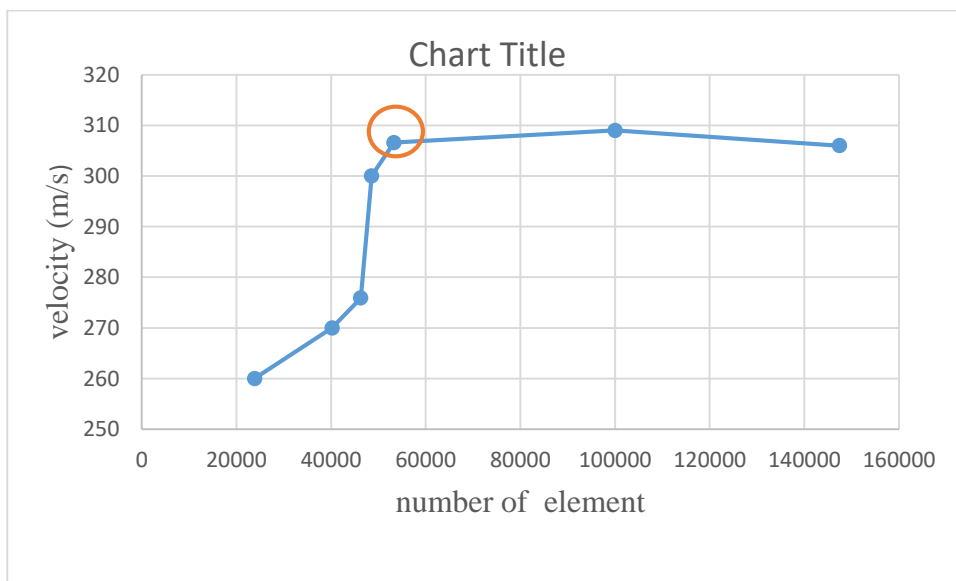


Figure 3-14: Velocity verses number of element

Table 3-9: Refinement ratio

r21	r32
1.404	1.351

Table 3-10: Grid independence index value

Order of convergence		Normal Error		Safety factor	Grid convergence index(GCI)	
P21	P32	ϵ_{21}	ϵ_{32}	F_s	GCI 21%	GCI 32%
8.28e+00	–	3.20E-02	1.40E-03	1.25	4.324	26.1

3.15.1. 2D model for combustion chamber simulation analysis

The 2D models developed on design modular. The dimensions of the reaction design chamber are 6mm for fuel inlet, 74mm for air inlet (80mm width) and 600mm in length which is axisymmetric, total fuel inlet 12mm, air inlet 148mm and 600mm in length in full dimensions. Before starting the reaction the 2D model were meshed using 2D mesh and define for its boundary condition in the software, fuel-inlet, and air-inlet, axis for symmetry, adiabatic wall and pressure outlet.

Mesh size; 53405 with medium mesh element size (35mm), depending on grid independence test.

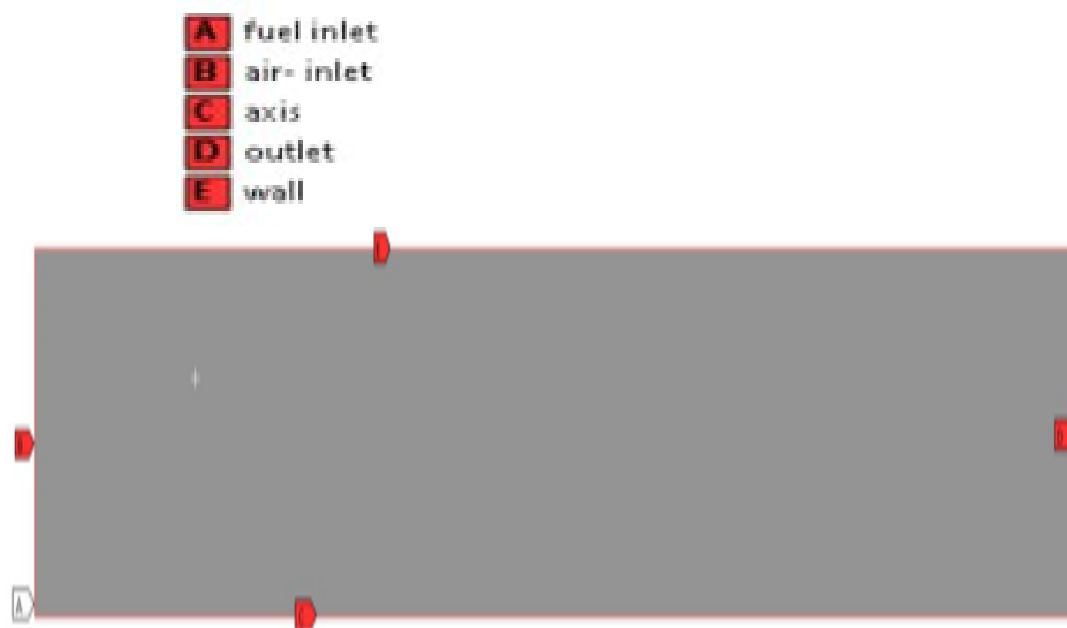


Figure 3-15: 2D model of combustion chamber

Species Transport Model, The species transport model is ideal for simulating combustion processes involving multiple chemical species. It solves conservation equations for each species, capturing the interaction between diesel fuel components and air during combustion.

k-ε Model (Standard), Widely used and well-validated for a broad range of turbulent flows. Provides a reasonable balance between accuracy and computational efficiency for many

combustion simulations. Eddy-dissipation, The process by which turbulent kinetic energy (TKE) in a fluid flow is converted into thermal energy due to viscous friction at small scale. Provide more accurate results for flows with complex turbulence characteristics. This is because they account for the energy transfer within the turbulent flow field. Later the NO_x model and soot model were activated to measure how much NO_x and soot were produced.

$$M_{air} = \frac{\pi}{4} B^2 * S * \rho_{air} \quad \frac{M_{air}}{M_{fuel}} = 14.5:1 \quad (4.66)$$

3.15.2. Boundary condition and possible assumption

In ANSYS, boundary conditions are used to define the interactions between the computational domain and the external environment or system. Applying appropriate boundary conditions is essential for the accuracy and convergence of the numerical simulation, some common reasons for using boundary conditions in ANSYS include:

- ✓ Defining the flow inlet and outlet conditions: This includes specifying the velocity, pressure, temperature, and other relevant parameters at the inlet and outlet of the computational domain.
- ✓ Modeling the interaction with solid surfaces: Boundary conditions are used to represent the interaction between the fluid flow and the solid walls, such as no-slip conditions, heat transfer, and wall roughness.
- ✓ Accounting for symmetry or periodic conditions: Boundary conditions can be used to simplify the computational domain by exploiting symmetry or periodicity in the problem.
- ✓ Incorporating external effects: Boundary conditions can be used to represent the influence of external factors.

Assumptions: In addition to boundary conditions, making appropriate assumptions is also essential for ANSYS simulations. Assumptions help to simplify the problem, reduce computational complexity, and focus on the most critical aspects of the system. Some common assumptions made in ANSYS simulations include: Fluid properties, Flow regime, Heat transfer mechanisms, Geometrical simplifications, Material properties.

Table 3-11: Boundary Conditions and related input values

Mass flow of air and fuel (kg/s)	0.000118, 0.000108
Total temperature(k)	300
Air-Hydraulic diameter(mm)	148
Wall	Adiabatic
Symmetric axis	Axis
Turbulence intensity (%) of air and fuel	15
Fuel-Hydraulic diameter(mm)	12
Outlet-Pressure profile multiplier	1
Backflow turbulence intensity (%)	15
Backflow hydraulic diameter(mm)	160

Solution schemes used

The numerical approach employed for solving this system of multiple equations utilizes a coupled scheme. This scheme solves all governing equations. (Pressure, momentum, turbulence kinetic energy, species concentrations of C₁₀H₂₂, O₂, CO₂, H₂O, and soot, and energy) simultaneously. For enhanced accuracy, a second-order spatial discretization is implemented. To accelerate convergence towards stable-state solution, a global time scaling technique is combined with a pseudo-time scaling technique. That tracks the actual time progression of the simulation. Finally, the solution is initialized using a hybrid approach.

3.15.3. ANSYS fluent meshing watertight (polyhedral mesh)

The Ansys Fluent Meshing Watertight Geometry workflow is a structured process designed to efficiently generate high-quality computational fluid dynamics (CFD) meshes from clean watertight CAD geometries. It's ideal for generating meshes for internal flow simulations within pipes. Step-by-step process for creating a watertight mesh for a multiple cylindrical pipe geometry in ANSYS Fluent Meshing.

Import geometry: This involves importing the 3D CAD model or geometry that represents the physical system to analyze.

Add Local Sizing: Local mesh sizing refers to the ability to specify different mesh element sizes in different regions of the geometry. This is useful for finer mesh in critical areas, such as regions with high gradients or complex geometrical features, to capture the necessary details. Also Defining local sizing allows for a more efficient mesh, concentrate the

computational resources where they are most needed, rather than using a uniform mesh size throughout the entire domain.

Generate Surface Mesh: This step involves creating a surface mesh, which is a discretization of the 3D geometry into smaller, interconnected surface elements (quadrilaterals). Serves as the foundation for the subsequent volume resolution of the surface directly impact on quality and accuracy of the final volume mesh.

Describe Geometry: providing additional information about the geometry, such as identifying different surfaces, edges, or vertices. Can be used to apply boundary conditions, define regions, or specify other simulation-specific properties. Accurately describing the geometry.

Apply Share Topology: the process of identifying and connecting common surfaces or edges between adjacent regions or components of the geometry. This step is crucial for ensuring a seamless transition between different parts of the model, which is essential for accurate simulation results. This share topology helps maintain the integrity of the geometry and ensures that the mesh generation process can be carried out effectively.

Enclose Fluid Regions (Capping): In the context of computational fluid dynamics (CFD), the fluid regions need to be clearly defined and enclosed within the computational domain. Capping involves adding virtual surfaces or boundaries to enclose the fluid regions, ensuring that the fluid flow can be properly simulated.

This step is particularly important for open or partially enclosed geometries, where the fluid domain needs to be explicitly defined for the analysis.

Create Regions: Regions are defined areas or volumes within the computational domain that are associated with specific properties or boundary conditions. crucial for applying the correct boundary conditions and material properties during the simulation.

Update Regions: After the initial region creation, it may be necessary to update or refine the region definitions based on the specific simulation requirements or the results of the initial analysis. This step allows to adjust the region boundaries, merge or split regions, or modify the properties associated with each region. Updating regions is an iterative process that can help improve the accuracy and relevance of the numerical model.

Add Boundary Layers: Boundary layers are thin regions near solid surfaces where the flow is strongly affected by viscous effects. Adding boundary layers to the mesh ensures that the simulation can accurately capture the velocity gradients and other flow phenomena near the

walls. Proper boundary layer modeling is particularly important for simulations involving boundary layer separation, turbulence, or heat transfer.

Generate the Volume Mesh: The volume mesh is the final discretization of the computational domain, where the entire 3D space is divided into smaller, interconnected volumetric elements, the volume mesh generation step builds upon the previously created surface mesh and incorporates the defined regions, boundary layers, and other simulation-specific requirements. The quality and resolution of the volume mesh directly impact the accuracy and convergence of the numerical simulation.

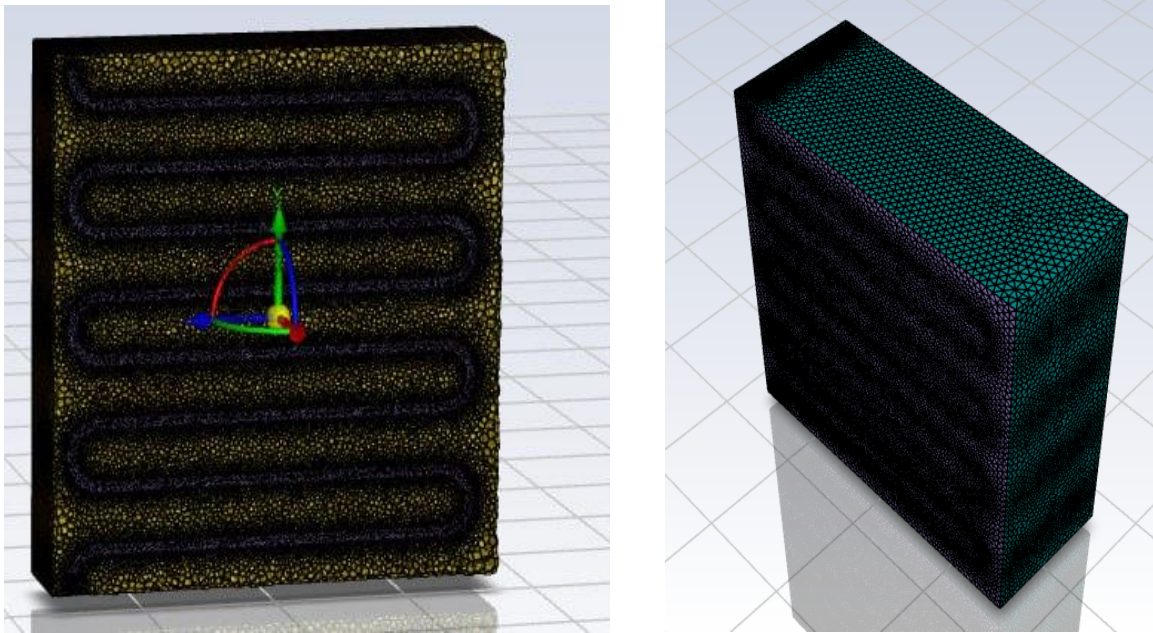


Figure 3-16: Polyhedral mesh multiple cylindrical pipe

Table 3-12: Boundary condition

Energy	ON
Viscose	k-epsilon(standard)
Used Material	<ul style="list-style-type: none"> ✓ Fluid: (water-liquid- H₂O), air ✓ Solid (aluminum)
Cell zone	Inlet-cooling pipe(water-liquid)
Boundary condition	<ul style="list-style-type: none"> ✓ P-inlet: T⁰(298,296,294, 292k) ✓ Gas-inlet: velocity(10m/s), T⁰(1235k)
Solution initialization	Hybrid
Run calculation	Iteration (30)

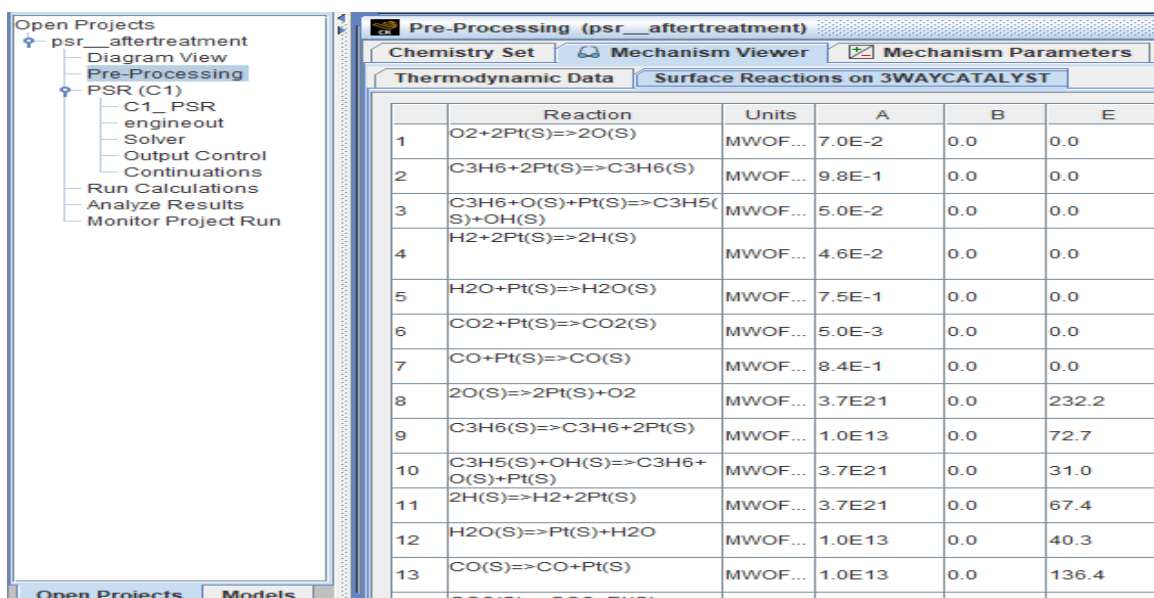
3.16. Engine exhaust-after-treatment with a transient inlet flow

This sample stores the engine-out conditions as a function of time in a text file using tabs to separate each line. The contents of file are read by a user-editable subroutine, which then uses the information to create a transient possible on stirred reactor model by extracting the temperature, instantaneous flow rate, and time-dependent intake composition.

Simulating a 3-way catalytic converter, where reactor removes pollutants like NO_x, CO, and HC over surface reactions on a platinum/rhodium based catalyst. Ready-to-use in Chemkin Interface, this sample user routine eliminates the required for a FORTRAN compiler. Customizing the sample user routine requires appropriate FORTRAN compiler on the computer running Chemkin. This enabling users to modify the subroutine's code by reconstructing it for easy Chemkin integration. The pre-compiled routine offers adaptability in modifying engine-out data (inlet composition, temperature, flow rate) without recompiling the user routine. This allows for quick updates to the simulation input.

3.16.1. Project setup

Featuring a streamlined design with a single gas inlet, this reactor utilizes a perfectly-stirred reactor (PSR) model to analyze rate of reaction. Occurring in the exhaust system. The model can be used to predict the performance of the after-treatment system under different operating conditions, Analyzing exhaust gas properties like temperature, pressure, and composition is the focus of this reactor setup. A sample user subroutine (psr-after-treatment.ckprj) in the Chemkin installation's user routines defines the inlet conditions



	Reaction	Units	A	B	E
1	O ₂ +2Pt(S)=>2O(S)	MWOF...	7.0E-2	0.0	0.0
2	C ₃ H ₆ +2Pt(S)=>C ₃ H ₆ (S)	MWOF...	9.8E-1	0.0	0.0
3	C ₃ H ₆ +O(S)+Pt(S)=>C ₃ H ₅ (S)+OH(S)	MWOF...	5.0E-2	0.0	0.0
4	H ₂ +2Pt(S)=>2H(S)	MWOF...	4.6E-2	0.0	0.0
5	H ₂ O+Pt(S)=>H ₂ O(S)	MWOF...	7.5E-1	0.0	0.0
6	CO ₂ +Pt(S)=>CO ₂ (S)	MWOF...	5.0E-3	0.0	0.0
7	CO+Pt(S)=>CO(S)	MWOF...	8.4E-1	0.0	0.0
8	2O(S)=>2Pt(S)+O ₂	MWOF...	3.7E21	0.0	232.2
9	C ₃ H ₆ (S)=>C ₃ H ₆ +2Pt(S)	MWOF...	1.0E13	0.0	72.7
10	C ₃ H ₅ (S)+OH(S)=>C ₃ H ₆ +O(S)+Pt(S)	MWOF...	3.7E21	0.0	31.0
11	2H(S)=>H ₂ +2Pt(S)	MWOF...	3.7E21	0.0	67.4
12	H ₂ O(S)=>Pt(S)+H ₂ O	MWOF...	1.0E13	0.0	40.3
13	CO(S)=>CO+Pt(S)	MWOF...	1.0E13	0.0	136.4

Figure 3-17: Surface reaction on 3-way catalyst

This chemical mechanism describes reactions on a Pt/Rh three-way catalyst. It includes NO reduction on Pt, CO oxidation on Rh, and unburned hydrocarbon (C_3H_6) oxidation on Pt. published work serves as the foundation for this response mechanism (Design, 2016). Recommendation for a 75% Pt and 25% Rh catalyst surface, this reaction mechanism accounts for the unique activation energies associated with this specific composition. This chemistry set neglects gas-phase kinetics. Thus, the gas-phase kinetics input file consists of the following, This system contains nine species (O, H, C, N, Rh, Pt) but, no reactions observed between these elements and the following molecules: C_3H_6 , O_2 , NO_2 , H_2 , CO_2 , H_2O , CO , NO , and N_2 . The chemistry that takes place on a single material named 3way-catalyst, which has two site types, each of which represents a different metal Platinum and Rhodium is described. Surface occupancy in the input file defines how molecules interact with the catalyst. Platinum has 18 possible sites, with Pt(S) acting as unoccupied site. $C_3H_6(S)$ is the only species capable of occupying two Pt sites simultaneously. Rhodium, with its simpler chemistry involving only 5 surface species, has Rh (S1) as its unoccupied site. For some surface species, thermochemical data are available, whereas placeholder values are available for others. Since all surface reactions are irreversible, rates for reverse reactions cannot be determined using any of the thermochemical data. One significant observation is that the mechanism's platinum site density ($2.04e^{-9}$ mol/cm²) significantly matches the value determined using solid platinum features ($2.717e^{-9}$ mol/cm²). For chemistry in order to explain some of the effects of the catalyst material's high surface area. When implementing this method in other systems, this factor should be taken into consideration.

47 irreversible events, incorporating interactions between attached species, simple and dissociative adsorptions, and simple and associative desorption, are described for the oxidation of C_3H_6 (or UHCs) on platinum. The latter comprise different division of adsorbed hydrocarbon species and oxidative reactions for deposited hydrocarbon species, ranging from a global description of $C_3H_5(S)$ oxidation to more step-wise oxidation reactions for various hydrocarbon pieces by hydrogen transfer to Pt(S) species. Five reactions involving NO reduction on platinum and nine more involving CO oxidation and NO reduction on rhodium are detailed. All of the reactions involve adsorptions, desorption, and interactions among adsorbed species. Sticking coefficients are used to characterize some reactions, reaction-order overrides are present in some reactions, and activation energy for a reaction sometimes fluctuates significantly depending on how much of the surface is covered by one or more species. This all on samples2023\psr\after-treatment.

Table 3-13: Psr-after-treatment input parameter

Parameters	Values
Project setup name	psr-after-treatment.ckprj
Reactor volume	1400cm ³
Reactive (internal) surface area	59000cm ³
Initial temperature of reactor	296.15 K (23°C)
Pressure	1 atm
System is treated	Adiabatic(no heat loss)
Specify O(S)	Platinum
Specify CO (S1)	Rhodium
Site species Pt/Rh	1.0
End time of simulation	100 sec
maximum Solver Time Step	1 msec
Time Interval to printing the solution	10 sec
Time Interval for Saving Data	1 sec.

3.16.2. Configuration of reactor

Within the Chemkin interface, under the "C1_PSR" panel. The Reactor Physical Properties tab, choose "Solve Gas Energy Equation" as the problem type. Additionally, select the Transient Solver option. PSR model a zero-dimensional reactor model, meaning it does not consider spatial variations in temperature or species concentrations. Instead, it assumes that there is perfect mix in the reactor surface, and therefore the temperature and species concentrations are uniform throughout the reactor. Solving the gas energy equation allows the PSR model to determine the heat and species concentrations at each time step, taking into account the heat release or absorption due to the chemical reactions occurring in the reactor

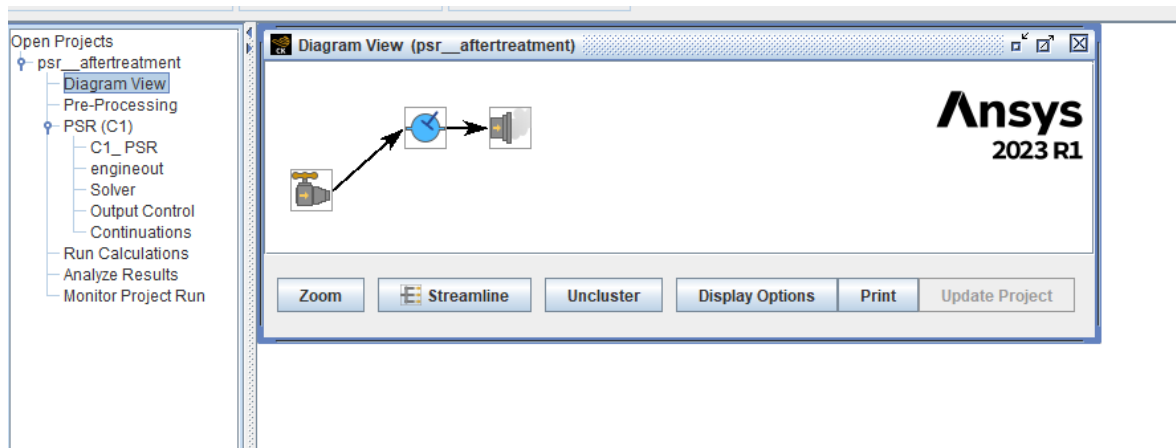


Figure 3-18: Perfectly-stirred reactor model (PSR).

The reactor's internal space, equivalent to the empty volume within the converter's honeycomb or porous media. Also known pore volume (the volume of empty space or void within the material which is not occupied by the solid phase) (the space with the reactor honeycomb structure not filled with catalyst) this volume is constant and is used to calculate Average time reactants spend in the reactor. Total volume of honeycomb, multiply length, width and height of honeycomb (porous media), this volume includes both solid catalyst support and empty space (void). Volume of solid reactor is multiplication of density and mass of solid catalyst Therefore Reactor Void volume is subtraction of total volume of honeycomb from volume of solid reactor. The reactor volume is specified as 1400 cm^3 , internal porosity of the converter media. This volume is constant and is used to calculate the Average time reactants hold on the reactor Catalytic reactions a 3-way catalytic converter occur on the surface of the catalyst material, typically a precious metal such as platinum (Pt) or rhodium (Rh).

The rate of these surface reactions have direct relationship with the surface area available on the catalyst. A larger reactive surface area provides more sites for the reactants (NO_x , CO, and unburned hydrocarbons) to interact with the catalyst and undergo the desired conversion reactions. The converter's internal reaction zone, characterized by its surface area is 59000 cm^2 , which is used to calculate the rate of reaction between the reactants and the surface of the converter. The initial temperature of the reactor is set to 294.15K and the system operates under atmospheric pressure. This simplifies analysis and allows for a consistent starting point for the simulation. For this simulation, the reactor is considered to be thermally insulated ensures that the energy balance is maintained without any heat exchange with the surrounding

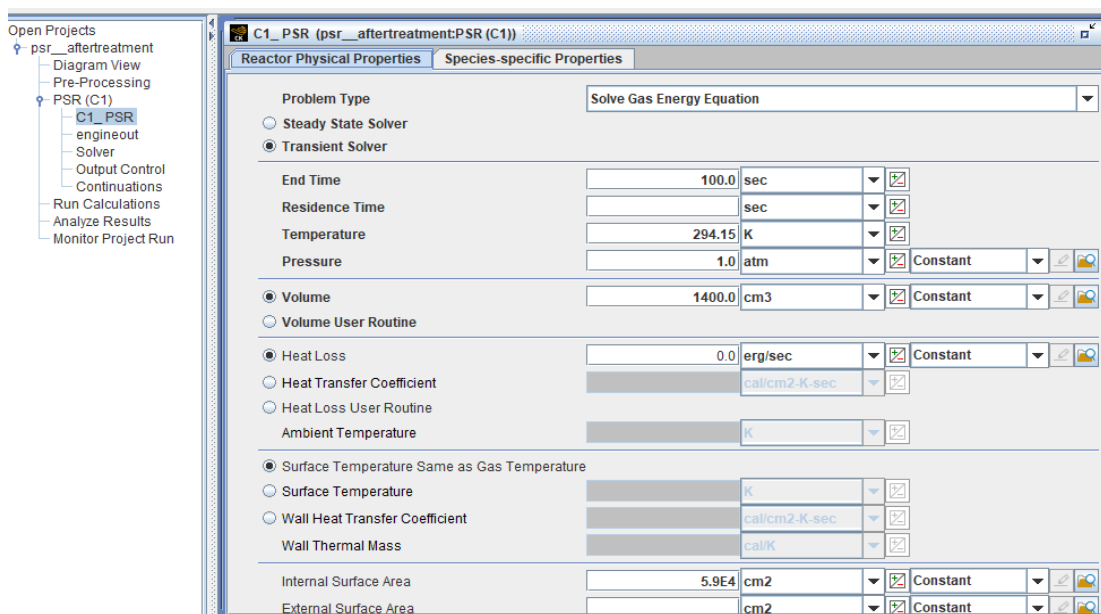


Figure 3-19: C1_PSR (psr_after_treatment) (C1)

Chemkin C1_PSR panel allows specifying the converter's initial state. On the Species-specific Properties tab, air is assumed as the starting composition before exhaust gas enters the system. This initial gas composition is entered under the Initial Gas Fraction sub-tab. Surface site fractions, while are estimated based on the knowledge of the surface chemistry or over preliminary mechanism testing. Giving initial estimate for surface site occupancy can improve convergence in Chemkin. Without this input, Chemkin assigns an even distribution of sites. Identify O(S) as the site for the platinum catalyst surface at the beginning, and CO (S1) for the rhodium portion. These dominant site species are set to a value of 1.0 on the Surface Fraction sub-tab to define the initial state of the catalyst surface.

3.16.3. Engine-out

The inlet, named engine-out is to reflect its source, utilizes a user-defined routine in Chemkin. This routine, accessed through the Stream Properties Data tab within the engine-out panel, inlet data (composition, flow rate, temperature) from a pre-programmed Chemkin subroutine. This subroutine reads a text file named engineout.txt. The inlet conditions, similar to real engine exhaust data (shown in Appendix I), change over time due to variations in engine load. These variations can impact exhaust properties like flow rate and composition. This setup provides mole or mass fractions for a limited number of key species (CO, NO, UHCs, and O₂).

For simplicity, assume the remaining gas composition of N₂, with C₃H₆ representing the unburned hydrocarbons. Additionally, the panel's Use SCCM for User Inlet Routine option

is selected. This signifies that flow rates are provided in volumetric units (SCCM) instead of mass units.

3.16.4. Solver panel

The simulation runtime is set to 100 seconds within the Chemkin solver's Basic tab. where the input data covers a longer timeframe, this duration is sufficient for our demonstration. The solver configuration includes a maximum time step of 1 millisecond, with solution data printed to the text output file every 10 seconds and saved every 1 second. No additional controls are required on the Continuations panels for this specific problem.

3.17. Catalyst selection

Three main component used in catalytic convertor, substrate, catalyst, and washcoat

3.17.1. Catalyst

Internal combustion engines produce harmful pollutants like HCs, CO, and NO_x during combustion. To address this, vehicles use catalytic converters. These devices employ catalysts to trigger chemical reactions that transform these pollutants into less hazardous substances through redox reactions. Three-way catalytic converters are widely used to tackle all three pollutants simultaneously.

The honeycomb design of the converter's internal structure, known as a monolithic catalyst. This structure maximizes the surface area of the catalyst layer exposed to exhaust gases. As honeycomb with large surface area. This surface area, the more exhaust gas can interact with the catalyst. The catalyst itself is a combination of metals deposited on the honeycomb. Rhodium takes the lead in reduction reactions, a small amount of Platinum is also present, contributing to both processes. These reactions occur directly on the metal surfaces of the catalyst. The honeycomb structure provides a stage for the catalyst to perform its reaction. By maximizing the surface area, the converter ensures the most efficient interaction between exhaust gases and the catalyst, leading to optimal conversion of Pollutants (Balaji et al., 2018)

3.17.2. Substrate

High surface area and some ability for heat and mass transfer alterations are features of ceramic honeycomb substrate designs. When more flexible designs with efficient thermal management are added, additional benefits of reduced emissions can be realized. The standard way of producing cordierite honeycomb substrates is extrusion.

A the honeycomb monolith, usually made by extrusion, having thousands of straight, parallel, flow-through channels covered in noble metals (Al_2O_3), which are in charge of catalytic reactions.

The substrate have two purposes in the simple channel design, first, it maintains the catalyst in place; second, it enhances the catalyst's interaction with exhaust gases. This is made possible by the limitations of the extrusion process, which result in thin barriers separating the numerous channels. In order to achieve low thermal inertia and effective heat transfer, washcoat needs to be applied to the substrate. Boost the surface area relative to the volume (Kovacev et al., 2021).

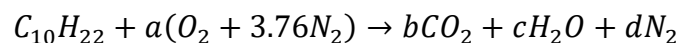
3.17.3. Catalytic coating material (washcoat)

The washcoat is an oxide barrier with pores, coating on the substrates from a mixture of diluted water, dried out also heated. It acts as a carrier for a precious metal catalyst. The most widely used substance for washcoat is aluminum oxide. Washcoat is to offer the significant surface area required for the distribution of catalytic metals, which is critical for the stability and catalytic activity of the catalyst. Furthermore, the washcoat has the ability to isolate and prevent unwanted interactions between the various parts of a complex catalytic system.

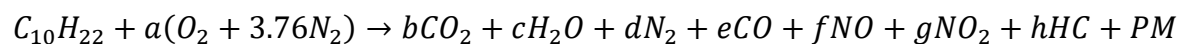
Inorganic base metal oxides such as TiO_2 , SiO_2 , and Al_2O_3 are typical washcoat materials. Thermal stability are characteristics of good washcoat materials (Majewski, 2022). Aluminum oxide has high wear resistance qualities and is a highly hard substance. Its helpful stiffness-to-weight ratio, minimal thermal expansion, thermal stability, and high corrosion durability are all present (Rajendran et al., 2020).

Combustion of Diesel fuel in diesel engine and its products

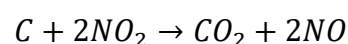
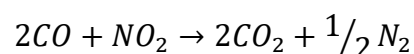
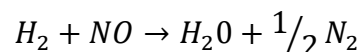
1. For Complete combustion

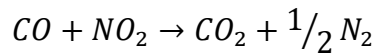


2. Incomplete combustion(with emission)

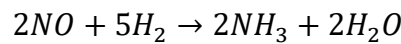
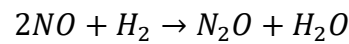
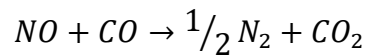
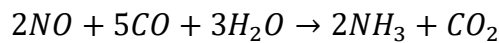
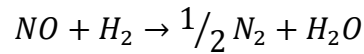
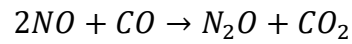


Reaction takes place during conversion





Platinum they accelerate the oxidation of carbon dioxide and hydrocarbons, with platinum being particularly active in this process. In one or more of the subsequent processes, rhodium facilitates the reaction of NOx.



$$\Delta CO\% = \frac{CO_{ref} - CO_{sol}}{CO_{ref}} * 100$$

$$\Delta NO_x\% = \frac{NO_{xref} - NO_{xsol}}{NO_{xref}} * 100$$

3.18. Temperature range of catalytic convertor

Primary elements of an emission control system's overall durability are its mechanical and emission performance. The catalyst coating's quality and other operational factors, including temperature or the amount of catalyst chemicals in the exhaust flow, affect how long an emission lasts. The necessary mechanical durability must be provided by the catalytic converter design. Under the operating circumstances of the vehicle's exhaust system, which include exposure to high temperatures and thermal shock, dampness and corrosive environments, as well as mechanical vibration, catalytic converters must offer sufficient protection for the substrate. If the converter's heat losses are significant, they must be taken into account when designing the converter. Close-coupled gasoline converters are often double-walled and adjusted for cold start hydrocarbon performance, with either air gaps or ceramic fiber insulation. For diesel catalytic converters, cold start and low temperature performance have also become more crucial in both light- and heavy-duty applications. Diesel converters should be positioned close to the exhaust manifold or exhaust system insulation should be added due to the low temperature of diesel exhaust gases in order to ensure adequate catalyst performance (Kahlon, 2016).

Table 3-14: Temperature range for specific condition in a catalytic convertor adapted

Operation	Temperature(K)
light-out	523.15 - 573.15
Best Operating	723.15 – 920.33
Pt burn	973.15
Alumina burn	1073.15 - 1173.15
Pt-Rd and pt-pd alloy form	873.15 - 973.15
Softening of ceramic monolith	1573.15 - 1673.15
A monolith of metal burns	1773.15 - 1873.15
Burning particles	>2173.15

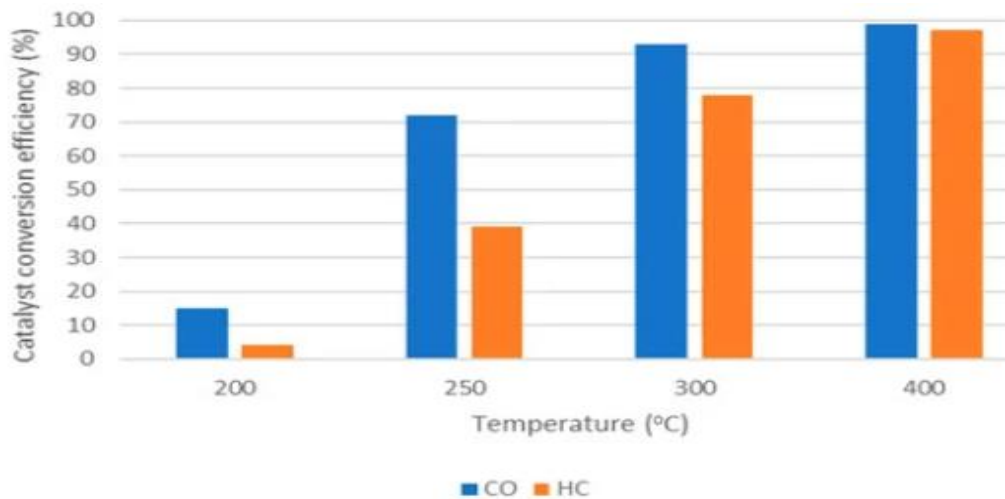


Figure 3-20: Conversion efficiency for CO and HC as a function of temperature

The graph indicates that at sufficiently high temperatures (between 350 and 450 °C), the steady-state conversion efficiencies of CO and HC are generally 95 percent or higher and 98–99 percent, respectively. High temperatures used to be a limiting factor for converter designs because they can cause sintering, which lowers the amount of metal available for catalytic reactions to occur and increases coating aging when the converter's gas inlet temperature rises above 700 °C (Kritsanaviparkporn et al., 2021).

3.19. Water cooling through single pipe

Temperature of water from ambient temperature should have to drop 292k(19 °C) in where the temperature of the tank drop at this temperature is drop as far as required to cool the tank temperature therefore to do that fan selection is important. In order to achieve to drop 30k of temperature from circulating water

3.19.1. Newton cooling law

which takes into consideration the temperature differential between the body and its surroundings, provides a linear differential equation controlling the rate of heat loss of a heated body (Keeratisiwakul et al., 2023).

Newton cooling law formula is given

$$-\frac{dQ}{dt} = k(T_{sur} - T_0) \quad (4.67)$$

$$-\frac{dQ}{dt} = k(T_{sur} - T_0)$$

$$-\frac{dQ}{dt}, \text{ is cooling state}$$

$$\frac{dQ}{dt} = mc \frac{dT_o}{dt}$$

Where:

- ✓ M_ mass of air 3600kg/hr
- ✓ C_ specific heat capacity of air 1005k
- ✓ T_o_ target temperature
- ✓ T_s_ surface temperature
- ✓ T_t_ time based temperature
- ✓ K_ cooling constant
- ✓ e: base of the natural logarithm (approximately 2.71828)
- ✓ σ : Stefan-Boltzmann constant ($5.67 \cdot 10^{-8} \text{ wm}^{-2} \text{ k}^{-4}$)
- ✓ θ_0 : Initial temperature of the object (in Kelvin)
- ✓ A_t: total surface area of the tank

$$A_t = A_1 + A_2 + A_3 = 2.25\text{m}^2$$

$$-mc \frac{dT_o}{dt} = k(T_{suf} - T_o), \frac{-k}{mc} dt = -kdt \quad (4.68)$$

$$k = \frac{k}{mc} \text{ cooling constant}$$

$$T_{(t)} = T_o + (T_s - T_o)e^{-kt} \quad (4.69)$$

$$k = \frac{4e\sigma\theta_0^3 A}{mc} = 0.02 \quad (4.70)$$

Table 3-15: Time based temperature variation

Time (sec)	Temperature (k)
0	300
0.7	299.88
6.7	298.9967
14.4	297.9981
23.6	296.99
34.6	295.9966
49.1	294.9965
69.6	293.9886
180	292.2186

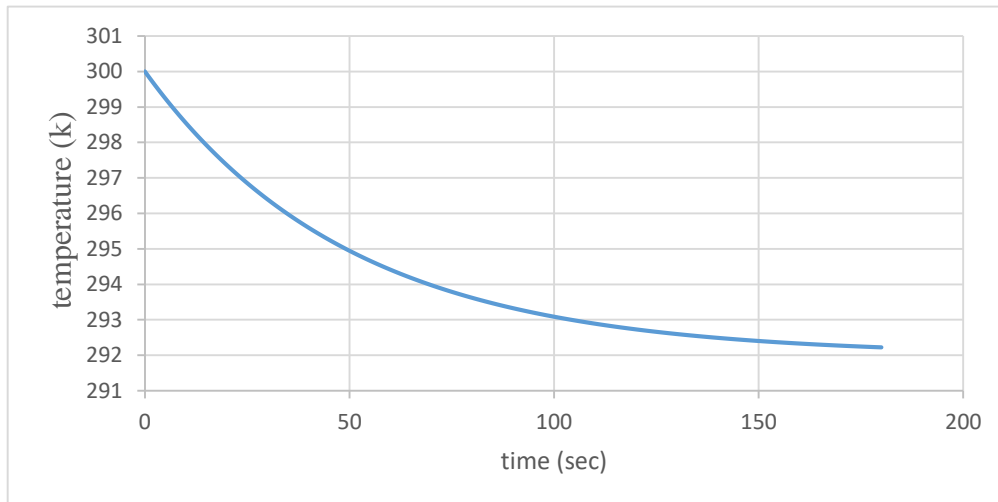


Figure 3-21: Temperature verses time

The graph indicate that the required temperature 292k (19 °C)of water is cold at a time of 180sec. at this time temperature drop from 298k to 292k (25 to19 °C). as far as fan ventilation is there.

CHAPTER FOUR

4. RESULTS AND DISCUSSIONS

4.1.. Results from ANSYS 2023 R1 fluent reaction

The contour of static temperature, pressure, and velocity are given below. The concentration of species, reactants and products in their mass fraction are also given. The results of NOx model and Soot model are also given below.

The static temperature: of the system varies from inlet to outlet. It increases toward the outlet as a reaction take place from 300 K to 1800 K.

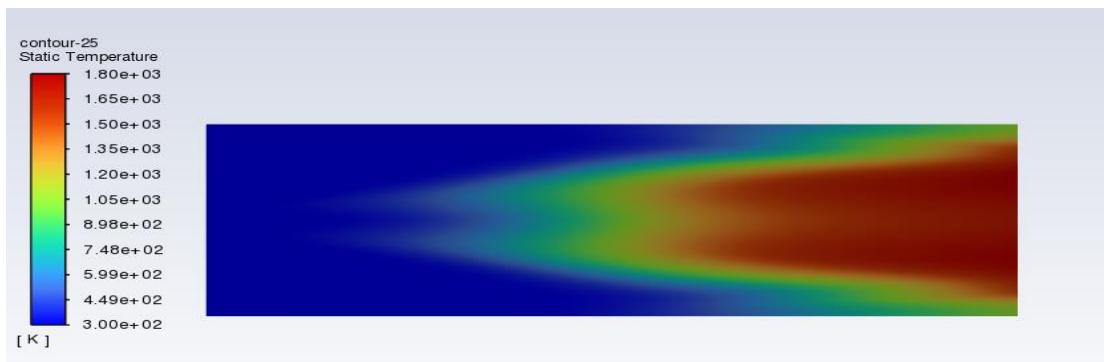


Figure 4-1: Contour static temperature

Pollutant NO (thermal or prompt): The thermal NO_x is the NO_x formed by the nitrogen present in the air. The prompt NO_x is formed by the reaction at the flame front. The NO concentration increases from the air inlet to the outlet, NO concentration peaks at the outlet where temperatures are highest and residence time is longest, The high NO concentration at the outlet indicates efficient combustion.





Figure 4-2: Contour Pollutant NO (thermal or prompt)

Mass fraction of $C_{10}H_{22}$ Concentration: will be greatest near the fuel inlet before it mixes with air and undergoes combustion. As the fuel and air mix and react, the mass fraction of unburnt fuel will decrease throughout the combustion chamber, being lowest at the outlet where the combustion products exit.

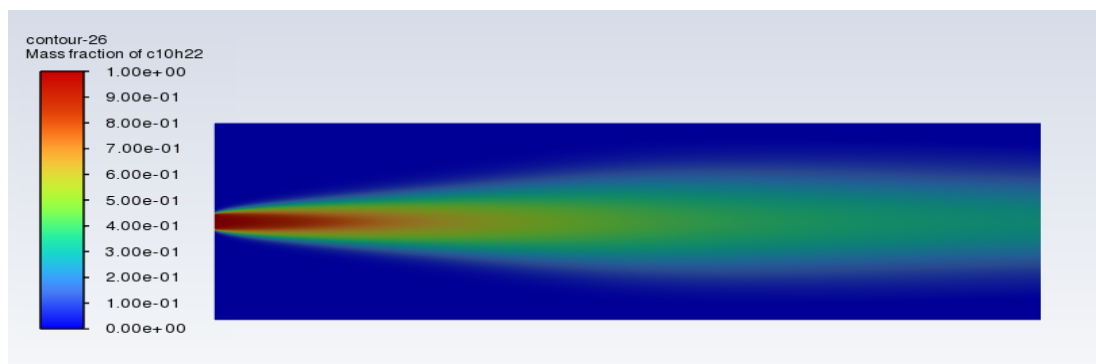


Figure 4-3: Contour Mass fraction of $C_{10}H_{22}$

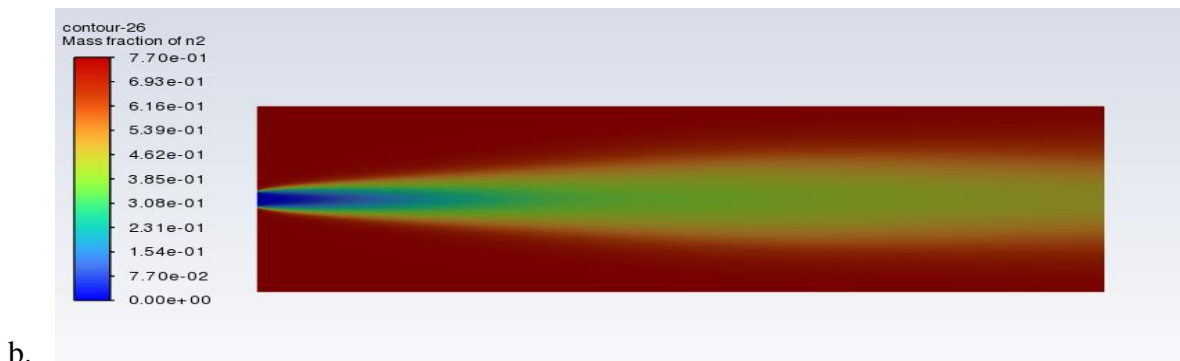
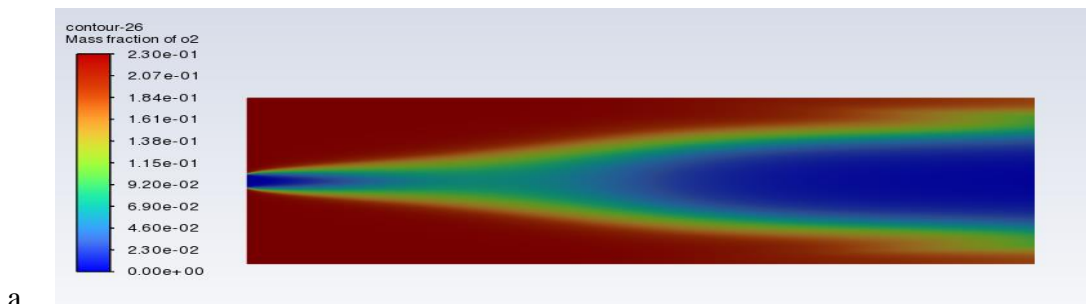
Rate of soot: As the combustion products reach the outlet, most of the soot has been oxidized, resulting in a lower soot concentration at the outlet

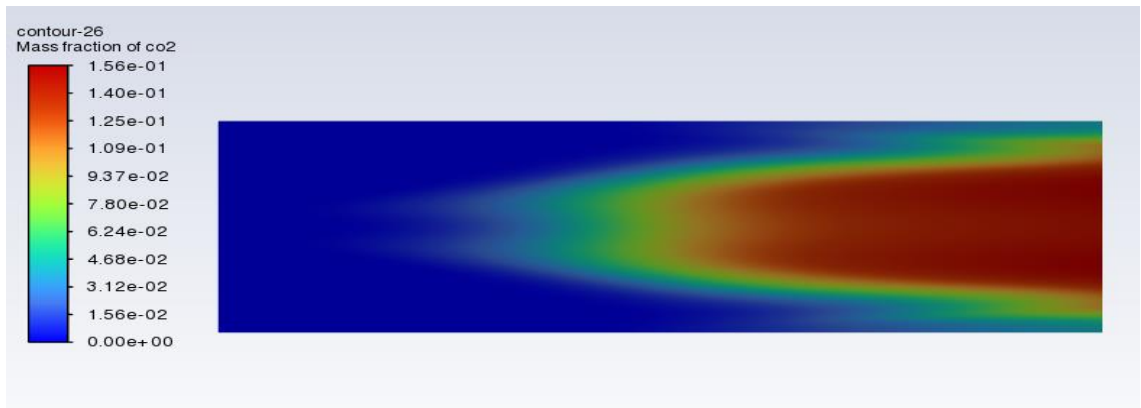
Soot accumulates at the outlet of combustion chambers due to incomplete combustion, lower temperatures, inadequate mixing, fuel characteristics, and chamber design. The figure below show some amount of soot is at outlet of combustion chamber



Figure 4-4: Rate of soot

Oxygen enters the chamber as part of the air intake, It will be more concentrated near the air inlet initially, but turbulence and mixing will distribute it throughout the chamber. Nitrogen also be distributed throughout the chamber due to turbulence and mixing. Its concentration might be slightly higher near the air inlet regions. The mass fraction of CO₂ is highest at the exhaust. as air with fuel react to produce CO₂ as a combustion product. At the fuel inlet, the mass fraction of CO₂ is very low, as the unburnt fuel has not yet reacted. Nitrogen will also be distributed throughout the chamber due to turbulence and mixing. Its concentration might be slightly higher near the air inlet regions. The mass fraction of H₂O increases as the fuel mixes with air and combustion occurs within the chamber, producing H₂O and CO₂



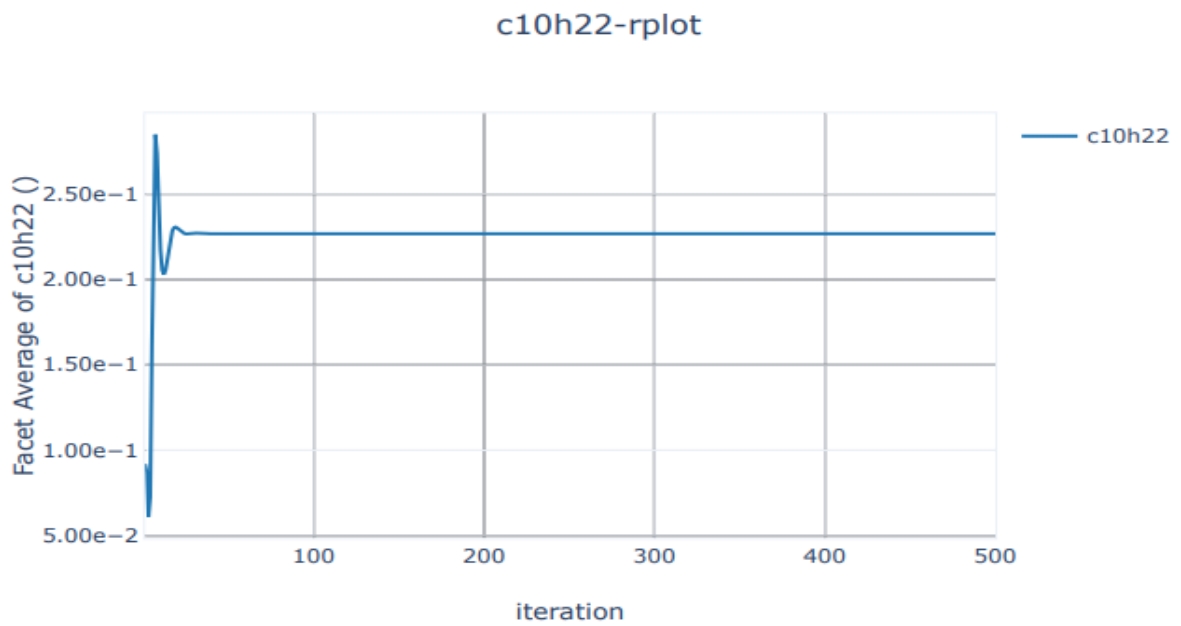


c.

Figure 4-5: Contour mass fraction of O₂, N₂, and CO₂

Table 4-1: Average mass fraction at combustion chamber outlet

No	Pollutant component	Ansys result
1	NO _x	0.0352337
2	Soot	0.03473795
3	C ₁₀ H ₂₂	0.02267992
4	O ₂	0.09229683
5	CO ₂	0.07120362
6	N ₂	0.6963224
7	H ₂ O	0.03206168



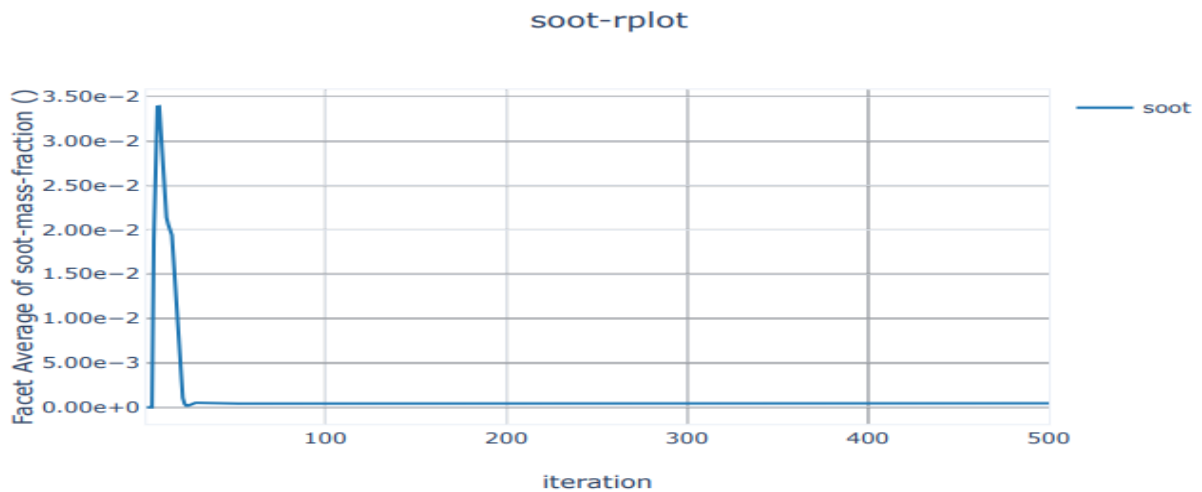


Figure 4-6: Mass fraction of $C_{10}H_{22}$, and soot

The high exhaust temperature of 1235K (962°C) is a critical concern when it comes to the design and operation of a catalytic converter. Catalytic converters are designed to operate within a specific temperature range, typically between 450-650°C, in order to maintain optimal catalytic activity and efficiency. This excess temperature of 312°C can have several detrimental effects on the converter's performance and longevity.

Firstly, the high temperature can lead to a phenomenon known as sintering. Sintering is a process in which the small metal particles or catalyst coatings within the converter begin to fuse together due to the high heat. As the surface area decreases, the contact between the exhaust gases and the catalytic materials is reduced, leading to a significant drop in the converter's efficiency. Additionally, the elevated temperature can accelerate the aging and degradation of the catalyst coatings. Responsible for facilitating the catalytic reactions that convert harmful exhaust emissions into less toxic substances. The high heat can cause the catalyst coatings to break down or lose their effectiveness over time, further compromising the converter's performance. To address this temperature discrepancy, one approach is to utilize multiple cylindrical pipes.

4.2. Cylindrical multiple pipe

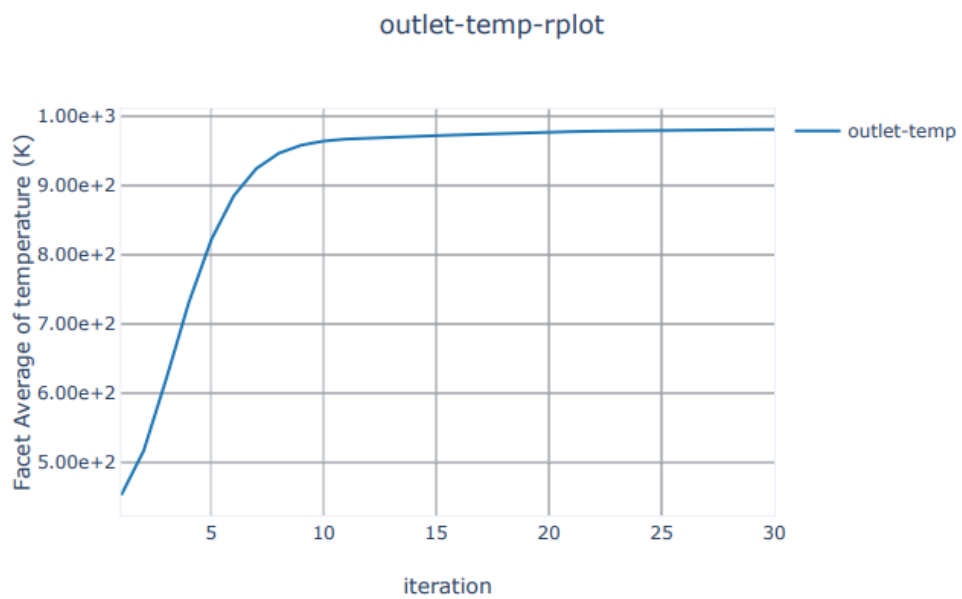
In- order to drop the hot exhaust temperature from engine- out enters to the compartment circulating water through the pipe the initial temperature of exhaust or wall temperature is 1235k (962°C). The room temperature of water was taken or pipe temperature is 298k (25°C), circulate through pipe drop temperature by convective heat transfer to 981.25k (708°C) figure (a) at the outlet of the gas domain. As far as the required temperature is not achieved the pipe temperature at inlet changed to 296, 294, 292k (23, 21, 19 °C) respectively

then the outlet gas domain temperature drop to 964, 929, 919k (691, 656, 646°C), figure b, c and d. at the pipe temperature inlet 292k the optimum temperature of gas domain is obtained. Next as far as the temperature of water is drop from 25°C to 19 °C, extra cooling system of water is required to.

Table 4-2: Temperature inlet and outlet gas domain

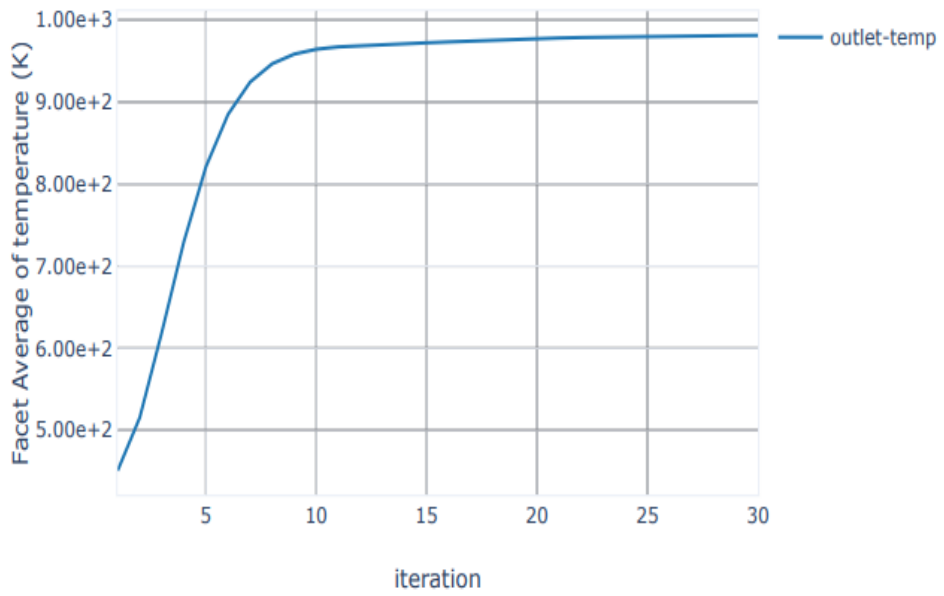
Number	Inlet-pipe temperature(k)	Outlet temperature(k)
1	298	981.25
2	296	963.3
3	294	929.14
4	292	919.61

outlet-temp-rplot



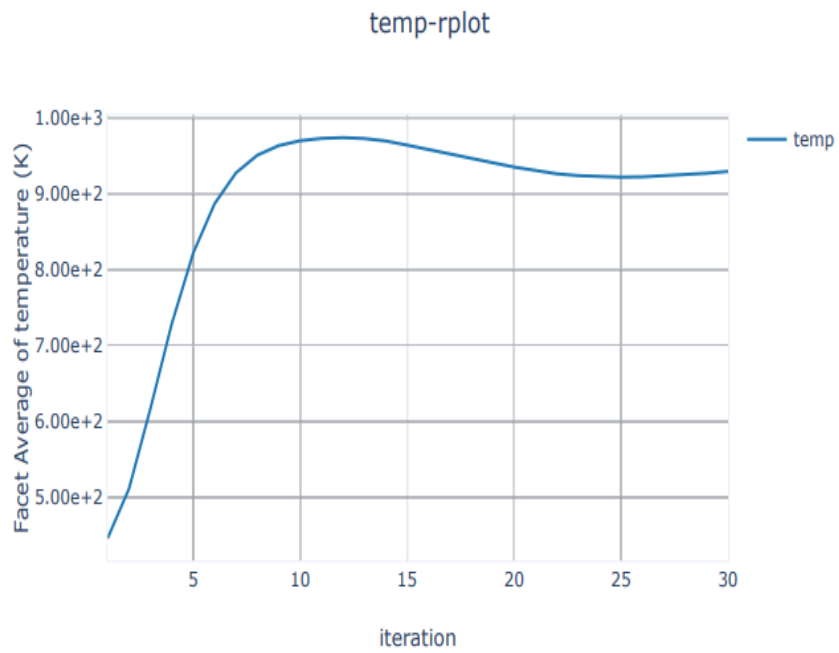
1

outlet-temp-rplot



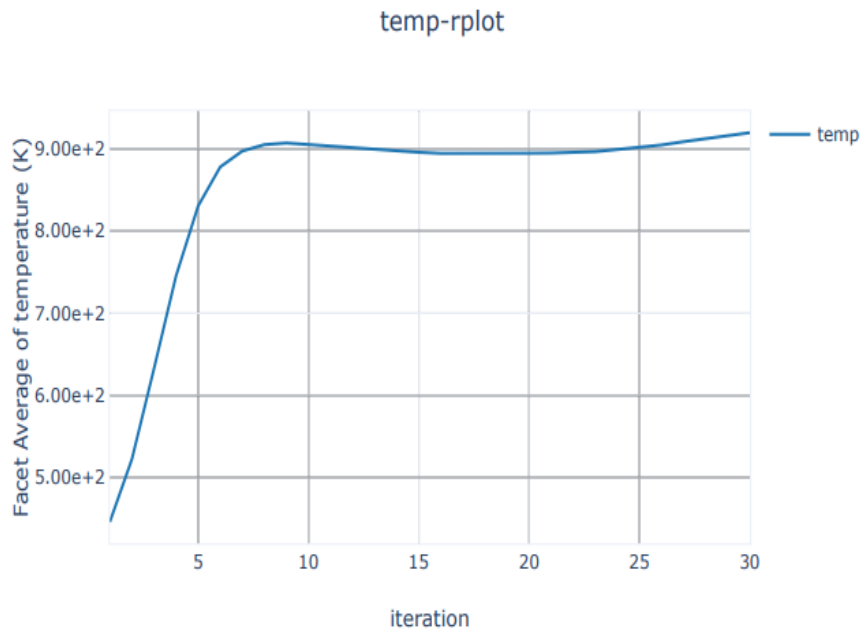
2

temp-rplot



3

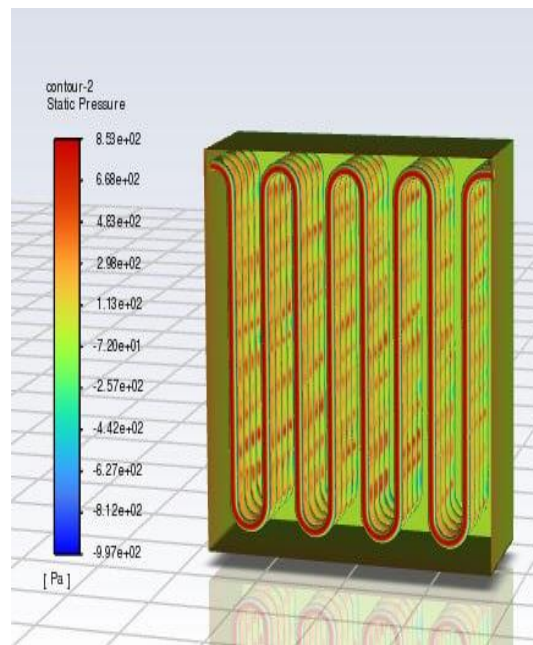
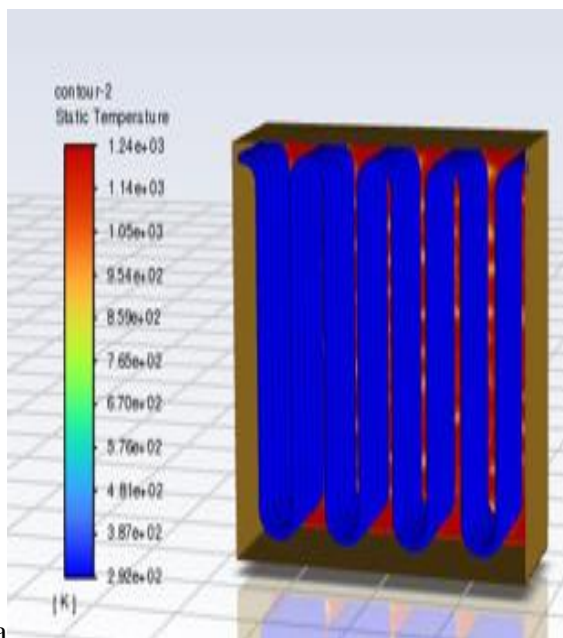
temp-rplot



4

Figure 4-7: temperature drop due to cold circulating water

The temperature contour indicate that 1235k inlet gas domain is drop along the pipe. The pipe temperature increases from 292k to 387k at outer pipe due to convective heat transfer



a

b.

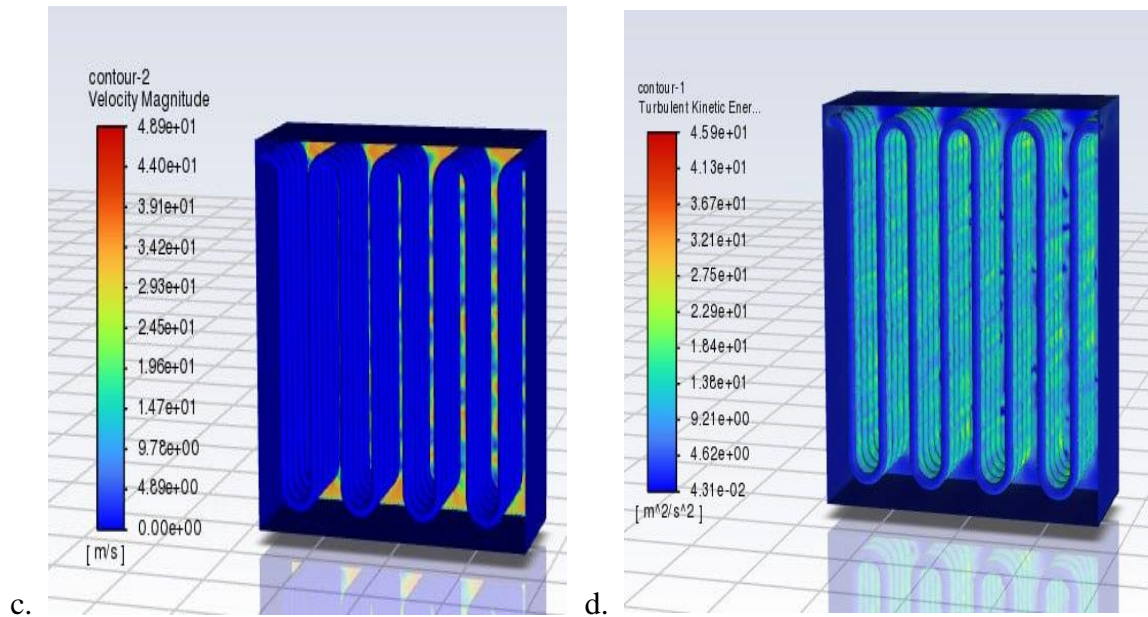
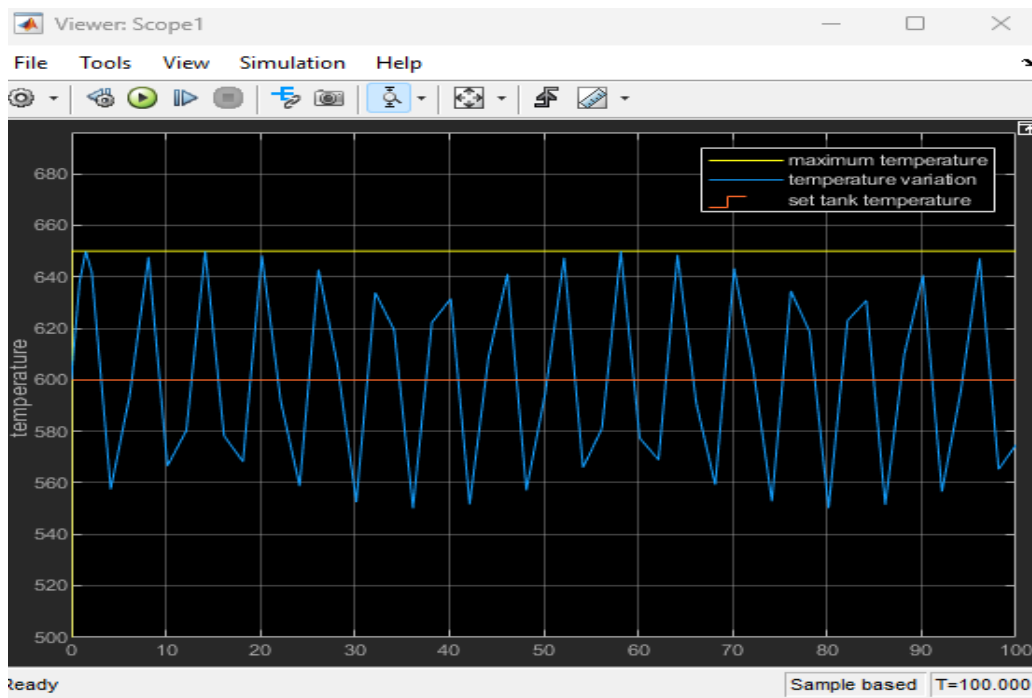
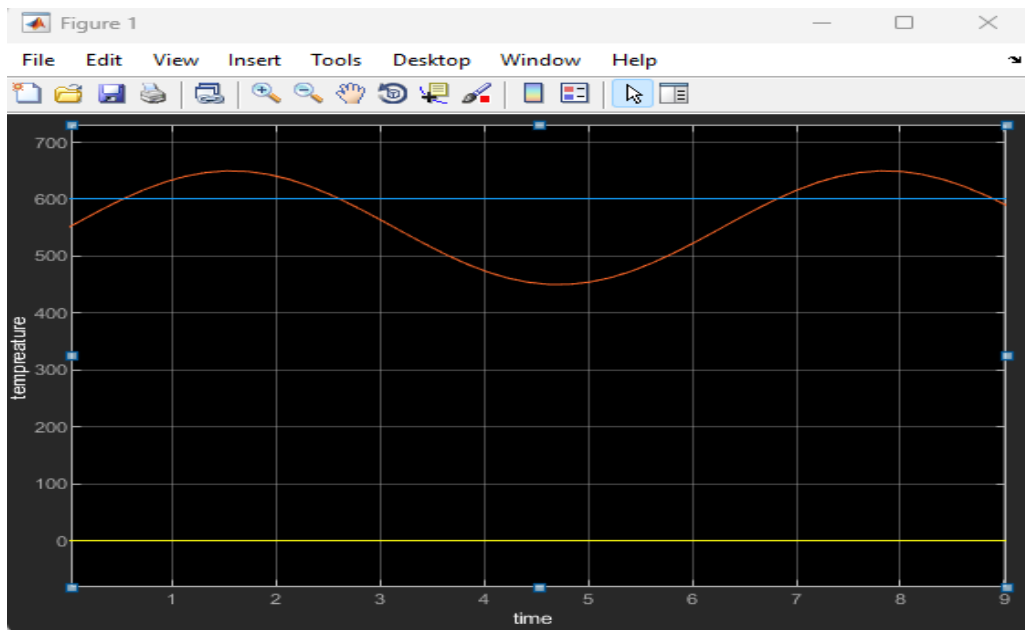


Figure 4-8: Pressure, temperature, turbulence kinetic energy and velocity distribution inside the multiple circular pipe

As long as the moderate temperature of catalytic convertor is obtained to keep the temperature variation temperature control system is model on open circuit on matlab/Simulink By using Simulink, the temperature control system can be effectively modeled and simulated, allowing for the optimization of the system's performance and the validation of the control algorithm's ability to maintain the tank temperature within the specified moderate range.

The tank component interacts with the heater and thermostat components within the overall temperature control system. The heater provides the heat input, while the thermostat controls the heater based on the tank temperature feedback. The external air temperature influences the heat loss through the tank walls.



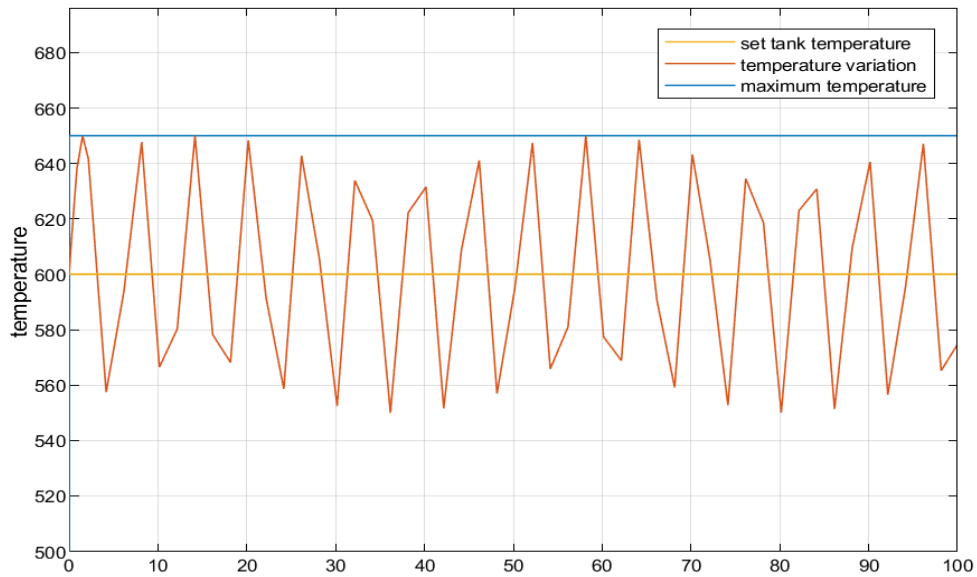
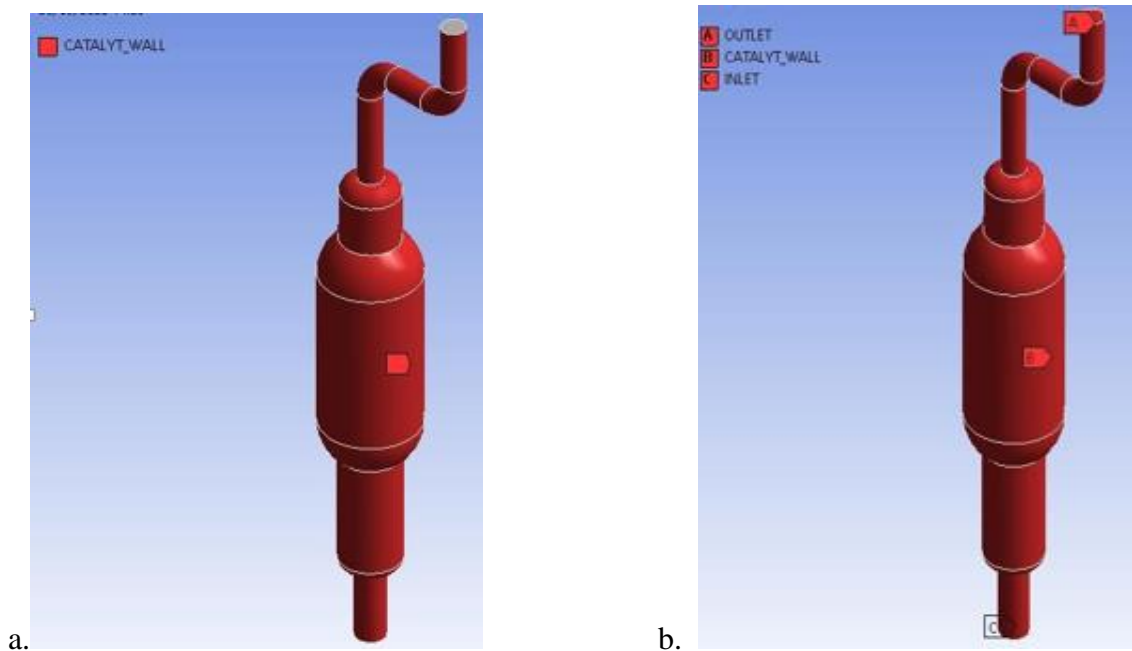


Figure 4-9: Temperature variation

4.3. Catalytic convertor

Catalytic wall and boundary condition, pressure contour and velocity streamline



Velocity distribution at the inlet 4.59m/s but at out increase to 18.3m/s this indicate velocity might decrease slightly at the inlet due to the flow restriction caused by the catalyst and pipe diameter. The pressure at the outlet(31.4pa) is lower than the pressure at the inlet(233pa). Throughout the converter, the exhaust gas experiences friction as it flows through the

channels and interacts with the catalyst. This friction causes a gradual loss of energy, leads to decrease in pressure.

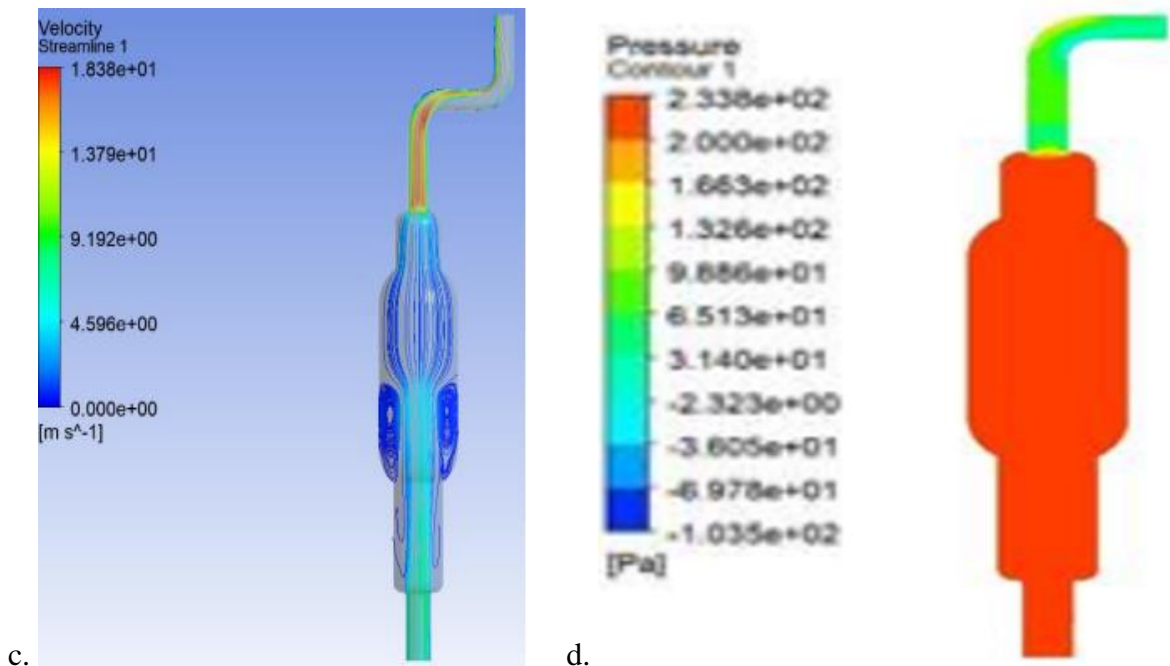


Figure 4-10: Catalytic wall, boundary condition, pressure contour, velocity streamline

4.4. The temperature versus time variation:

As the reduction reactions start, the temperature at the catalytic converter's input rises. on catalyst's surface are exothermic, which means that heat is released as a byproduct. Heat is released as a result of oxidation-reduction processes between the reactants, which include carbon monoxide and unburned hydrocarbons, and the catalyst.

At around 78 seconds, the catalyst reaches its maximal temperature on the figure 5-11 the temperature inside the catalytic converter reaches a high of 910 K, or roughly 637°C. The moment at which the catalytic reactions are most active and efficient, producing the most heat output, is correlated with this peak temperature.

The temperature profile and the location of the converter's peak temperature are largely dependent on the catalyst material and its design. Temperature Drop at the Outlet as it passes through the catalytic converter and the catalytic processes continue. The surroundings transmission nearby components are two of the reasons for this temperature drop.

Reduction of the reactants (HC and CO) during the transformation process into H₂O and CO₂. Potentially occurring endothermic events within the converter, such as steam reforming, may have a cooling effect. The significance of the catalyst minimal temperature

until temperature rises over around 500 K (227°C), the catalyst is ineffective. Pollutant conversion is greatly decreased and the catalyst loses its effectiveness below the light-off temperature. Temperature Production and Catalyst Efficiency, The three-way catalytic converter's overall performance depends on the exothermic nature of the catalytic processes. As a result of the heat produced during the reactions, the catalyst is kept at its ideal operating temperature and the pollutants' (CO, HC, and NO_x) conversion efficiency is sustained. However, excessive heat generation can also lead to thermal degradation of the catalyst, which can decrease its long-term performance and durability. The temperature variation within the catalytic converter is a dynamic process that depends on the interplay between the exothermic catalytic reactions, heat transfer mechanisms, and the design of the converter. Understanding and optimizing the temperature profile is essential for achieving effective emissions reduction and ensuring the long-term reliability of the catalytic converter system.

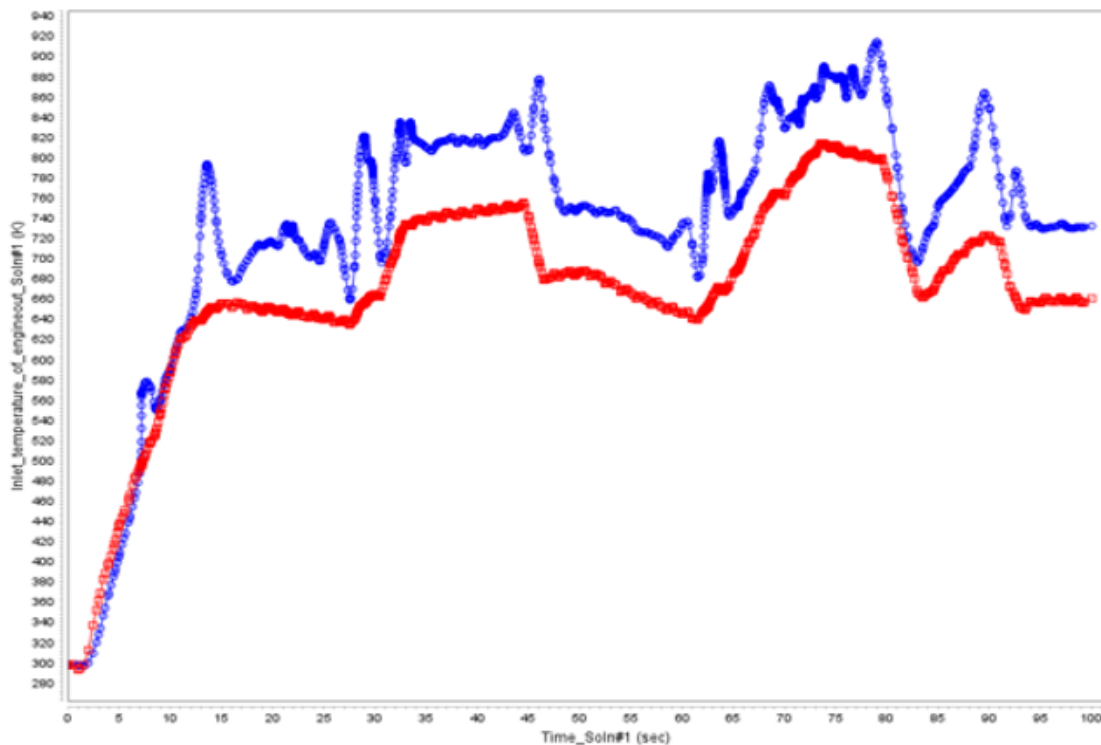


Figure 4-11: Temperature versus time

4.5. Oxygen concentration (in mass-fraction)

The starting point content is highest when catalytic converter initially turned on. This is because engine functioning in high air combustion, where there is excess air (and thus, oxygen) compared to the amount of fuel. Catalytic Reactions Consumption of Oxygen A drop in the concentration of oxygen occurs exhaust gases flow over catalytic converter. This

results from the oxygen being used up in catalytic oxidation reactions, which turn CO and HC to CO₂ and H₂O

Rate of oxygen consumption depends on the activity and efficiency of the catalyst, When catalytic converter is fresh and the exhaust gas is lean (excess oxygen), the oxygen can be stored within the catalyst by being adsorbed onto the catalyst surface. This oxygen storage capacity helps to maintain a sufficient oxygen supply during the periods of rich (excess fuel) exhaust gas conditions.

As the catalyst ages and the exhaust gas composition oscillates between lean and rich, the stored oxygen can be released or liberated from the catalyst surface. Temporary Oxygen Concentration Rise, When the exhaust gas becomes rich (excess fuel) and there is insufficient oxygen in the gas stream to fully oxidize the CO and HC, the liberated oxygen from the catalyst storage can react with the excess CO and HC. This temporary rise in oxygen concentration occurs before the liberated oxygen is eventually consumed by the catalytic reactions. Oxygen Concentration Stabilization As long as the catalytic converter runs, the amount of oxygen in the exhaust gas tends to stabilize, while there may be some variations based on the catalyst's condition and the engine's operating parameters. Maintaining a somewhat constant oxygen content is essential for the effective functioning of device and this is made possible by catalyst's capacity to store and release oxygen.

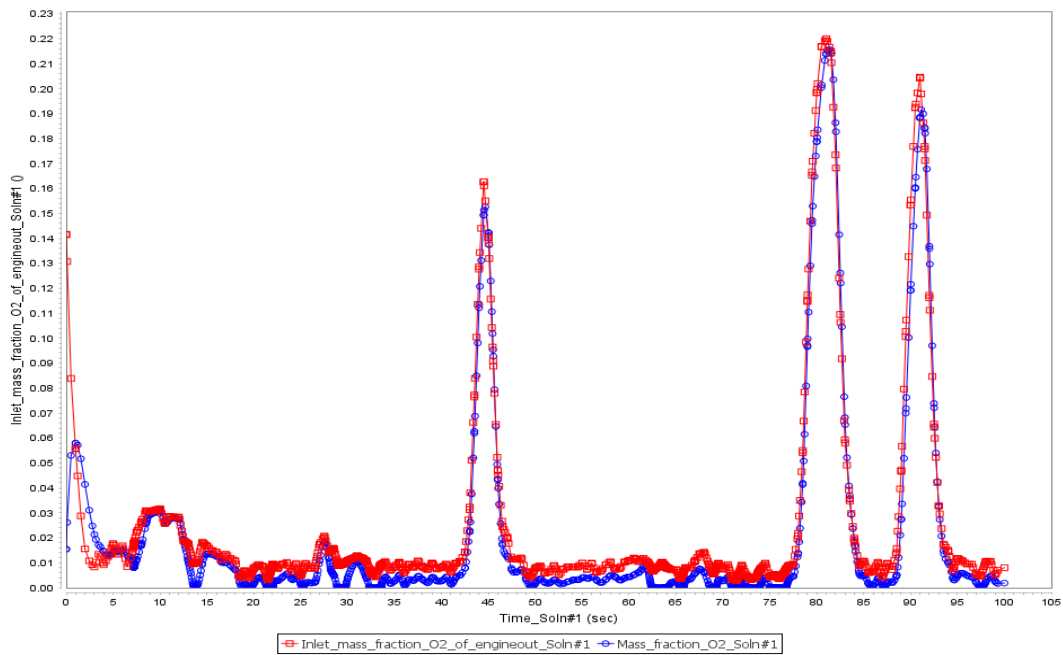


Figure 4-12: Oxygen concentration (mass fraction)

4.6. Nitrogen concentration (in mass fraction)

The mass fraction of nitrogen at the outlet of the catalytic converter remains relatively constant compared to the inlet, because does not participate in the catalytic reactions

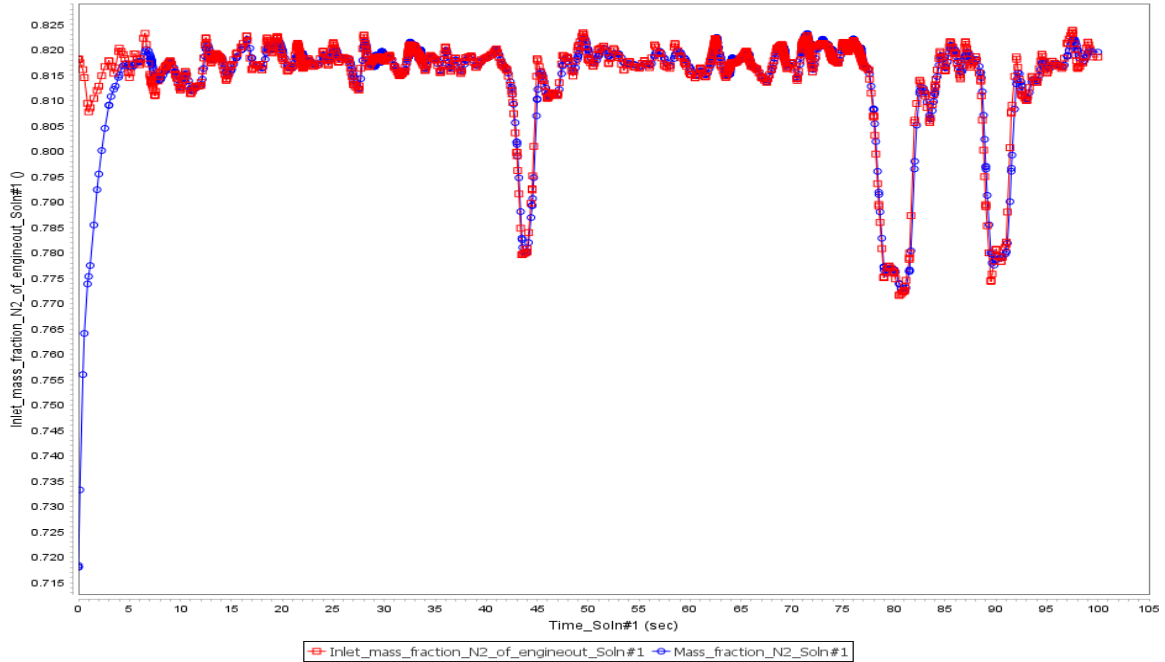
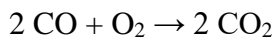


Figure 4-13: Concentration of nitrogen (mass fraction)

4.7. CO₂ concentration (mass fraction)

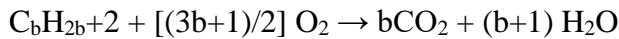
The following reactions occur

1. CO oxidation



The platinum catalyst facilitates the reaction between CO and oxygen, converting carbon monoxide into carbon dioxide.

2. Oxidation of HC



The palladium catalyst promotes the reaction between hydrocarbons and oxygen, converting them into carbon dioxide and water. These oxidation reactions lead to a significant increase carbon dioxide concentration at the outlet of the catalytic converter compared to the inlet

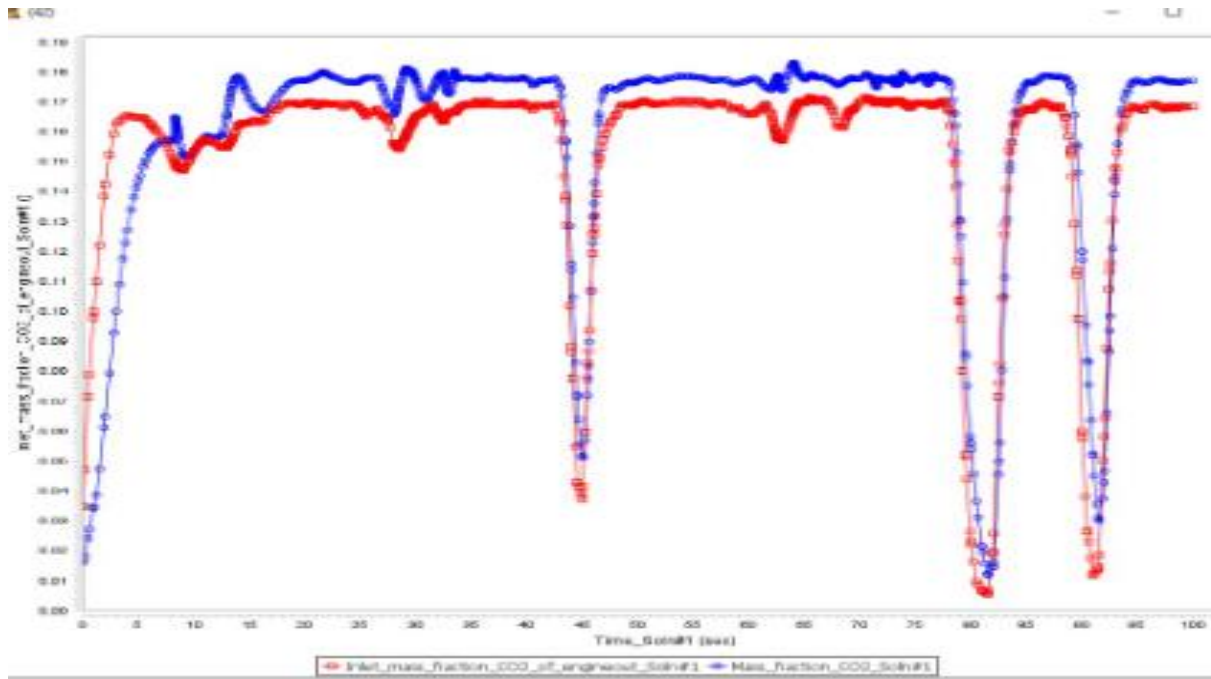


Figure 4-14: CO₂ concentration (mass fraction)

4.8. CO concentration (mass fraction)

Platinum acts as a facilitator, reducing the amount of energy needed for the reaction to activate. Energy of activation like a bump that the molecules need to overcome to react. Platinum lowers this bump, allowing the reaction to happen at a much faster rate and at the lower temperatures found in exhaust gas. Oxidation reaction takes place on platinum surface catalyst helps oxidize combine with oxygen and HC to CO₂ and H₂O. The carbon monoxide concentration after- treatment is given below. The CO concentration is very high at inlet (0.038g/s) and gradually reduced to 0.024g/s in the reduction chamber. Lastly the CO concentration in the reduction system brought to the minimum level.

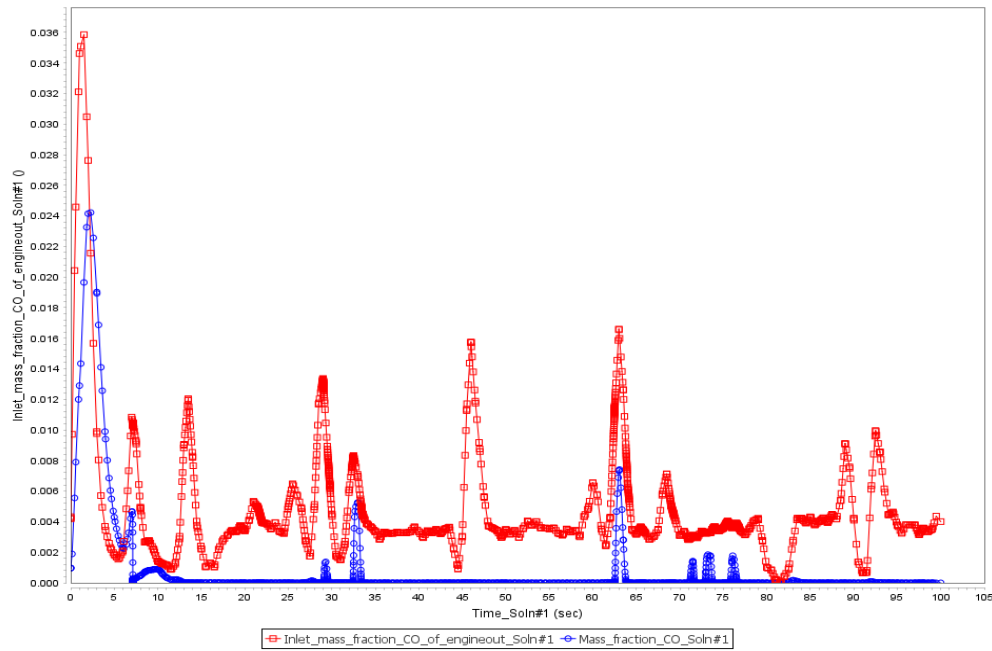


Figure 4-15: CO concentration (mass fraction)

4.9. NOx concentration (in mass-flow)

The primary nitrogen oxides present in the exhaust gas are NO and N₂O. Of nitric oxide is typically the dominant species and exists in a higher quantity compared to the other nitrogen oxides. Engine-Out NOx Concentration, The figure 5-16, shows the concentration of NO (in mass-flow) at the engine-out stage, typically its high due to the high-temperature combustion process in the engine, which favors the formation of nitrogen oxides.

Rhodium in a catalytic converter plays a crucial role in reducing nitrogen oxides through catalytic reactions. When NO and CO molecules enter a catalytic converter, they bind to rhodium surfaces. This attachment weakens the link in the nitric oxide molecule between the atoms of N₂ and O₂, making it more susceptible to change. In some cases, this bond weakens to the point where the nitrogen and oxygen atoms separate completely. Pairs of nitrogen atoms can then combine and leave the surface as nitrogen gas, while oxygen atoms can combine with CO molecules on the surface, leaving as carbon dioxide. This catalytic process facilitated by rhodium in the converter leads to the conversion nitric oxide in the exhaust stream to nitrogen and carbon dioxide.

Therefore Rh reducing NO through catalytic reactions. NO and CO enter a converter, they bind to Rh by Adsorption, Weakening of the NO bond (N&O), Dissociation of NO, breaking of NO, reduction of NO convert to N₂ & H₂O. 0.00045g/s reduced 0.00038g/s

Outlet NO_x Concentration, The figure below shows the concentration of NO (in mass-flow) at the outlet of the catalytic converter, after the reduction reactions have taken place. The outlet concentration is significantly lower than the engine-out concentration, demonstrating the effectiveness of the catalytic converter in reducing nitrogen oxides. The specific outlet concentration depends on after-treatment device efficiency the catalyst's performance, and the overall exhaust gas composition.

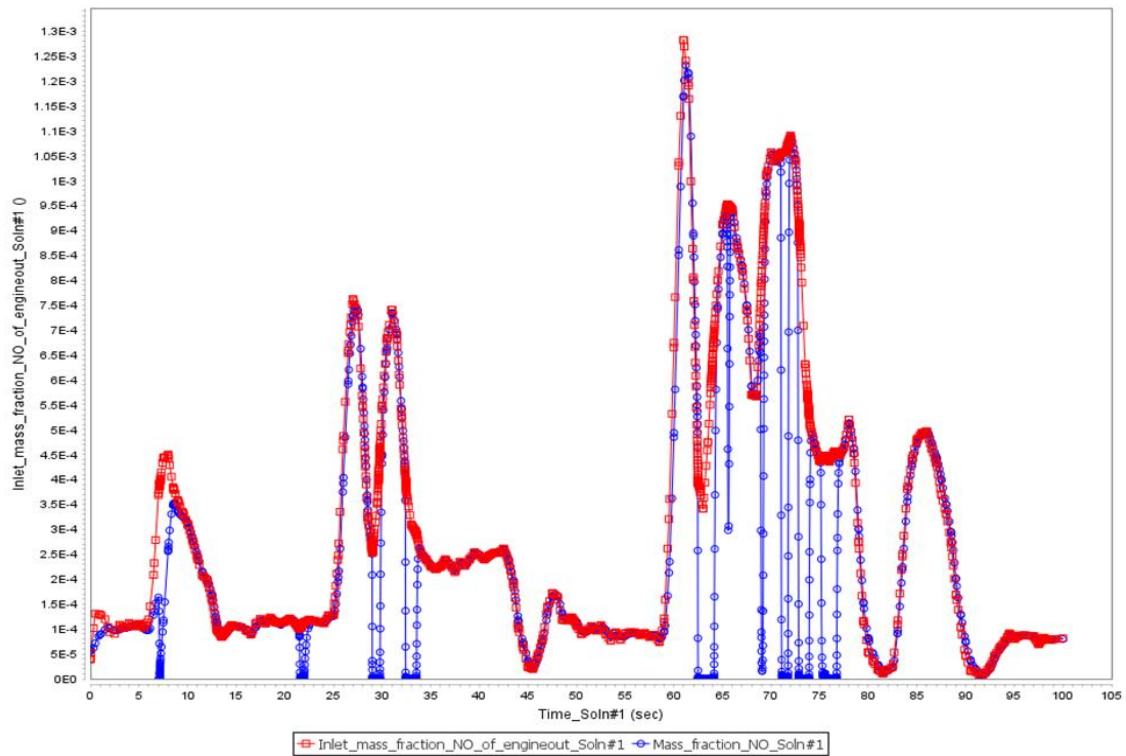


Figure 4-16: NO_x concentration (mass fraction)

4.10. Concentration of HC (mass fraction)

Pt-catalyzed oxidation of hydrocarbons is a crucial step HC&O₂ Adsorption on Pt, Pt activation adsorbed HC & O₂ raise rxn & weak bond of HC & O₂, after adsorption & activation Oxidation takes place form CO₂ &H₂O, remove byproduct by Desorption and Increased rxn rate by Pt lower activation energy for HC oxidation

After passing over the surface of reactor, the mass fraction of HC decreases from the inlet to the outlet due to the catalytic reactions. Achieving an 60.08 percent reduction means that 60.08 percent of the unburned hydrocarbons that enter the catalytic converter are successfully converted into water and carbon dioxide.

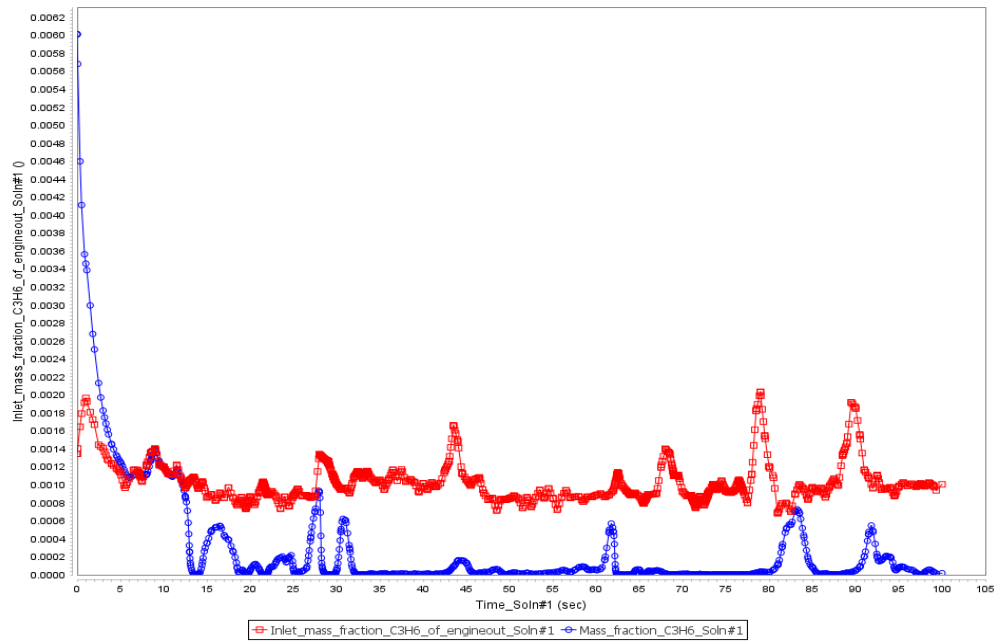


Figure 4-17: HC concentration (mass fraction)

The engine-out data for heavy-duty vehicle used for is validated according this paper, to NO_x engine-out varies $5.02e^{-2}$ plus or minus $3.03e^{-7}$, CO engine-out $1.91e^{-2}$ plus or minus $3.321e^{-9}$ HC engine out $2.13e^{-3}$ plus or minus $4.23 e^{-6}$ (Clevert et al., 2016)

Table 4-3: Percentage Conversion of CO

Time (s)	Mass fraction of CO at Inlet (engine out)	Mass fraction of CO at Exit	Percentage of Conversion (%)
0.00	0.004207374	0.0009633208	
1.00	0.03461898	0.01293041	
10	0.001422877	8.85e-04	
::	0.00335681	1.27E-06	
::	0.003569015	4.29E-07	
100	0.004002606	1.04E-06	
Average	0.005321431	3.72E-04	73.3%

As it is given in the table above CO conversion is proportional to its production. The emission gas reduction system is effective in reducing the CO emission using platinum as a catalyst; it is possible to reduce the CO emission in the exhaust line up to the optimum range of 73.3% using the exhaust gas treating system.

Table 4-4: Percentage Conversion of NO

Time (s)	Mass fraction of NO at inlet (engine-out)	Mass fraction of NO at exit	Percentage of conversion (%)
0.00	3.95e ⁻⁰⁵	5.71e ⁻⁰⁵	
1.00	1.29e ⁻⁰⁴	8.83e ⁻⁰⁵	
10	3.11e ⁻⁰⁴	3.14e ⁻⁰⁴	
::	2.26e ⁻⁰⁴	2.28e ⁻⁰⁴	
::	4.37e ⁻⁰⁴	4.41 e ⁻⁰⁴	
100	8.13e ⁻⁰⁵	7.96 e ⁻⁰⁵	
Total average 1 to 100sec	4.1e ⁻⁰⁴	2.00 e ⁻⁰⁴	

The NO_x emission is formed at a higher temperature of combustion around 700 K and above. From the components nitrogen oxide emission of IC engine NO is the dominant one or exist in higher quantity than others. In this designed system, 51% can be converted into non harmful components by using platinum catalyst in the emission treating system. This system found very efficient in the conversion of NO components.

Table 4-5: Percentage Conversion of UHC

Time (s)	Mass fraction of HC at inlet (engine-out)	Mass fraction of HC at exit	Percentage of conversion (%)
0.00	0.001345428	0.006012533	
1.00	0.001966222	0.003460935	
10	0.00120154	0.001201758	
::	0.001054509	1.03E-05	
::	9.31E-04	6.96E-07	
100	0.001005496	1.72E-05	
Total average 1sec to 100sec	0.001023461	0.000297584	

As given in the table above one of the component of the emission in diesel engine is unburned hydrocarbon (UHC). Those are released to the environment as a byproduct from IC engine

and cause environmental and health problems. This designed emission treating system has ability to reduce the UHC by 60.08% using platinum catalyst which is the efficient catalyst.

4.11. Inlet flow rate of engine out

The inlet flow rate of an engine refers to the mass or volume of fluid that enters the engine per unit time. It's a crucial parameter for the impacts engine performance in terms of, Power output, a higher inlet flow rate typically allows for more fuel intake and combustion. Fuel efficiency. The engine's efficiency in converting fuel into usable power is also affected by the inlet flow rate. Emissions, The amount of pollutants released by the engine is partly influenced by the inlet flow rate. The number average weight 6.69093392g/s indicate proportion of a specific component within the mixture.

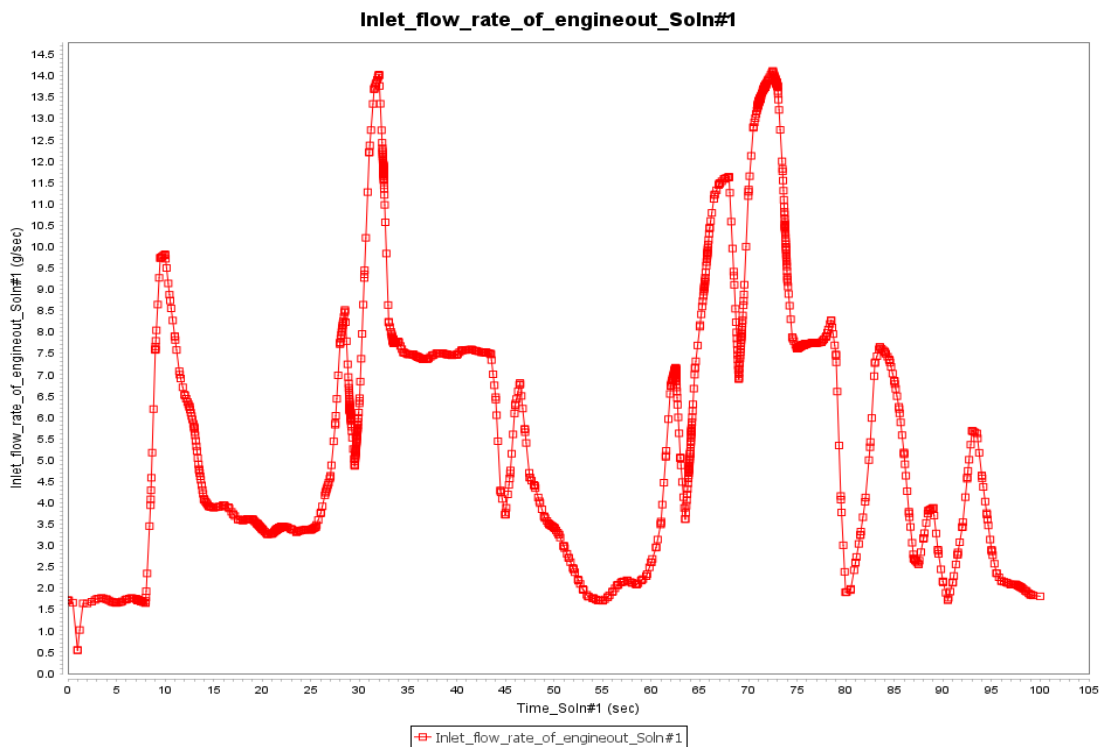


Figure 4-18: inlet flow rate of engine-out

The average weight for figures shown below NO_x $4.1\text{E-}04\text{g/s}$, HC 0.001023461g/s , CO 0.005321431g/s is in mass fraction, because of turbulence indicated on the graph not possible to take at random time (sec), rather than the average weight form 0 to 100sec, and is possible.as temperature of catalytic convert reaches to maximum $750.44\text{k}(449.44\text{ }^\circ\text{C})$, those HC , CO and NO_x , decreases to, $1.58\text{e-}4$, $6.84\text{e-}6$, $1.15\text{e-}4$, from 0.001473 , 0.002221 , 0.0000198 respectively.

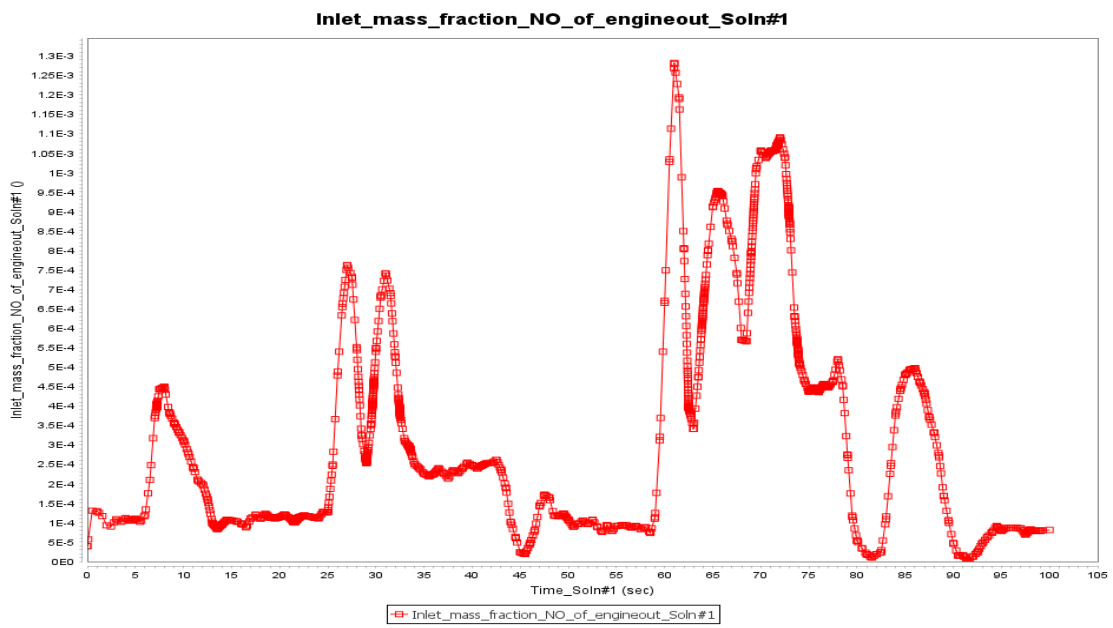
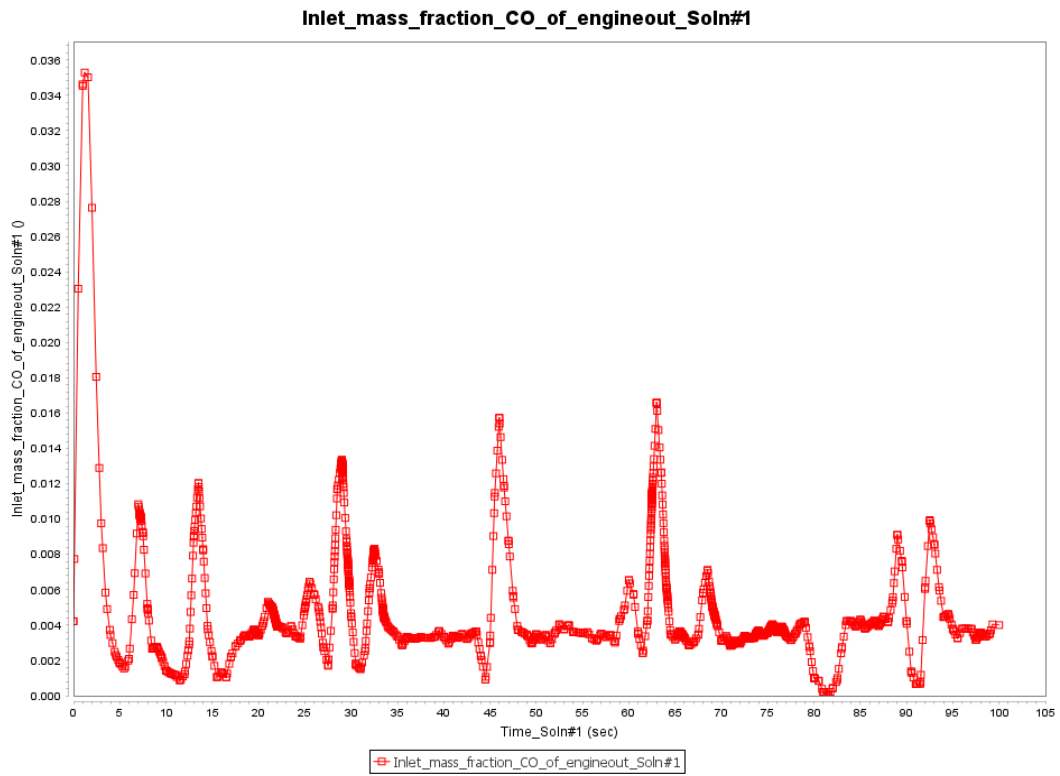


Figure 4-19: engine-out, CO, and NO

Table 4-6: Overall Average mass-fraction

No	Inlet engine-out	After-treatment outlet
1	Inlet_mass_fraction_O2_of_engineout	Mass_fraction_O2
	✓ 0.01804082	✓ 0.012493971
2	Inlet_mass_fraction_CO2_of_engineout	Mass_fraction_CO2
	✓ 0.15870891	✓ 0.168856063
3	Inlet_mass_fraction_CO_of_engineout	Mass_fraction_NO
	✓ 0.005321431	✓ 3.72E-04
4	Inlet_mass_fraction_CO_of_engineout	Mass_fraction_NO
	✓ 4.1E-04	✓ 2.00E-04
5	Inlet_mass_fraction_C3H6_of_engineout	Mass_fraction_C3H6
	✓ 0.001023461	✓ 0.000297584

4.12. Verification

For validate the research based on the material used as a catalyst by different research paper and compare the effectiveness of three-way catalytic converters utilizing platinum/rhodium catalysts aluminum oxide as washcoat and ceramic monolith substrates, how much percent they reduce after a treatment.

(Ghofur et al., 2018) ash was extracted from the coal decline of a steam-electric power station and used as a catalyst. After being cleaned with distilled water, it was dried at 60 °C until its weight kept constant. 9M H₂SO₄ was used to further activate the fly ash. After adding 1.5 liters of 9M H₂SO₄ to a flask containing 500 grams of fly ash, the flask was permitted to anneal for 24 hours at room temperature. After filtering the mixture, distilled water was used to wash the fly ash until it reached a PH of 7. Next, the fly ash was dried for three hours at 110 °C. Finished substance afterwards filtered in 100-mesh (0.15 mm), called the activated catalyst. Subsequently the catalyst shaped into a circle using a pipe-mild steel that have 50 mm diameter and a 5 cm length. A total of 700 and 900 g of catalyst were used to produce the catalytic converter, which has a length of 7 and 9 cm, respectively. Fly ash molding was adhered to using cement. Consequently, the use of activated fly ash as a catalytic converter could cut carbon monoxide and hydrocarbon emissions by up to 45% and 48 percent, respectively.

the paper done by (Kumar & Mathiselvan, 2017), base solutions with entirely different liquid molar and weight ratios were employed in this research. As a metal oxide catalyst, cobalt oxide and titanium dioxide were employed. Since titanium dioxide is the oxidant and the agent, pure CO is utilized. It is the most often used carrier in the selective catalytic reduction of NO_x from stationary pollution sources due to its surface characteristics and inertness to the production of sulphates. In order to prepare the substrate for oxidation, 900 milliliters of distilled water were mixed with 275 grams of TiO₂ and 38 grams of CaO, and the mixture was agitated for ten minutes at a specific rotational speed. Stirring is mostly used to facilitate efficient mixture generation. After coated with an oxidizing agent (TiO₂), the circular stainless steel wire web substrate pieces are placed into a solution, the slurry removed, and allowed to dry at room temperature. Once the stainless steel wire meshes are completely dried out, preheat them in an oven at 600°C for four hours, and then assemble the wire mesh onto the converter. Preparing the substrate for reduction: 900 milliliters of distilled water are mixed with 240 grams of MSG₃+36 grams of MSG₂ according to the required ratios. Stirring is mostly used to facilitate efficient mixture generation. Coating wire mesh components with CO₃O₄ reducing agent. After having been immersed in slurry, circular portions of stainless steel wire mesh substrate are removed and allow evaporate at room temperature. After drying, assemble the circular stainless steel wire meshes to the converter by heating them for four hours at 600°C in an oven. It was discovered that catalytic converters based on TiO₂ and CO₃O₄ may therefore lower NO, HC, and CO emissions by 27%, 37%, and 32%, respectively.

CHAPTER FIVE

5. CONCLUSION AND RECOMMENDATION

5.1. Conclusion

This thesis work aimed to design and analyze an effective emission treatment system for vehicle repair workshops, addressing the environmental concerns posed by the scattered, unplanned distribution of such facilities throughout the city. The study highlights the importance of emission control, especially in cases where proper ventilation or existing treatment systems are lacking.

Key Findings: The computational fluid dynamics (CFD) modeling approach using ANSYS Fluent software provided reliable data on engine-out emissions, which are difficult to measure directly from the exhaust manifold due to the varying and non-constant operating conditions of the engine. The detailed 2D model of the combustion chamber of the WD615.69, 336HP engine allowed for accurate simulation of the complex processes inside, enabling the determination of the composition and characteristics of the exhaust gases leaving the engine. The CFD modeling of the catalytic converter downstream of the engine provided valuable insights into the velocity streamlines, pressure distributions, and temperature gradients within the catalytic device. The MATLAB/Simulink-based temperature variation control system effectively modeled and simulated the cooling system components, including the thermostat controller, cooling plant, and temperature-controlled tank environment, ensuring accurate and effective temperature regulation.

The integration of the CFD-derived engine-out data with the CHEMKIN-PRO simulation of the after-treatment system demonstrated that the platinum catalyst-based emission treatment device can effectively convert 73.3% of CO, 51% of NO, and 60.08% of unburnt hydrocarbons (UHCs) into less-harmful substances, while also contributing 67.6% of CO₂ and 30.7% of O₂ to the surrounding workshop environment.

Accomplishment of Study Objectives: This research successfully achieved its intended goals. The designed emission treatment system demonstrates significant reductions in harmful pollutants within vehicle repair shops. This translates to a positive impact on both the natural environment and the health of workers in these facilities.

In Conclusion: This thesis effectively designed and analyzed an emission treatment system, directly addressing environmental concerns in vehicle repair shops. The results demonstrate the potential to significantly improve worker health by minimizing exposure to harmful

pollutants, thereby creating a healthier working environment. This, in turn, can minimize the impact of vehicle emissions on surrounding areas.

5.2. Recommendation

It is very important to research on emission treating areas to improve and develop effective emission controlling systems that may work at stationary in workshop or installed on vehicle. An important study of lean burn combustion technology could be essential to gain more understanding of the emissions reduction possibility via different combustion conditions such as changing the compression ratio or ignition timing etc. Emissions of some potentially important pollutants such as carbonyls (especially carbonyls other than formaldehyde and acetaldehyde) have not been thoroughly investigated for pure fuels such as ethanol, methanol or other fuels. In terms of end-use properties and exhaust emissions, gasoline fuels to be used for lean burn combustion are not problem-free. For instance their use reportedly results in the increase of aromatic hydrocarbons and carbonyls release into the environment.

5.3. Future work

The design of emission treating is basically give a better treating if it include new emission reduction approaches, In order to enhance the emission treatment system, it would be advantageous to incorporate a (1) Ammonia/urea, sometimes referred to as diesel emission fuel, is introduced into the exhaust gasses in the chamber and allowed to mix throughout until the content in the chamber reacts spontaneously in order to reduce emissions in advance of time. This will enable the mixture to mix properly and burn all harmful gases, converting them into harmless byproducts like nitrogen, carbon dioxide, and water. Additionally Considering the potentially high noise levels during vehicle maintenance activities, incorporating. (2) Diesel Particulate Filter (DPF) with a regenerative cleaning mechanism. Particulate matter would be efficiently captured by this DPF before it builds up and restricts exhaust flow. The trapped soot is released by the regenerative cleaning mechanism, which usually uses high temperatures to oxidize it and turn it into gaseous byproducts that can be safely released from the exhaust stream. (3) Silencers into the design is recommended. This would significantly contribute to a more comfortable and noise-free working environment for repair workshop. (4) putting fins on the surface of outer pipe in order to remove heat of superheated water when discharged from the multiple cylindrical pipe, as long as the temperature of water get hot through convective and conductive heat transfer, before it enters to the cold water tank

REFERENCES

- Adgate, J. L., Ramachandran, G., Pratt, G. C., Waller, L. A., & Sexton, K. (2002). Spatial and temporal variability in outdoor, indoor, and personal PM_{2.5} exposure. *Atmospheric Environment*, *36*(20). [https://doi.org/10.1016/S1352-2310\(02\)00326-6](https://doi.org/10.1016/S1352-2310(02)00326-6)
- Afroz, R., Hassan, M. N., & Ibrahim, N. A. (2003). Review of air pollution and health impacts in Malaysia. *EnviroAbdulwahid, A. A. (2020). Heat and mass transfer mechanisms in a wet scrubber.*
- Abutu Francis. (2018). *Emission and Pollution Control Needs in the Automobile Mechanic Workshop in Benue State, Nigeria.* 73–80.
- Ahmad, I., & Balkhyour, M. A. (2020). Occupational exposure and respiratory health of workers at small scale industries. *Saudi Journal of Biological Sciences*, *27*(3), 985–990. <https://doi.org/10.1016/j.sjbs.2020.01.019>
- Almomani, H., & Almutairi, N. (2020). Vehicles maintenance workshops layout and its management to reduce noise pollution and improve maintenance quality. *Journal of Environmental Treatment Techniques*, *8*(4), 1352–1356. [https://doi.org/10.47277/JETT/8\(4\)1356](https://doi.org/10.47277/JETT/8(4)1356)
- AMCA. (2018). *STANDARD ANSI / AMCA Standard 208-18 Calculation of the Fan Energy Index Association International ANSI / AMCA Standard 208-18 Calculation of the Fan Energy Index.*
- Ataro, Z., Geremew, A., & Urgessa, F. (2018). Occupational health risk of working in garages: Comparative study on blood pressure and hematological parameters between garage workers and haramaya university community, harar, Eastern Ethiopia. *Risk Management and Healthcare Policy*, *11*(3099067), 35–44. <https://doi.org/10.2147/RMHP.S154611>
- Balaji, G., Premnath, D., Yuvaraj, R., & Kohli, A. S. (2018). Experimental analysis of exhaust emissions using catalytic converter. *IOP Conference Series: Materials Science and Engineering*, *402*(1). <https://doi.org/10.1088/1757-899X/402/1/012200>
- Blejchař, T., Konvička, J., Von Der Heide, B., Malý, R., & Maier, M. (2018). High Temperature Modification of SNCR Technology and its Impact on NO_x Removal Process. *EPJ Web of Conferences*, *180*(X), 1–7. <https://doi.org/10.1051/epjconf/201818002009>

- Braga da Costa Campos, L. M. (2020). Steady Heat Conduction. *Complex Analysis with Applications to Flows and Fields*, 388, 607–634. <https://doi.org/10.1201/b13580-44>
- Chawla, A., & Lavania, A. K. (2008). Air pollution and fuel vapour induced changes in lung functions: Are fuel handlers safe? *Indian Journal of Physiology and Pharmacology*, 52(3), 255–261. <https://doi.org/10.4103/abr.abr>
- Chen, G. J., & Zhang, Z. M. (2013). Study on integrated system of SCR and muffler for heavy-duty diesel vehicle. *Applied Mechanics and Materials*, 427–429, 41–44. <https://doi.org/10.4028/www.scientific.net/AMM.427-429.41>
- Clevert, D. A., Unterthiner, T., & Hochreiter, S. (2016). Fast and accurate deep network learning by exponential linear units (ELUs). *4th International Conference on Learning Representations, ICLR 2016 - Conference Track Proceedings*, 2024. <https://doi.org/10.1016/j.ijheat>
- Couper, J. R., Penney, W. R., Fair, J. R., & Walas, S. M. (2012). 17 - *Chemical Reactors*. 591–653. http://www.sciencedirect.com/science/article/pii/B9780123969590000173%5Cnhttp://pdn.sciencedirect.com/science?_ob=MiamiImageURL&_cid=282457&_user=464374&_pii=B9780123969590000173&_check=y&_origin=article&_zone=toolbar&_coverDate=31-Dec-2012&view=c&originC
- Denton, T. (2020). *Advanced automotive fault diagnosis: automotive technology: vehicle maintenance and repair*. Routledge.
- Design, R. (2016). ANSYS Chemkin Tutorials Manual. *Design, December*, 1–274.
- Dutra, N., & Victório, C. (2020). Automobile repair shops have a negative impact on the environment. *Acta Scientiae et Technicae*, 8(2), 5–19. <https://doi.org/10.17648/uezoast-v8i2.292>
- Flynn, M. R., & Susi, P. (2012). Local exhaust ventilation for the control of welding fumes in the construction industry - A literature review. *Annals of Occupational Hygiene*, 56(7), 764–776. <https://doi.org/10.1093/annhyg/mes018>
- Fornalczyk, A., Przylucki, R., Golak, S., & Willner, J. (2016). Modelling methods of magnetohydrodynamic phenomena occurring in a channel of the device used to wash out the spent automotive catalyst by a liquid metal. *Archives of Metallurgy and Materials*, 61(2A), 713–718. <https://doi.org/10.1515/amm-2016-0122>

- Gas, G., & Standards, E. (2023). *Heavy-Duty Vehicles , Air Pollution , and Climate Change. August 2021*, 14–16.
- Ghofur, A., Soemarno, Hadi, A., & Putra, M. D. (2018). Potential fly ash waste as catalytic converter for reduction of HC and CO emissions. *Sustainable Environment Research*, 28(6), 357–362. <https://doi.org/10.1016/j.serj.2018.07.003>
- Gholami, F., Tomas, M., Gholami, Z., & Vakili, M. (2020). Technologies for the nitrogen oxides reduction from flue gas: A review. *Science of the Total Environment*, 714, 136712. <https://doi.org/10.1016/j.scitotenv.2020.136712>
- Guo, J., & Wang, C. (2018). *Analysis of Contaminants in Vehicle Maintenance and Repair Enterprise. 159(Icaset)*, 228–232. <https://doi.org/10.2991/icaset-18.2018.46>
- Guoquan, X., Huaming, W., Lin, C., & Xiaobin, H. (2021). Predicting unsteady heat transfer effect of vehicle thermal management system using steady velocity equivalent method. *Science Progress*, 104(2), 419–449. <https://doi.org/10.1177/00368504211025933>
- Gupta, V., Chaturvedi, K., Dubey, M., & Rao, N. M. (2017). Catalytic Converters for treatment of Exhaust Gas Emission in Automobiles: A Review. *International Journal of Scientific & Engineering Research*, 8(2), 95–99. <http://www.ijser.org>
- Horton, R., Murphy, C., Pielke, R., Raymond, C., Thorne, P., & Wilby, R. L. (2024). *enhancement methodologies 2 PCMs AND APPLICATIONS*. 2024.
- James, A. (2018). Gas Turbine Combustion Chamber. *2nd Ed. New York: Taylor and Francis*, 50–57.
- Jason, A., May, L., & Louison, J. (2024). *Exhaust Gas Pressure / Blowdown Calculations*. 2024.
- Kahlon, A. (2016). *Catalytic Converters. May 1995*, 1–24. http://chemwiki.ucdavis.edu/Core/Physical_Chemistry/Kinetics/Case_Studies:_Kinetics/Catalytic_Converters
- Kamp, C. J., Zhang, S., Bagi, S., Wong, V., Monahan, G., Sappok, A., & Wang, Y. (2017). Ash Permeability Determination in the Diesel Particulate Filter from Ultra-High Resolution 3D X-Ray Imaging and Image-Based Direct Numerical Simulations. *SAE International Journal of Fuels and Lubricants*, 10(2), 608–618. <https://doi.org/10.4271/2017-01-0927>

- Keeratisiwakul, K., Anantachaisophon, S., & Vatiwutipong, P. (2023). A modification of Newton's cooling law with correlation to fractional derivative. *Journal of Physics: Conference Series*, 2431(1). <https://doi.org/10.1088/1742-6596/2431/1/012027>
- Knotek, S., Schmelter, S., & Olbrich, M. (2021). Assessment of different parameters used in mesh independence studies in two-phase slug flow simulations. *Measurement: Sensors*, 18. <https://doi.org/10.1016/j.measen.2021.100317>
- Kovacev, N., Li, S., Zeraati-Rezaei, S., Hemida, H., Tsolakis, A., & Essa, K. (2021). Effects of the internal structures of monolith ceramic substrates on thermal and hydraulic properties: additive manufacturing, numerical modelling and experimental testing. *International Journal of Advanced Manufacturing Technology*, 112(3–4), 1115–1132. <https://doi.org/10.1007/s00170-020-06493-2>
- Kritsanaviparkporn, E., Baena-Moreno, F. M., & Reina, T. R. (2021). Catalytic Converters for Vehicle Exhaust: Fundamental Aspects and Technology Overview for Newcomers to the Field. *Chemistry (Switzerland)*, 3(2), 630–646. <https://doi.org/10.3390/chemistry3020044>
- Kumar, D., & Mathiselvan, G. (2017). *Design and Development of Non Novel Based Catalytic Converter for DI Diesel Engine*. 10(4), 1520–1525.
- Li, H. M., Zhang, N., Guo, X., Dou, M. Y., Feng, Q., Zou, S., & Huang, F. C. (2020). Summary of Flue Gas Purification and Treatment Technology for Domestic Waste Incineration. *IOP Conference Series: Earth and Environmental Science*, 508(1). <https://doi.org/10.1088/1755-1315/508/1/012016>
- Li, K., & Luo, X. (2023). *Research Progress on Catalytic Combustion of Volatile Organic Compounds in Industrial Waste Gas*.
- Liu, A. F. (2020). Mechanical Properties Data for Selected Aluminum Alloys. *Mechanics and Mechanisms of Fracture*, 397–409. <https://doi.org/10.31399/asm.tb.mmfi.t69540397>
- Majewski, W. A. (2022). Catalytic Coating Materials. *Dieselnet*, 2022. https://dieselnet.com/tech/cat_mat.php
- Mizell, B., Brewer, M., Walton, M., Wooley, M., Fox, R., Smith, D., Jason, H., Jason, H., Hines, A., Hines, A., Jason, H., & Jason, H. (2024). *How To Calculate Muffler Size and Exhaust Pipe Diameter achieve THAT OR GET THE CORRECT SIZE AND WHAT IS*

THIS DOING TO MY TRUCK ? 2024.

- Nunez, A. M. (2019). High temperature corrosion in exhaust application for heavy-duty trucks. *Thesis*, 81. <http://urn.kb.se/resolve?urn=urn:nbn:se:kth:diva-259660%0Ahttps://drive.google.com/open?id=1RCXUwS0OO8371BE2tSztMsm74orTZZJR>
- Parrish, D. D., & Stockwell, W. R. (2015). Urbanization and air pollution: Then and now. *Eos (United States)*, 96(1), 10–15. <https://doi.org/10.1029/2015eo021803>
- Pronobis, M., Wejkowski, R., Jagodzińska, K., & Kress, T. (2017). Simplified method for calculating SNCR system efficiency. *E3S Web of Conferences*, 14, 1–10. <https://doi.org/10.1051/e3sconf/20171402003>
- Rajendran, R., Logesh, U., Praveen, N. S., & Subbiah, G. (2020). Optimum design of catalytic converter to reduce carbon monoxide emissions on diesel engine. *AIP Conference Proceedings*, 2311(December). <https://doi.org/10.1063/5.0034427>
- Redho, A., Irawan, D., Julianto, E., & Fadhilah, R. (2023). Effect of Cooling Using Added Peltier Ice Pack on Cool Box. *International Journal of ...*, 8, 72–79. [https://www.iaras.org/iaras/filedownloads/ijme/2023/012-0011\(2023\).pdf](https://www.iaras.org/iaras/filedownloads/ijme/2023/012-0011(2023).pdf)
- Roy, D., Chakraborty, T., Basu, D., & Bhattacharjee, B. (2020). Feasibility and performance of ground source heat pump systems for commercial applications in tropical and subtropical climates. *Renewable Energy*, 152, 467–483. <https://doi.org/10.1016/j.renene.2020.01.058>
- Shan, W., Yu, Y., Zhang, Y., He, G., Peng, Y., Li, J., & He, H. (2021). Theory and practice of metal oxide catalyst design for the selective catalytic reduction of NO_x with NH₃. *Catalysis Today*, 376(x), 292–301. <https://doi.org/10.1016/j.cattod.2020.05.015>
- Swallow, K. (2023). *Author*. 2023.
- Tan, Y., Thomas Durbin Co-PIs, by D., Johnson, K. C., Karavalakis, G., Wayne Miller, J., Jiang, Y., B Ventura, L. M., Clark, N., & McKain, D. (2019). *Final Report Heavy-duty On-Road Vehicle Inspection and Maintenance Program Contract No. 15RD022. 15.*
- Tannous, M. (2024). *Recent Advances in the Catalytic Treatment of Volatile Organic Compounds: A Review Based on the Mixture Effect*. 2024.
- Trivedi, S., & Prasad, R. (2018). A four-way catalytic system for control of emissions from

- diesel engine. *Sadhana - Academy Proceedings in Engineering Sciences*, 43(8), 2023.
<https://doi.org/10.1007/s12046-018-0884-0>
- Truth, T., Heat, A. U., & Vapor, P. (2023). *Standard and Thin Heat Pipe Vapor Chamber Component Parts How Do Heat Pipes Work | Heat Telltale Signs You Might Need a Heat Pipe or Types of Heat Sinks Used with Two-Phase Related Links Typical Uses of Heat Pipes*. 22793.
- Vaghela, J., Rota, R., & Morbidelli, M. (2024). *CFD Analysis of Catalytic Converter for Mitigation of Emission* *CFD Analysis of Catalytic Converter for Mitigation of Emission September 1998 · Industrial & Engineering Chemistry Research*. 2024.
<https://doi.org/10.13140/RG.2.2.23868.13447>
- Weitekamp, C. A., Kerr, L. B., Dishaw, L., Nichols, J., Lein, M., & Stewart, M. J. (2020). A systematic review of the health effects associated with the inhalation of particle-filtered and whole diesel exhaust. *Inhalation Toxicology*, 32(1), 1–13.
<https://doi.org/10.1080/08958378.2020.1725187>
- Wuryanti, S., & Fitriyani, Y. (2019). The effect of brine mass rate on circumferential and longitudinal stress in vertical type separator design. *Cogent Engineering*, 6(1).
<https://doi.org/10.1080/23311916.2019.1679062>
- Abdulwahid, A. A. (2020). *Heat and mass transfer mechanisms in a wet scrubber*.
- Abutu Francis. (2018). *Emission and Pollution Control Needs in the Automobile Mechanic Workshop in Benue State, Nigeria*. 73–80.
- Ahmad, I., & Balkhyour, M. A. (2020). Occupational exposure and respiratory health of workers at small scale industries. *Saudi Journal of Biological Sciences*, 27(3), 985–990.
<https://doi.org/10.1016/j.sjbs.2020.01.019>
- Almomani, H., & Almutairi, N. (2020). Vehicles maintenance workshops layout and its management to reduce noise pollution and improve maintenance quality. *Journal of Environmental Treatment Techniques*, 8(4), 1352–1356.
[https://doi.org/10.47277/JETT/8\(4\)1356](https://doi.org/10.47277/JETT/8(4)1356)
- AMCA. (2018). *STANDARD ANSI / AMCA Standard 208-18 Calculation of the Fan Energy Index Association International ANSI / AMCA Standard 208-18 Calculation of the Fan Energy Index*.
- Ataro, Z., Geremew, A., & Urgessa, F. (2018). Occupational health risk of working in

- garages: Comparative study on blood pressure and hematological parameters between garage workers and haramaya university community, harar, Eastern Ethiopia. *Risk Management and Healthcare Policy*, 11(3099067), 35–44. <https://doi.org/10.2147/RMHP.S154611>
- Balaji, G., Premnath, D., Yuvaraj, R., & Kohli, A. S. (2018). Experimental analysis of exhaust emissions using catalytic converter. *IOP Conference Series: Materials Science and Engineering*, 402(1). <https://doi.org/10.1088/1757-899X/402/1/012200>
- Blejchař, T., Konvička, J., Von Der Heide, B., Malý, R., & Maier, M. (2018). High Temperature Modification of SNCR Technology and its Impact on NO_x Removal Process. *EPJ Web of Conferences*, 180(X), 1–7. <https://doi.org/10.1051/epjconf/201818002009>
- Braga da Costa Campos, L. M. (2020). Steady Heat Conduction. *Complex Analysis with Applications to Flows and Fields*, 388, 607–634. <https://doi.org/10.1201/b13580-44>
- Chawla, A., & Lavania, A. K. (2008). Air pollution and fuel vapour induced changes in lung functions: Are fuel handlers safe? *Indian Journal of Physiology and Pharmacology*, 52(3), 255–261. <https://doi.org/10.4103/abr.abr>
- Chen, G. J., & Zhang, Z. M. (2013). Study on integrated system of SCR and muffler for heavy-duty diesel vehicle. *Applied Mechanics and Materials*, 427–429, 41–44. <https://doi.org/10.4028/www.scientific.net/AMM.427-429.41>
- Clevert, D. A., Unterthiner, T., & Hochreiter, S. (2016). Fast and accurate deep network learning by exponential linear units (ELUs). *4th International Conference on Learning Representations, ICLR 2016 - Conference Track Proceedings*, 2024. <https://doi.org/10.1016/j.ijheat>
- Couper, J. R., Penney, W. R., Fair, J. R., & Walas, S. M. (2012). 17 - *Chemical Reactors*. 591–653. http://www.sciencedirect.com/science/article/pii/B9780123969590000173%5Cnhttp://pdn.sciencedirect.com/science?_ob=MiamiImageURL&_cid=282457&_user=464374&_pii=B9780123969590000173&_check=y&_origin=article&_zone=toolbar&_coverDate=31-Dec-2012&view=c&originC
- Denton, T. (2020). *Advanced automotive fault diagnosis: automotive technology: vehicle maintenance and repair*. Routledge.

- Design, R. (2016). ANSYS Chemkin Tutorials Manual. *Design, December*, 1–274.
- Dutra, N., & Victório, C. (2020). Automobile repair shops have a negative impact on the environment. *Acta Scientiae et Technicae*, 8(2), 5–19. <https://doi.org/10.17648/uezo-ast-v8i2.292>
- Flynn, M. R., & Susi, P. (2012). Local exhaust ventilation for the control of welding fumes in the construction industry - A literature review. *Annals of Occupational Hygiene*, 56(7), 764–776. <https://doi.org/10.1093/annhyg/mes018>
- Fornalczyk, A., Przylucki, R., Golak, S., & Willner, J. (2016). Modelling methods of magnetohydrodynamic phenomena occurring in a channel of the device used to wash out the spent automotive catalyst by a liquid metal. *Archives of Metallurgy and Materials*, 61(2A), 713–718. <https://doi.org/10.1515/amm-2016-0122>
- Gas, G., & Standards, E. (2023). *Heavy-Duty Vehicles , Air Pollution , and Climate Change. August 2021*, 14–16.
- Ghofur, A., Soemarno, Hadi, A., & Putra, M. D. (2018). Potential fly ash waste as catalytic converter for reduction of HC and CO emissions. *Sustainable Environment Research*, 28(6), 357–362. <https://doi.org/10.1016/j.serj.2018.07.003>
- Gholami, F., Tomas, M., Gholami, Z., & Vakili, M. (2020). Technologies for the nitrogen oxides reduction from flue gas: A review. *Science of the Total Environment*, 714, 136712. <https://doi.org/10.1016/j.scitotenv.2020.136712>
- Guo, J., & Wang, C. (2018). *Analysis of Contaminants in Vehicle Maintenance and Repair Enterprise. 159(Icaset)*, 228–232. <https://doi.org/10.2991/icaset-18.2018.46>
- Guoquan, X., Huaming, W., Lin, C., & Xiaobin, H. (2021). Predicting unsteady heat transfer effect of vehicle thermal management system using steady velocity equivalent method. *Science Progress*, 104(2), 419–449. <https://doi.org/10.1177/00368504211025933>
- Gupta, V., Chaturvedi, K., Dubey, M., & Rao, N. M. (2017). Catalytic Converters for treatment of Exhaust Gas Emission in Automobiles: A Review. *International Journal of Scientific & Engineering Research*, 8(2), 95–99. <http://www.ijser.org>
- Horton, R., Murphy, C., Pielke, R., Raymond, C., Thorne, P., & Wilby, R. L. (2024). *enhancement methodologies 2 PCMs AND APPLICATIONS*. 2024.
- James, A. (2018). Gas Turbine Combustion Chamber. *2nd Ed. New York: Taylor and*

Francis, 50–57.

- Jason, A., May, L., & Louison, J. (2024). *Exhaust Gas Pressure / Blowdown Calculations*. 2024.
- Kahlon, A. (2016). *Catalytic Converters*. May 1995, 1–24. http://chemwiki.ucdavis.edu/Core/Physical_Chemistry/Kinetics/Case_Studies:_Kinetics/Catalytic_Converters
- Kamp, C. J., Zhang, S., Bagi, S., Wong, V., Monahan, G., Sappok, A., & Wang, Y. (2017). Ash Permeability Determination in the Diesel Particulate Filter from Ultra-High Resolution 3D X-Ray Imaging and Image-Based Direct Numerical Simulations. *SAE International Journal of Fuels and Lubricants*, 10(2), 608–618. <https://doi.org/10.4271/2017-01-0927>
- Keeratisiwakul, K., Anantachaisophon, S., & Vatiwutipong, P. (2023). A modification of Newton's cooling law with correlation to fractional derivative. *Journal of Physics: Conference Series*, 2431(1). <https://doi.org/10.1088/1742-6596/2431/1/012027>
- Knotek, S., Schmelter, S., & Olbrich, M. (2021). Assessment of different parameters used in mesh independence studies in two-phase slug flow simulations. *Measurement: Sensors*, 18. <https://doi.org/10.1016/j.measen.2021.100317>
- Kovacev, N., Li, S., Zeraati-Rezaei, S., Hemida, H., Tsolakis, A., & Essa, K. (2021). Effects of the internal structures of monolith ceramic substrates on thermal and hydraulic properties: additive manufacturing, numerical modelling and experimental testing. *International Journal of Advanced Manufacturing Technology*, 112(3–4), 1115–1132. <https://doi.org/10.1007/s00170-020-06493-2>
- Kritsanaviparkporn, E., Baena-Moreno, F. M., & Reina, T. R. (2021). Catalytic Converters for Vehicle Exhaust: Fundamental Aspects and Technology Overview for Newcomers to the Field. *Chemistry (Switzerland)*, 3(2), 630–646. <https://doi.org/10.3390/chemistry3020044>
- Kumar, D., & Mathiselvan, G. (2017). *Design and Development of Non Novel Based Catalytic Converter for DI Diesel Engine*. 10(4), 1520–1525.
- Li, H. M., Zhang, N., Guo, X., Dou, M. Y., Feng, Q., Zou, S., & Huang, F. C. (2020). Summary of Flue Gas Purification and Treatment Technology for Domestic Waste Incineration. *IOP Conference Series: Earth and Environmental Science*, 508(1).

<https://doi.org/10.1088/1755-1315/508/1/012016>

- Li, K., & Luo, X. (2023). *Research Progress on Catalytic Combustion of Volatile Organic Compounds in Industrial Waste Gas*.
- Liu, A. F. (2020). Mechanical Properties Data for Selected Aluminum Alloys. *Mechanics and Mechanisms of Fracture*, 397–409. <https://doi.org/10.31399/asm.tb.mmfi.t69540397>
- Majewski, W. A. (2022). Catalytic Coating Materials. *Dieselnet*, 2022. https://dieselnet.com/tech/cat_mat.php
- Mizell, B., Brewer, M., Walton, M., Wooley, M., Fox, R., Smith, D., Jason, H., Jason, H., Hines, A., Hines, A., Jason, H., & Jason, H. (2024). *How To Calculate Muffler Size and Exhaust Pipe Diameter achieve THAT OR GET THE CORRECT SIZE AND WHAT IS THIS DOING TO MY TRUCK ? 2024*.
- Nunez, A. M. (2019). High temperature corrosion in exhaust application for heavy-duty trucks. *Thesis*, 81. <http://urn.kb.se/resolve?urn=urn:nbn:se:kth:diva-259660%0Ahttps://drive.google.com/open?id=1RCXUwS00O8371BE2tSztMsm74orTZZJR>
- Parrish, D. D., & Stockwell, W. R. (2015). Urbanization and air pollution: Then and now. *Eos (United States)*, 96(1), 10–15. <https://doi.org/10.1029/2015eo021803>
- Pronobis, M., Wejkowski, R., Jagodzińska, K., & Kress, T. (2017). Simplified method for calculating SNCR system efficiency. *E3S Web of Conferences*, 14, 1–10. <https://doi.org/10.1051/e3sconf/20171402003>
- Rajendran, R., Logesh, U., Praveen, N. S., & Subbiah, G. (2020). Optimum design of catalytic converter to reduce carbon monoxide emissions on diesel engine. *AIP Conference Proceedings*, 2311(December). <https://doi.org/10.1063/5.0034427>
- Redho, A., Irawan, D., Julianto, E., & Fadhilah, R. (2023). Effect of Cooling Using Added Peltier Ice Pack on Cool Box. *International Journal of ...*, 8, 72–79. [https://www.iaras.org/iaras/filedownloads/ijme/2023/012-0011\(2023\).pdf](https://www.iaras.org/iaras/filedownloads/ijme/2023/012-0011(2023).pdf)
- Roy, D., Chakraborty, T., Basu, D., & Bhattacharjee, B. (2020). Feasibility and performance of ground source heat pump systems for commercial applications in tropical and subtropical climates. *Renewable Energy*, 152, 467–483. <https://doi.org/10.1016/j.renene.2020.01.058>

Shan, W., Yu, Y., Zhang, Y., He, G., Peng, Y., Li, J., & He, H. (2021). Theory and practice of metal oxide catalyst design for the selective catalytic reduction of NO_x with NH₃. *Catalysis Today*, 376(x), 292–301. <https://doi.org/10.1016/j.cattod.2020.05.015>

Swallow, K. (2023). *Author*. 2023.

Tan, Y., Thomas Durbin Co-PIs, by D., Johnson, K. C., Karavalakis, G., Wayne Miller, J., Jiang, Y., B Ventura, L. M., Clark, N., & McKain, D. (2019). *Final Report Heavy-duty On-Road Vehicle Inspection and Maintenance Program Contract No. 15RD022. 15*.

Tannous, M. (2024). *Recent Advances in the Catalytic Treatment of Volatile Organic Compounds: A Review Based on the Mixture Effect*. 2024.

Trivedi, S., & Prasad, R. (2018). A four-way catalytic system for control of emissions from diesel engine. *Sadhana - Academy Proceedings in Engineering Sciences*, 43(8), 2023. <https://doi.org/10.1007/s12046-018-0884-0>

Truth, T., Heat, A. U., & Vapor, P. (2023). *Standard and Thin Heat Pipe Vapor Chamber Component Parts How Do Heat Pipes Work | Heat Telltale Signs You Might Need a Heat Pipe or Types of Heat Sinks Used with Two-Phase Related Links Typical Uses of Heat Pipes*. 22793.

Vaghela, J., Rota, R., & Morbidelli, M. (2024). *CFD Analysis of Catalytic Converter for Mitigation of Emission CFD Analysis of Catalytic Converter for Mitigation of Emission September 1998 · Industrial & Engineering Chemistry Research*. 2024. <https://doi.org/10.13140/RG.2.2.23868.13447>

Weitekamp, C. A., Kerr, L. B., Dishaw, L., Nichols, J., Lein, M., & Stewart, M. J. (2020). A systematic review of the health effects associated with the inhalation of particle-filtered and whole diesel exhaust. *Inhalation Toxicology*, 32(1), 1–13. <https://doi.org/10.1080/08958378.2020.1725187>

Wuryanti, S., & Fitriyani, Y. (2019). The effect of brine mass rate on circumferential and longitudinal stress in vertical type separator design. *Cogent Engineering*, 6(1). <https://doi.org/10.1080/23311916.2019.1679062>

nmental Research, 92(2). [https://doi.org/10.1016/S0013-9351\(02\)00059-2](https://doi.org/10.1016/S0013-9351(02)00059-2)

Ahmad, I., Rehan, M., Balkhyour, M., Abbas, M., Basahi, J., Almeelbi, T., & Ismail, I. M. (2016a). Review of environmental pollution and health risks at motor vehicle repair

workshops challenges and perspectives for Saudi Arabia. *Int J Agric Environ Res*, 2(1), 1–23.

Ahmad, I., Rehan, M., Balkhyour, M., Abbas, M., Basahi, J., Almeelbi, T., & Ismail, I. M. (2016b). Review of environmental pollution and health risks at motor vehicle repair workshops challenges and perspectives for Saudi Arabia. *Int J Agric Environ Res*, 2(1), 1–23.

Ahmad, I., Rehan, M., Balkhyour, M., Abbas, M., Basahi, J., Almeelbi, T., & Ismail, I. M. (2016c). Review of environmental pollution and health risks at motor vehicle repair workshops challenges and perspectives for Saudi Arabia. *Int J Agric Environ Res*, 2(1), 1–23.

Alharbi, B. H., Pasha, M. J., & Tapper, N. (2014). Assessment of ambient air quality in Riyadh City, Saudi Arabia. *Current World Environment*, 9(2), 227.

Arriaga-Colina, J. L., West, J. J., Sosa, G., Escalona, S. S., Ordunez, R. M., & Cervantes, A. D. M. (2004). Measurements of VOCs in Mexico City (1992–2001) and evaluation of VOCs and CO in the emissions inventory. *Atmospheric Environment*, 38(16), 2523–2533.

Arunkumar, M., Visagavel, K., & AbdulZubar, H. (2014). Assessment of indoor air quality in an automobile industry. *Int. J. of Res. Eng. Technol*, 3(11), 265–272.

Ashmore, M. R., Batty, K., Machin, F., Gulliver, J., Grossinho, A., Elliott, P., Tate, J., Bell, M., Livesley, E., & Briggs, D. (2000). Effects of traffic management and transport mode on the exposure of schoolchildren to carbon monoxide. *Environmental Monitoring and Assessment*, 65(1–2). https://doi.org/10.1007/978-94-010-0932-4_6

APPENDIX I: Engine-out data for Chemkin

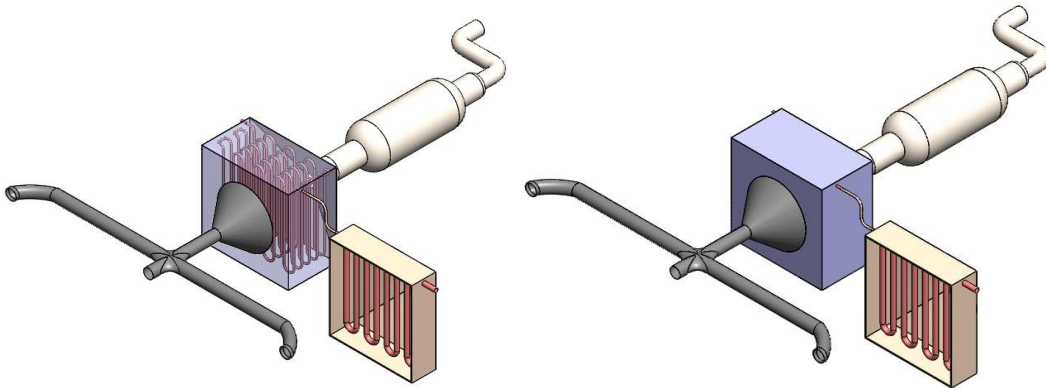
Time(s)	Inlet T ^o (C)	Flow(SLM)	parts per million Co	parts per million of CO ₂	parts per million NO _x	parts per million O ₂
0.001	24.3	85.02	4341	22764	38	12786
0.5	25	85.49	23557	49535	127	77187
1	20.1	27.15	36212	66499	126	50914
1.5	22.6	81,89	1267	37984		
2	39.1	81.2	37984	95735	92	14359
2.5	66.2	83.17	18119	104492	89	9577
3	88.2	86	10391	110148	108	7744
3.5	111.3	87.08	5786	111276	101	13012
4	125.4	85.42	3663	112346	111	8645
4.5	141.2	82.53	2532	111864	104	11867
5	163	81.1	1967	111803	110	16508
5.5	175.2	82.43	1619	111685	101	12255
6	189.8	85.28	2224	110433	119	15728
6.5	208.9	87.06	6022	108765	207	7865
7	218.2	86.12	11532	107414	366	12835
8	244.3	81.27	5259	102752	446	24211
8.5	251.6	193	2823	100132	381	28629
9	272.1	374.28	2942	99228	354	28534
9.5	297.4	479.67	2355	101356	331	28906
10	313.6	483.61	1514	103822	309	29511
10.5	333.2	439.87	1343	105570	276	23807

APPENDIX II: Result value from design calculation

Parameters	Values
Catalyst volume	0.003566m ³
Length of catalytic	600mm
Diameter of catalytic	200mm
Temperature when exhaust valve opens	1335k
Pressure when exhaust valve opens	1603kpa
Mas of exhaust valve open	0.00578kg
Velocity of exhaust valve open	122m/s
Exhaust Temperature	1125k
Exhaust pressure	1487kpa
volumetric flow of air	470CFM
Mass flow rate	0.027kg/s
Temperature of tank(k)	1235
constant gas J/(mol·K)	8.214
for diesel engine(k)	1.35
Pipe temperature out(k)	646
thickness of heat pipe	0.3mm
Diameter of heat pipe	10mm
Longitudinal Stress and total resisting force	316.67kpa
Circumferential or hoop stress for cylindrical shell.	633.3kp
diameter (δd)	0.000065mm
length (δl)	1.08*10 ⁻⁵ mm
volume	1.219mm ³
Fuel-air flow rate of Mass (kg/s)	0.000108, 0.000118
Density of air (kg/m ³)	1.2
Pipe duct area (m ²)	50.24
Initial room temperature of water (K)	296
required temperature (K)	270
Specific heat pressure constant (Cp)	1.005
Volumetric flow rate m ³ /s	0.221
CFM _for hose	470

CFM_ For fan Cubic Feet per Minute	43.661
Static Pressure at cold flow (pa) @43.661cfm	106
FPM. – Feet Per Minute,	0.869
VP- velocity pressure	4.7×10^{-5}
TP Total Pressure,	106.000047
AHP– Air Horsepower	Hp, 0.7281kw (536W)
Safety Factor (k) assumed from 1-3 range	1-3
Volumetric flow of air	$0.0232 \text{m}^3/\text{s}$
Area of single pipe with divergent cover	50.24m^2
Mass flow rate	0.002496kg/s

APPENDIX III: Full assembly design



APPENDIX IV: Data from Chemkin inlet engine out and after treatment at transient

A

Time (sec)	Volume (cm ³)	External_surface_area (cm ²)	Inlet-flow-rate engine-out(g/sec)
0	1400	59000	1.71441
1.03E-05	1400	59000	1.714409
6.33E-04	1400	59000	1.714387
0.509256	1400	59000	1.675297

0.852051	1400	59000	0.8849598
1	1400	59000	0.5419079
1.119715	1400	59000	0.8044099
1.508884	1400	59000	1.642091
1.806302	1400	59000	1.639871
2	1400	59000	1.638392
2.483389	1400	59000	1.683323
2.726961	1400	59000	1.713063
3	1400	59000	1.747065
3.165226	1400	59000	1.75505
3.967512	1400	59000	1.739636
4	1400	59000	1.737439
4.210805	1400	59000	1.712768
4.528552	1400	59000	1.677311
4.629382	1400	59000	1.671637
4.799234	1400	59000	1.662075
4.947377	1400	59000	1.653733
5	1400	59000	1.650768

B

Inlet_mass_fraction_CO	Inlet_mass_fraction_CO	Inlet_mass_fracti C3H6
0.004207374	3.95E-05	0.001345428
0.004207755	3.95E-05	0.001345437
0.004230918	3.96E-05	0.001345993
0.006647343	5.15E-05	0.001404025
0.01671958	1.01E-04	0.001645913
0.02287374	1.31E-04	0.001791667
0.03109202	1.30E-04	0.001913805
0.03461898	1.29E-04	0.001966222
0.03498539	1.27E-04	0.001928984
0.0359916	1.20E-04	0.001808737
0.0309133	1.04E-04	0.001725017

0.02762593	9.32E-05	0.001670822
0.01741621	8.99E-05	0.001445446
0.01374517	9.84E-05	0.001425008
0.009760323	1.09E-04	0.001409742
0.008327464	1.06E-04	0.001368599
0.006956139	1.04E-04	0.001329222
0.00550504	1.02E-04	0.001287555
0.004916218	1.04E-04	0.001272675
0.003565812	1.11E-04	0.001239248
0.003436405	1.12E-04	0.001236045
0.002988866	1.09E-04	0.001215762
0.00234466	1.05E-04	0.001185085
0.002237534	1.06E-04	0.001175005
0.00205713	1.08E-04	0.001158028
Average weight 0.005321431kg/s	Average weight 0.000411531kg/s	Average weight 0.001023461kg/s

C

Mass_fraction_NO	Mass_fraction_NO	Mass_fraction_C3H6
9.63E-04	5.71E-05	0.006012533
9.63E-04	5.71E-05	0.006012478
9.66E-04	5.71E-05	0.006009184
0.001283437	5.63E-05	0.005681015
0.004058061	6.19E-05	0.004598428
0.006746971	7.13E-05	0.004111708
0.01158095	8.55E-05	0.003564702
0.01293041	8.83E-05	0.003460935
0.01400097	9.03E-05	0.003386841
0.01955171	9.86E-05	0.002995485
0.02310145	1.02E-04	0.002678339
0.02417692	1.01E-04	0.002505718
0.02334942	9.74E-05	0.002132366

0.02153645	9.66E-05	0.001971728
0.01893829	9.85E-05	0.001826134
0.01721738	1.00E-04	0.001750203
0.01558397	1.01E-04	0.001681803
0.01386763	1.01E-04	0.001613338
0.01252022	1.02E-04	0.001561511
0.009647575	1.00E-04	0.001455704
0.009400642	1.00E-04	0.001446944
0.007947866	1.00E-04	0.001395029
0.006176441	1.00E-04	0.00132988
0.005704382	1.00E-04	0.001311676
0.005001352	1.00E-04	0.001282975
0.004467941	1.00E-04	0.001259648
0.004293777	1.00E-04	0.00125169
0.004013855	1.00E-04	0.001237087
0.003593254	1.00E-04	0.001208067
0.003176076	1.00E-04	0.001169166
0.002909222	1.00E-04	0.001138326
0.002654201	9.82E-05	0.001109647
0.002269414	9.72E-05	0.001081034
Weighted average 3.72E-04 kg/s	Weighted average 2.00E- 04	Average weight 0.000187584